

FLUCTUATION RELATIONS, THEIR CONSEQUENCES AND SOME EXAMPLES

By

SOURABH LAHIRI

PHYS07200604033

Institute of Physics, Bhubaneswar

A thesis submitted to the

Board of Studies in Physical Sciences

In partial fulfillment of requirements

For the Degree of

DOCTOR OF PHILOSOPHY

of

HOMI BHABHA NATIONAL INSTITUTE



April, 2013

STATEMENT BY AUTHOR

This dissertation has been submitted in partial fulfillment of requirements for an advanced degree at Homi Bhabha National Institute (HBNI) and is deposited in the Library to be made available to borrowers under rules of the HBNI.

Brief quotations from this dissertation are allowable without special permission, provided that accurate acknowledgement of source is made. Requests for permission for extended quotation from or reproduction of this manuscript in whole or in part may be granted by the Competent Authority of HBNI when in his or her judgment the proposed use of the material is in the interests of scholarship. In all other instances, however, permission must be obtained from the author.

Date:

(Sourabh Lahiri)

DECLARATION

I, hereby declare that the investigation presented in the thesis has been carried out by me. The work is original and has not been submitted earlier as a whole or in part for a degree/diploma at this or any other Institution/University.

Date:

(Sourabh Lahiri)

To my parents

ACKNOWLEDGEMENTS

It is a great pleasure for me to thank all the people who have helped me to attain the successful completion of my thesis. Firstly, I would like to express my deep sense of gratitude towards my thesis advisor, Prof. A. M. Jayannavar, who has not only guided me through the PhD course at the institute, but has encouraged and supported me in every step of my work. His critical approach towards any topic, has helped in bolstering my concepts and knowledge in several areas. His amicable nature has also made my process of learning a pleasant one.

I would like to extend my sincere thanks to all the members of my annual review committee, for various fruitful and illuminating discussions regarding my work. Their constructive comments and suggestions have helped me to get further insights into the problems. I have also benefited a lot from the lectures delivered by our teachers in the predoctoral course.

I am grateful to Prof. M. Mahato, Prof. G. Tripathy, Prof. K. Kundu and Dr. Mamata Sahoo for kindly correcting the introduction to my thesis. I am also thankful to all my collaborators, namely, Dr. Navinder Singh, Dr. Arnab Saha, Dr. Mamata Sahoo, and Mr. Shubhashis Rana. Working with them has never allowed monotonicity to seep in, and has been a great learning experience. I would like to especially thank Mr. Shubhashis Rana for being a great friend and companion throughout, ever since we have begun our collaboration.

My heartfelt gratitude goes to all the scholars at IOP who have made my stay at the institute a pleasant one. A special thanks is in order for Mr. Trilochan Bagarti, whose lively nature and curiosity in physical problems have led to several informative discussions, from which I have gained substantially.

I have got immense help from our library staff, who have readily offered their helping hands whenever there has been any problem in the library matters, in particular while searching for a book or a journal.

I am indebted to my teachers who had taught us with ardent zeal during my B. Sc. and M. Sc. courses. My deep regards would be ever-present for Prof. D. Raichaudhuri, Prof. D. Shyam, Prof. S. P. Khastgir, Prof. S. Kar and Prof. S. Bharadwaj, for their inspirational teachings. I am greatly indebted to Partha sir, who, in our school days, had instilled in us a

deep interest in the subject.

The list would remain largely incomplete if I do not express my deep regards and gratitude towards my family members. Hereby I take the opportunity to express my trifling acknowledgement of the generosity with which my parents have encouraged me to pursue the subject of my choice. Their love and affection have always remained an invaluable source of inspiration for me. I am greatly thankful to my wife Jayasree, who has been a very good friend of mine ever since our period of association, and have comforted me whenever I have gone through any stressful moment. The support that I have received from my family has helped me to circumvent many difficulties, and to remain focussed on my journey through my academic career.

Date:

(Sourabh Lahiri)

Contents

Synopsis	xi
1 Introduction	1
1.1 Langevin equation and stochastic thermodynamics	6
1.2 Second law at mesoscales	9
1.3 Fluctuation theorems	11
1.3.1 The Jarzynski and Crooks relations	11
1.3.2 The Integral Fluctuation Theorem (IFT) for total entropy	15
1.3.3 The Detailed Fluctuation Theorem (DFT)	17
1.4 Fluctuation theorems for systems making transition between steady states . . .	17
1.5 The dual trajectory formalism	19
1.6 Stochastic resonance	20
1.7 Plan of the thesis	22
2 Entropy production theorems and some consequences	25
2.1 Introduction	25
2.2 The model	26
2.2.1 Case I: A particle in a harmonic trap subjected to an external time- dependent force	26
2.2.2 Case II: $P(\Delta s_{tot})$ for particle in a dragged harmonic oscillator	33
2.2.3 Case III: Entropy production with athermal initial condition: a case study for a relaxation dynamics	35

2.3	Some relations resulting from the average entropy production fluctuations over finite time	38
2.4	Conclusion	43
3	Fluctuation theorems in presence of information gain and feedback	45
3.1	Introduction	45
3.2	The System	46
3.3	Rederivation of previous results	47
3.3.1	Extended Jarzynski equality	47
3.3.2	Detailed Fluctuation Theorem	49
3.3.3	The generalized Jarzynski equality and the efficacy parameter	51
3.4	Modification in Seifert's and Hatano-Sasa identities	53
3.5	Quantum case	55
3.6	Conclusion	59
4	Universal interpretation of efficacy parameter in perturbed nonequilibrium systems	60
4.1	Introduction	60
4.2	Extended Jarzynski Equality	63
4.2.1	Blind time-reversal of protocol	63
4.2.2	Using feedback to generate reverse process	64
4.2.3	The general case	66
4.3	Efficacy parameter in presence of general feedback	68
4.4	The three detailed fluctuation theorems	70
4.4.1	Total entropy	71
4.4.2	Nonadiabatic entropy	72
4.4.3	Adiabatic entropy	73
4.5	Conclusion	75

5	Total entropy production fluctuation theorems in a nonequilibrium time-periodic steady state	76
5.1	Introduction	76
5.2	The Model	77
5.3	Results and Discussions	80
5.4	Conclusion	87
6	Energy fluctuations in a biharmonically driven nonlinear system	89
6.1	Introduction	89
6.2	The Model: Brownian particle in a Rocked Double Well Potential	90
6.3	Results and Discussions	92
6.3.1	SR as a function of noise strength	92
6.3.2	SR in the presence of static tilt	95
6.3.3	SR as a function of driving frequency	96
6.3.4	Energy fluctuations over a single period	97
6.3.5	Effect of phase difference on SR	99
6.3.6	Energy fluctuations and SSFT	101
6.4	Conclusion	104
7	Summary and Conclusions	106
A	Derivation of Crooks work theorem and Seifert’s detailed fluctuation theorem for total entropy	108
A.1	Crooks Theorem for forward and reverse trajectories	108
A.2	Crooks work theorem	110
A.3	Seifert’s detailed fluctuation theorem for the total entropy	112
B	Dual dynamics and heat exchanges in steady state	113
B.1	The Hatano-Sasa identity	113
B.2	Dual dynamics and its relation to steady state heat exchanges	114

C	Calculation of variance of W, and the Fourier transform of $P(\Delta s_{tot})$ for a system in a harmonic potential	117
C.1	Calculation of variance of W :	117
C.2	Calculation of cross correlation $\langle Wx \rangle - \langle W \rangle \langle x \rangle$:	119
C.3	Calculation of the Fourier transform of $P(\Delta s_{tot}, t)$	121
C.4	Proof of $\langle \Delta F(\tau) \rangle \geq \Delta F$ for harmonic potential	122
C.5	Explicit expressions for free energy changes in a sinusoidally driven system in harmonic potential	123
D	Heun's method of numerical integration	125

Synopsis

When a macroscopic system exchanges energy with its surroundings or some external drive in the form of work or heat, it is usually given by a sharp distribution whose mean is large compared to its variance. However, as we go towards mesoscopic systems, we find that the fluctuations from the mean become comparable to the mean itself. At these scales, the thermal fluctuations experienced by the system owing to its interaction with the surroundings, begin to dictate its evolution in phase space.

At the macroscopic level, even for a single experiment, we expect the second law to hold. For example, the work done on the macroscopic system, in presence of a heat bath at constant temperature, will be found with overwhelming probability to be greater than or equal to the change in its free energy. In other words, the probability of finding a deviation from the second law is fantastically small, even if we consider a single event instead of an ensemble. However, this is not true for a mesoscopic system, where such deviations can occur with appreciable probabilities. So the second law inequalities must hold only in terms of the *ensemble averaged* work or entropy.

Recent advances in experimental techniques have allowed us to carry out exact manipulations on mesoscopic systems like RNA molecules, nanosized particles, molecular motors, etc. As a result, the study of the thermodynamics of these systems has transformed itself from being of mere academic interest to that of practical concern. It is now well-established that the inequalities of the second law strictly hold for averaged thermodynamic variables for these systems. More interestingly, it turns out that inclusion of fluctuations actually helps us to find stronger relations for the variables in terms of exact *equalities*, which produce the second law

inequalities as their corollaries. The last couple of decades have observed the development of several such powerful theorems, called *fluctuation theorems* (FTs) [1, 2], which dictate the amount by which these energy exchanges can violate our expectations. These relations have recently gained a lot of attention. They have been derived for several different scenarios: for deterministic as well as stochastic dynamics, and also for quantum dynamics. We have FTs that apply to driven systems in transient state (for example, the Crooks' work fluctuation theorem), or to systems in nonequilibrium steady state (for example, Seifert's detailed fluctuation theorem for total entropy). They exist for systems that begin in a state of canonical, microcanonical or grand canonical ensembles. There are FTs for different variables like work done on the system, heat exchanged with the reservoir, exchanged charge, information, etc. These relations are very robust and remain valid even when the system is driven far away from equilibrium, where the linear response theory breaks down.

In this thesis, we would concentrate primarily on various FTs that are significant mainly for mesoscopic systems. Some model systems are considered in order to analytically verify different results connected to FTs. Apart from these, several new FTs have been predicted. In one of our works [3], we show that in the very special case when the system begins from thermal equilibrium and the confining potential is harmonic, the detailed fluctuation theorem for the change in total entropy holds even in the transient regime. This happens in spite of the fact that the theorem is supposed to hold only for systems in a nonequilibrium steady state. The nature of entropy production during the relaxation of a system to equilibrium is analyzed. The averaged entropy production over a finite time interval gives a better bound for the average work performed on the system than that obtained from the well-known Jarzynski equality. Further, in the same work, a new quantifier for the irreversibility of a process, namely, the average change in the total entropy, has been introduced.

Using feedback-controlled protocol to drive a system has attracted a lot of attention in recent years [2], primarily because it can drastically enhance the efficiency of the process. Using proper feedback, one can extract work from a system coupled to a single reservoir as well as reduce its entropy. In such processes, a system observable is measured at intermediate times,

and the form of the protocol is changed according to the outcomes of these measurements. In presence of feedback, the fluctuation theorems, along with the second law, need modification. The correction term includes the so-called *mutual information*. The mutual information essentially provides a measure of the information contained in the measurement outcomes about the actual values of the observables being measured, when the measuring device is in general subject to measurement errors. We first show that these extended fluctuation theorems can be trivially obtained from the original ones (that are valid in absence of feedback) [4]. Interestingly, the modified second law obtained on the application of the Jensen's inequality to the extended fluctuation theorems allows for the average change in total entropy to be negative. This is a consequence of the fact that we are actually ignoring the measuring apparatus from the "universe" consisting of the system and the reservoir. We have used this method to generalize the Hatano-Sasa identity [5] as well as the Seifert's fluctuation theorems for the total entropy [6,7]. We have also extended our analysis to derive the generalized form of the detailed as well as the integral form of fluctuation theorems for open systems in the quantum regime.

In addition to obtaining the modified relations for the work or entropy, one is also interested in how efficient a given feedback algorithm is. This measure is provided by the *efficacy parameter* defined by Sagawa and Ueda [8]. We show that other than computing the efficiency of a feedback process, this parameter actually serves to provide a useful generalized form of FTs for the thermodynamic variables like work or entropy [9]. The physical interpretation of the efficacy parameter remains the same, regardless of the feedback procedure used to generate the time-reversed process. This universal expression stands in contrast to the extended fluctuation relations that are more commonly used, which can be very different depending on the algorithm for feedback along the backward process. The latter relations also give rise to different bounds for the thermodynamic variables, depending on the feedback algorithm along the reverse process, while the efficacy parameter provides a universal bound.

One of the important examples where the random thermal fluctuations contrive to produce a very useful physical phenomenon is that of stochastic resonance (SR) [10]. It is a highly nonlinear phenomenon, and is usually modelled as a system transiting between the two wells of

a symmetric double-well potential subjected to an external periodic drive. This effect produces amplified output of an otherwise weak periodic input drive. We study the behaviour of average change in total entropy as well as of average work done in a cycle, as a function of both the noise strength and of the frequency of external drive [11]. We find that when noise strength is changed, the peak in the average work correctly characterizes the resonance condition, but not the peak in average total entropy change. In the second case, the averages of both total entropy change and work done peak when the resonance condition is met. It has also been shown that the probability distribution for total entropy change obeys the detailed fluctuation theorem given by Seifert, in the time-periodic steady state.

In a separate work [12], we show that if a biharmonic drive is applied to the potential in place of a single harmonic drive, then not only does the average energy show a sharper peak at stochastic resonance, it also leads to particle pumping into one of the wells. It is also observed that introduction of an additional phase difference between the two harmonics significantly affects the amount of particle pumping, and they also produce appreciable changes in the structures of the hysteresis loops. Along with this, we check that the work done and dissipated heat follow fluctuation theorems in the limit of a large number of cycles in each realization, when the contributions from the boundary terms become negligible.

Bibliography

- [1] C. Jarzynski, *Annu. Rev. Condens. Matter Phys.* **2**, 329 (2011).
- [2] U. Seifert, arxiv/cond-mat:1205.4176. models. *J. Phys. Soc. Jpn.*, 66:12341237, 1997.
- [3] A. Saha, S. Lahiri and A. M. Jayannavar, *Phys. Rev. E* **80**, 011117 (2009).
- [4] S. Lahiri, S. Rana and A. M. Jayannavar, *J. Phys. A: Math. Theor.* **45**, 065002 (2012).
- [5] T. Hatano and S. Sasa, *Phys. Rev. Lett.* **86**, 3463 (2001).
- [6] U. Seifert, *Phys. Rev. Lett.* **95**, 040602 (2005).
- [7] U. Seifert, *Eur. Phys. J. B* **64**, 423 (2008).
- [8] T. Sagawa and M. Ueda, *Phys. Rev. E* **85**, 021104 (2012).
- [9] S. Lahiri and A. M. Jayannavar, arxiv/cond-mat: 1206.3383.
- [10] L. Gammaitoni, P. Hänggi, P. Jung and F. Marchesoni, *Rev. Mod. Phys.* **70**, 223 (1998).
- [11] S. Lahiri and A. M. Jayannavar, *Eur. Phys. J. B* **69**, 87 (2009).
- [12] N. Singh, S. Lahiri and A. M. Jayannavar, *Pramana J. Phys.* **74**, 331 (2010).

Publications :¹

1. Published

- * (i) *Total entropy production fluctuation theorems in a nonequilibrium time-periodic steady state*. S. Lahiri and A. M. Jayannavar, Eur. Phys. J. B **69**, 87 (2009).
- * (ii) *Entropy production theorems and some consequences*, Arnab Saha, S. Lahiri and A. M. Jayannavar, Phys. Rev. E **80**, 011117 (2009).
- * (iii) *Energy fluctuations in a biharmonically driven nonlinear system*. Navinder Singh, S. Lahiri, A. M. Jayannavar, Pramana J. Phys. **74**, 331 (2010).
- (iv) *Classical diamagnetism revisited*, Arnab Saha, S. Lahiri and A. M. Jayannavar, Mod. Phys. Lett. B **24**, 2899 (2010).
- (v) *Fluctuation theorems and atypical trajectories*, Mamata Sahoo, S. Lahiri and A. M. Jayannavar, J. Phys. A: Math. Theor. **44**, 205001 (2011).
- (vi) *The role of soft versus hard bistable systems on stochastic resonance using average cycle energy as a quantifier*, S. Rana, S. Lahiri and A. M. Jayannavar, Eur. Phys. J. B **84**, 323 (2011).
- * (vii) *Fluctuation theorems in presence of information gain and feedback*, S. Lahiri, S. Rana and A. M. Jayannavar, J. Phys. A: Math. Theor. **45**, 065002 (2012).
- (viii) *Quantum Jarzynski Equality with multiple measurement and feedback for isolated system*, S. Rana, S. Lahiri, A. M. Jayannavar, Pramana J. Phys. **79**, 233 (2012).
- (ix) *Fluctuation relations for heat engines in time-periodic steady states*, S. Lahiri, S. Rana and A. M. Jayannavar, J. Phys. A: Math. Theor. **45**, 465001 (2012).
- (x) *Generalized entropy production fluctuation theorems for quantum systems*, S. Rana, S. Lahiri and A. M. Jayannavar, Pramana J. Phys. **80**, 207 (2013).

¹The starred publications are the ones on which the thesis is based.

2. Communicated

- * (i) *Universal interpretation of efficacy parameter in perturbed nonequilibrium systems*,
S. Lahiri and A. M. Jayannavar, arxiv/cond-mat: 1206.3383.

Chapter 1

Introduction

Statistical mechanics is the subject that strives to explain the macroscopic events from the properties of microscopic dynamics of the constituent particles. It is evidently computationally impossible to apply and solve Newton's laws of motion to all the particles present (typically of the order of 10^{23}) in a given macroscopic sample. Furthermore, often we are not interested in the entire system, but only in a part of it. Henceforth, we would call this part as our system of interest, or simply as the *system*. The remaining portion that we are not interested in would be termed as the *environment*. Together they form the *universe*, i.e., an isolated supersystem. Classical mechanics would not allow us to study the time-evolution of the properties of the system only, without taking into account the detailed time-evolution of the supersystem.

Statistical mechanics provides us a way to circumvent these difficulties by exploiting the properties arising precisely due to the presence of a large number of degrees of freedom [1]. These properties are described probabilistically. For example, consider an ideal gas at equilibrium with a thermal reservoir. Although we do not know the exact coordinates and momenta of each particle of the combined supersystem, we do know the probability distribution¹ of the states of the molecules in this system. Thus, as the number of degrees of freedom becomes very large, statistical laws come to our aid, and the job of solving a huge number of differential equations no more remains a necessity.

¹In this thesis, we would be using the terms “probability distribution” and “probability density” interchangeably, as long as there is no reason for confusion, although more often we would mean the latter.

The last couple of decades have observed a crescendo of effort going into the field of nonequilibrium thermodynamics and statistical mechanics of mesoscopic or smaller systems, having dimensions typically in the range 1 nm to 1 μm . This is mainly because of the advent of new high-precision measurements to probe these systems, as in RNA pulling experiments, dragged colloidal particles, molecular motors, etc. [2–6]. Thus, at present this field has transformed itself from being a problem of mere academic interest to a study dealing with practical applications. Any attempt to build machines at such small scales be preceded by a thorough understanding of how differently the systems behave at these scales. An efficient nano-engine need not be (and, in fact, is not) a simple scaled down version of an efficient macro-engine.

A major development in the field of nonequilibrium statistical mechanics has been a group of relations, collectively known as the *fluctuation theorems* (FTs) (see section 1.3) [5]. This thesis is primarily aimed at the verification of FTs in several different model systems, along with the derivation of some new theorems. These theorems provide rigorous relations for the probability distributions (over a large number of experimental realizations of a process) of various physical quantities like work, heat or entropy changes, in systems undergoing nonequilibrium processes (for details, see section 1.3). A knowledge of FTs is necessary to build efficient machines at small scales. We have also studied extension of the known FTs to the case when the externally applied drive is controlled by feedback. The meaning of feedback-controlled drive would be explained shortly. Such drives are of extreme importance, because they can drastically enhance the efficiency of a process. Other than fluctuation relations, the phenomenon of stochastic resonance (see section 1.6), which is of major significance in biological systems, has been studied.

The mathematical statement of the fluctuation theorems can be generically stated as

$$\frac{P(\Sigma)}{\tilde{P}(-\Sigma)} = e^{\alpha\Sigma}, \quad (1.1)$$

where Σ is the observed value of an extensive variable (dissipated work, dissipated heat, total entropy change, etc.), and α is a positive constant with inverse dimension of that of Σ . The

symbols P and \tilde{P} denote the probability density functions observed under the forward and time-reversed² external perturbations or *protocols*, whose time dependences are given by $\lambda(t)$ and $\lambda(\tau - t)$, respectively. Here, the period of observation begins at time $t = 0$ to and ends at time $t = \tau$. Since all the dissipative quantities scale with the system size, it is obvious that for a macroscopic system, the probability of observing a negative value of Σ will be fantastically small compared to that of observing a positive value of Σ . For a mesoscopic system, however, the probability of observing such events can become appreciable, as will be elaborated later (see the discussion on pages 4 and 5). The strength of these theorems lies in the fact that they remain valid no matter how far the system has been driven away from equilibrium. Moreover, they provide further insights into the microscopic basis for the second law of thermodynamics. We will see that the second law inequalities are readily obtained as corollaries, from these theorems. Most of these theorems have been verified experimentally [3, 7–17].

In general, the second law specifies that the total entropy of the universe (system plus environment) never decreases in a process. However, sometimes we need to apply a drive that is feedback-controlled. This means that during the process, we measure some observable (say, the position or the velocity) of the system, and depending on the outcome of the measurement, the form of the protocol is changed. In such a case, the second law inequality undergoes a modification. This is because, now the measuring device is also a part of our universe. Thus, if we still include only the system and the bath in our analysis, then we are actually ignoring a part of the universe. The modified inequalities involve correction terms that are encoded in the information recorded by the measuring device. We have studied these modified expressions for the fluctuation theorems in presence of feedback-controlled drive in chapters three and four.

In chapter three, the extended relations in presence of feedback have also been studied for quantum systems. Most of the fluctuation theorems have been generalized to the quantum regime [6, 18–21]. A particularly simple approach adopted for quantum systems is to consider the system to be initially prepared in a state sampled from some arbitrary distribution. Subsequently, it is kept isolated from its environment throughout the period of evolution so that the

²In chapter 4, we would find that certain fluctuation theorems hold for transformations other than simple time-reversal.

evolution operator is unitary. The other simplifying assumption is the use of projective measurements on the state of the system. Although these assumptions are highly simplistic, they provide a clear visualization of the process, and it is instructive to study such processes before embarking upon more general processes. For example, the work done on an isolated system is defined through two projective energy measurements at the initial and the final times. If the energy eigenvalues thus obtained are E_n and E_m respectively, then the work done on the system during that realization is defined as: $W = E_m - E_n$. Only by such an identification, work can be defined as an observable, which is difficult otherwise. Much more detailed treatments are called for in studying the quantum fluctuation theorems under more general conditions, and the subject is being studied intensively at present.

In this thesis, we would apply the FTs mainly to mesoscopic systems that undergo some nonequilibrium process. The FTs are useful only when applied these small systems, where thermal fluctuations become significant. In this regard, it would be useful to briefly discuss the terms “mesoscopic systems” and “nonequilibrium process” separately. We outline below the special features of each.

Let us first discuss the properties of *mesoscopic systems*. In general, the evolution of a system in phase space will not follow a unique trajectory, but will be subject to thermal fluctuations. Thermal fluctuations arise because of the system’s interaction with its environment. These fluctuations are ignored in macroscopic thermodynamics. This approach yields quite accurate results, as long as our system is itself macroscopic, so that deviations from the mean value are negligibly small compared to the mean value itself. However, when we direct our attention to systems at mesoscopic scales or smaller, this condition gets invalidated. We can, therefore, no more remain oblivious to the fluctuations [5, 22]. Consequently, we will find that the thermodynamic observables appearing in the second law inequality must be replaced by their averages over a large number of experimental realizations. Consider, for example, a corollary of the Clausius statement for the second law. It states that, if we consider a system in contact with a thermal reservoir, then we must have: $W_d \equiv W - \Delta F \geq 0$ (sect. 15 of [1]). Here, W is the work done *on* the system by the external force, and ΔF is the change in the

Helmoltz free energy of the system in the process. For a mesoscopic system, this inequality would be modified to $\langle W_d \rangle \geq 0$, where $\langle \cdot \cdot \cdot \rangle$ represents ensemble averaging.

The above fact has been shown diagrammatically in figure 1.1. The figure clearly shows that, when the mean value of W_d becomes comparable to the typical energy obtained from thermal fluctuations, there may be an appreciable number of events in the ensemble in which the dissipated work becomes negative. This is the shaded region in the figure. The phase space trajectories along which an observable seems not to behave in accordance with the second law are called *atypical trajectories*. Sometimes they are also termed as “transient second law violating trajectories”. Nevertheless, $\langle W_d \rangle$ remains positive, in conformity with the second law. In the above discussion, the dissipated work W_d is the observable Σ , in the context of eq. (1.1).

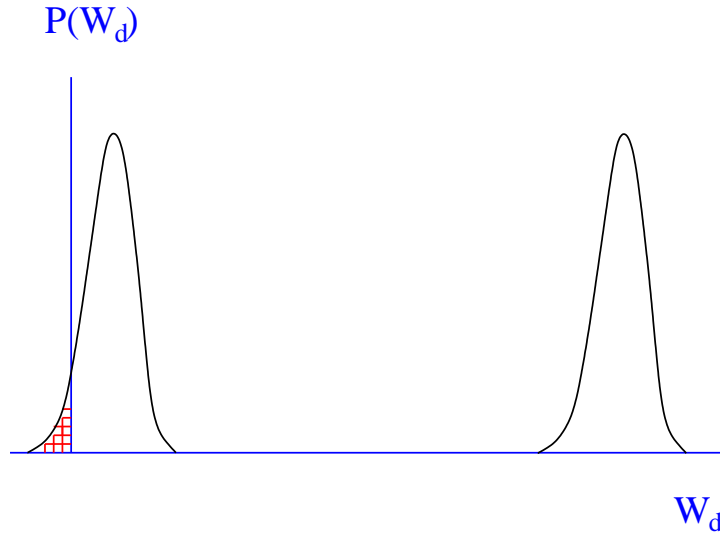


Figure 1.1: The distribution at the right is that for the dissipated work in a macroscopic system (diagram is not to scale). Obviously, because of the large value of the mean, there would be negligible probability of observing a process in which the dissipated work W_d is negative. On the other hand, the distribution for the mesoscopic system (left) may have an appreciable part of the distribution on the negative side (shaded part).

We now discuss the features of a *nonequilibrium process*. Nonequilibrium statistical mechanics studies processes where the system may be arbitrarily away from equilibrium. Although we have well-defined state variables for systems at equilibrium, it is usually difficult to define thermodynamic variables for a system that is far from equilibrium. Nevertheless, the energy remains unambiguously defined for any given microstate of the system, even if the

macrostate is no more well-defined. We will see that the variables like work, heat and internal energy can be defined using physical arguments in stochastic energetics [23, 24], even when system undergoes a highly nonequilibrium process.

We would next go through a little more detailed introduction to the basic concepts involved in the topics dealt with in this thesis, in sections 1.1–1.6 of this chapter. In section 1.7, the plan of this thesis will be outlined.

1.1 Langevin equation and stochastic thermodynamics

To get a proper understanding of the variables work, heat, internal energy and entropy at mesoscopic scales, we need to define them unambiguously. This has been done by Sekimoto in [23, 24], where he has used physical arguments to show how these variables naturally arise from the Langevin dynamics of a Brownian particle. The Langevin equation is the extension of the Newton’s equation of motion to the regime where the system interacts with environment, and its effect on the system is given by a systematic frictional force and a fluctuating force [48]. These fluctuations play a major role in determining the phase space trajectory of the system. We suppose that a mesoscopic particle is performing Brownian motion in a medium held at temperature T which we would treat as a heat bath. The particle may be subjected to an external time-dependent perturbation $f(t)$ that can be derived (say) from a time-dependent potential³. Let the full potential (including the perturbation) to which the system is subjected be $V(x, t)$. We then write the equation of motion for the system (in one-dimension) in the form:

$$m\dot{v} = -\frac{\partial V(x, t)}{\partial x} - \gamma v + \xi(t), \quad (1.2)$$

where $-\gamma v$ is the viscous force, and $\xi(t)$ contains all the random contributions. We would use an overhead dot to represent total time-derivatives. Throughout this thesis, we will assume that

³At the end of the section we would state the result in presence of a non-conservative force.

this random force follows a zero-mean Gaussian distribution, and is delta-correlated in time:

$$\langle \xi(t) \rangle = 0; \quad \langle \xi(t)\xi(t') \rangle = 2D\delta(t - t'). \quad (1.3)$$

In the above equation, D is the noise strength and is related to the bath parameters through the Einstein relation: $D = \gamma k_B T$, where k_B is the Boltzmann constant. Following Sekimoto [24], we will now trace the steps⁴ that lead to the definitions of the thermodynamic variables in this setup. We multiply both sides of (1.2) by dx and rearrange the terms to get

$$-[-\gamma v + \xi(t)]dx = -m \frac{dv}{dt} dx - \frac{\partial V}{\partial x} dx. \quad (1.4)$$

$(-\gamma v + \xi(t))$ consists of the forces that are generated by the bath. So, $-(-\gamma v + \xi(t))$ is the reaction force of the system on the bath. Thus, the left hand side is the work done by this reaction force of the system, on the bath. This work gets irretrievably lost into the huge number of degrees of freedom of the bath. We identify this term as the heat dissipated dQ (in a time step dt) into the medium:

$$dQ = [\gamma v - \xi(t)]dx. \quad (1.5)$$

We then have, after rewriting eq. (1.4), and using the chain rule $dV = \frac{\partial V}{\partial x} dx + \frac{\partial V}{\partial t} dt$,

$$dQ = -mvdv - dV + \frac{\partial V}{\partial t} dt = -d\left(\frac{1}{2}mv^2 + V\right) + \frac{\partial V}{\partial t} dt. \quad (1.6)$$

Finally, on integrating both sides, and writing the total change in the internal energy as $\Delta U = \Delta(\frac{1}{2}mv^2 + V)$, we obtain

$$Q = -\Delta U + \int \frac{\partial V}{\partial t} dt = -\Delta U + W, \quad (1.7)$$

⁴Although in [24], although Sekimoto had provided the derivation for an overdamped system, it is straightforward to see that it is easily applicable to underdamped systems as well.

where, on comparing with the first law, we have identified the second term on the right hand side as the thermodynamic work W performed on the system by the external parameter:

$$W = \int \frac{\partial V}{\partial t} dt. \quad (1.8)$$

Thus, we get the following expressions for Q , ΔU and W up to time τ :

$$Q(\tau) = \int_0^\tau (\gamma v - \xi(t)) \dot{x} dt = - \int_0^\tau \left(\frac{\partial V(x, t)}{\partial x} + m\dot{v} \right) v dt. \quad (1.9a)$$

$$\Delta U(\tau) = \frac{1}{2} m v^2(\tau) + V(x(\tau), \tau) - \frac{1}{2} m v^2(0) - V(x(0), 0). \quad (1.9b)$$

$$W(\tau) = \int_0^\tau \frac{\partial V(x, t)}{\partial t} dt. \quad (1.9c)$$

In eq. (1.9a), the integrand has been rewritten using eq. (1.2).

Overdamped case: Often in stochastic dynamics, we have systems whose momentum variable is a fast variable, i.e., the relaxation time $\tau_v \sim m/\gamma$, is very small compared to the time scale of change in the position distribution. We then say that the system is *overdamped* and the Langevin equation transforms to

$$\gamma \dot{x} = - \frac{\partial V(x, t)}{\partial x} + \xi(t). \quad (1.10)$$

Following a prescription similar to that of an underdamped system, we arrive at the following expressions for Q , ΔU and W :

$$\begin{aligned} Q(\tau) &= - \int_0^\tau \frac{\partial V(x, t)}{\partial x} \dot{x} dt; \\ \Delta U(\tau) &= V(x(\tau), \tau) - V(x(0), 0); \\ W(\tau) &= \int_0^\tau \frac{\partial V(x, t)}{\partial t} dt. \end{aligned} \quad (1.11)$$

Finally, in addition to the conservative force field that can be derived from the potential

function $V(x, t)$, a non-conservative force $f_{nc}(x, t)$ may also be present. This would simply modify the definition of work to [5]

$$W(\tau) = \int_0^\tau \frac{\partial V(x, t)}{\partial t} dt + \int_0^\tau f_{nc}(x, t) \dot{x} dt. \quad (1.12)$$

1.2 Second law at mesoscales

The second law for macroscopic *closed* systems (one that can exchange only energy with its surroundings) can be described through either of the following two statements, which arise from the Clausius inequality:

First statement: *Among all processes taking place between any two given thermodynamic states, the work done on the system is minimum for a reversible process.*

For a system in contact with a thermal reservoir, this gives rise to the inequality

$$W \geq \Delta F. \quad (1.13)$$

Here, the change in free energy ΔF is the work done during an isothermal reversible process [1]. The above equation, when rewritten in terms of work *extracted* from the system, gives the statement for the maximum work theorem [25].

Second statement: *The total entropy of the universe (which is a closed system consisting of the system of interest and the environment with which it interacts) can never decrease with time:*

$$\Delta S_{tot} \geq 0. \quad (1.14)$$

Here, ΔS_{tot} is the change in total entropy of the universe, which, according to the above statement, is always non-negative [26].

The second law has been formulated for macroscopic systems, where the effect of thermal fluctuations are negligible. At mesoscopic scales, as mentioned above (page 5), there would

be atypical trajectories, although the ensemble-averaged quantities must obey the second law. Thus the statements of the second law at mesoscales become:

$$\langle W \rangle \geq \Delta F; \quad \langle \Delta s_{tot} \rangle \geq 0. \quad (1.15)$$

Here, the angular brackets denote averages taken over a large number of realizations of the experiment, while the expressions within $\langle \rangle$ denote the values of the observables (work or change in total entropy) for each experiment, which in general vary from one realization of the experiment to the other. The change in total entropy, Δs_{tot} , for a given phase space trajectory (corresponding to a given experiment) is defined as the sum of the changes in medium entropy (Δs_m) and in system entropy (Δs) [28, 29] along that trajectory. A change in the medium entropy over a time interval τ is given by the heat dissipated into the medium divided by its temperature:

$$\Delta s_m(\tau) = \frac{Q(\tau)}{T}. \quad (1.16)$$

The nonequilibrium entropy S of the system is defined as

$$S(t) = - \int dx p(x, t) \ln p(x, t) = -\langle \ln p(x, t) \rangle, \quad (1.17)$$

where x would be replaced by both position and velocity for an underdamped system. This leads to the definition of the configurational entropy of the particle as [27–29]

$$s(t) = - \ln p(x, t). \quad (1.18)$$

The change in the system entropy for any trajectory of duration τ is given by

$$\Delta s(\tau) = - \ln \left[\frac{p_1(x_\tau)}{p_0(x_0)} \right], \quad (1.19)$$

where $p_0(x_0)$ and $p_1(x_\tau)$ are the probability densities of the particle positions at initial time $t = 0$ and final time $t = \tau$, respectively. Thus for a given trajectory, the system entropy $s(t)$

depends on the initial probability density and hence contains the information about the whole ensemble. The total entropy change over time duration τ is given by

$$\Delta s_{tot}(\tau) = \Delta s_m(\tau) + \Delta s(\tau). \quad (1.20)$$

1.3 Fluctuation theorems

As stated earlier, the fluctuation theorems have been one of the rare and significant developments in the field of nonequilibrium statistical mechanics. These theorems remain valid no matter how far the system has been driven away from equilibrium. Initially theorems of this kind were proved for the entropy production, from simulation of sheared fluids by Evans et al [30]. It was proved mathematically for deterministic systems in [31] and later by Gallavotti and Cohen [32]. Several new relations in this field have come up since then [20, 27–29, 33–43]. These theorems provide stringent restrictions on the fraction of atypical realizations (i.e., the ones that behave atypically with respect to the second law, as explained in page 5) in an ensemble. They give rigorous relations for the properties of distribution functions of physical variables like work, heat and entropy production for systems driven away from equilibrium, where Onsager relations no longer hold.

1.3.1 The Jarzynski and Crooks relations

An important development in the field of fluctuation theorems has been the Jarzynski equality [33, 34] which provides a way to compute the change in the equilibrium free energy of a system from measurements of the work done on it along a nonequilibrium process. Crooks [42] later provided a more detailed fluctuation theorem from which the Jarzynski equality automatically follows. We would first describe the Crooks theorem below and show how the Jarzynski equality appears as a corollary. Although these theorems have been proven for both deterministic as well as stochastic evolutions, we would outline only one of them below, namely for the stochastic dynamics.

Let us consider a system that has been equilibrated with a heat bath with temperature T at initial time $t = 0$ [33,34], corresponding to the value $\lambda(0) \equiv A$, of an external thermodynamic parameter (on which the system Hamiltonian depends explicitly). At $t = 0+$ we switch on the time-variation of the external perturbation $\lambda(t)$. The phase space coordinates of the particle evolve along a trajectory governed by stochastic dynamics, from time $t = 0$ to $t = \tau$, and the final value of the parameter is $\lambda(\tau) \equiv B$. The time-dependence of the protocol is arbitrary. However, in an ensemble of realizations of a given experiment, the same protocol is used repeatedly.

As an example, in a particular experiment, the system may consist of an RNA molecule, whose free ends are attached to two polystyrene beads. One of them is held fixed, while the other bead is moved using an optical trap, thereby either stretching or contracting the molecule. In this case, the external parameter would be the distance between the two beads, and the time-dependence $\lambda(t)$ of this parameter would specify the *protocol*.

The full trajectory of the system's evolution in phase space will be represented by $X(t)$, to differentiate it from the individual phase space points x_t .⁵ Now, any such point x_t in general consists of all the degrees of freedom associated with the particle, but we will stick to a one-dimensional overdamped motion to enhance the transparency of the following treatment. If the system is underdamped, x_t will denote both position and velocity of the particle at time t : $x_t \equiv (x, v; t)$. Unless clear from the context, whenever we are considering an overdamped system, we would always state this fact explicitly in this thesis. The treatment can be trivially generalized to multiple dimensions.

The probability distribution of the initial phase space point x_0 is given by the Boltzmann distribution:

$$p_0(x_0) = \frac{e^{-\beta H(x_0, A)}}{Z(A)}. \quad (1.21)$$

⁵If we discretize the time of observation as $\{t_0, t_1, \dots, t_N\}$, the corresponding phase space trajectory would be represented by a discrete set of points $\{x_0, x_1, \dots, x_N\}$. We are using the compact notation $x_k = x(t_k)$. The entire trajectory will then be denoted by $X \equiv \{x_0, x_1, \dots, x_N\}$.

Here, $H(x_0, A)$ is the system Hamiltonian at the initial state x_0 with the external parameter fixed at A , and $Z(A)$ is the initial partition function. $\beta = 1/k_B T$ is the inverse temperature of the bath.

For the reverse process, we at first equilibrate the system with the same heat bath, but now with the protocol value held fixed at B . Subsequently we apply the time-reversed protocol $\lambda(\tau - t)$ to the system⁶ Thus the system now has the following distribution to begin with:

$$p_1(\tilde{x}_\tau) = \frac{e^{-\beta H(\tilde{x}_\tau, B)}}{Z(B)}. \quad (1.22)$$

Here, the tilde symbol implies time-reversed variables defined through the operation executing the inversion of velocities. In other words, (x, v) goes to $(x, -v)$ under the tilde operation. In particular, the initial point of the reverse process is given by \tilde{x}_τ . According to our notation, \tilde{x}_t would mean the time-reversal of the variable x_t , where the time elapsed along the *forward* path is t . However, we must keep in mind that the actual time elapsed along the reverse trajectory is $\tau - t$, where τ is the total time of observation in either process.

As shown by Crooks [42], the ratio of the forward to the reverse trajectory is given by

$$\frac{P[X|x_0]}{\tilde{P}[\tilde{X}|\tilde{x}_\tau]} = e^{\beta Q}. \quad (1.23)$$

where time runs from 0 to τ , and Q is the heat dissipated into the heat bath during the forward process. Here, the notation $P[X|x_0]$ is a compact representation of the probability density for the entire trajectory $X(t)$, beginning from a given initial state x_0 , when the process is generated by the external protocol $\lambda(t)$. Similarly, $\tilde{P}[\tilde{X}|\tilde{x}_\tau]$ represents the probability density for the time-reversed path $\tilde{X}(t)$, beginning from the given initial point \tilde{x}_τ . The initial point of the reverse path is the time-reversed of the final state of the forward path. Symbolically, if the forward trajectory is denoted by $X(t) \equiv x_0 \rightarrow x_1 \rightarrow x_2 \rightarrow \dots \rightarrow x_\tau$, then the reverse trajectory will be given by $\tilde{X}(t) \equiv \tilde{x}_0 \leftarrow \tilde{x}_1 \leftarrow \tilde{x}_2 \leftarrow \dots \leftarrow \tilde{x}_\tau$. Another elegant proof for the relation (1.23)

⁶Note that this is not the same as the time-reversal of a movie of the forward process, as has been discussed in detail in [44].

is given in [41].

If both sides of eq. (1.23) are multiplied by $p_0(x_0)/p_1(\tilde{x}_\tau)$, we would get the ratio of the unconditional probability densities (i.e., for arbitrary initial points) for the forward path $P[X]$ and the corresponding reverse path $\tilde{P}[\tilde{X}]$ in phase space: $P[X] = P[X|x_0]p_0(x_0)$; $\tilde{P}[\tilde{X}] = \tilde{P}[\tilde{X}|\tilde{x}_\tau]p_1(\tilde{x}_\tau)$. A typical forward trajectory in phase space and its corresponding reverse trajectory is given in figure 1.2.

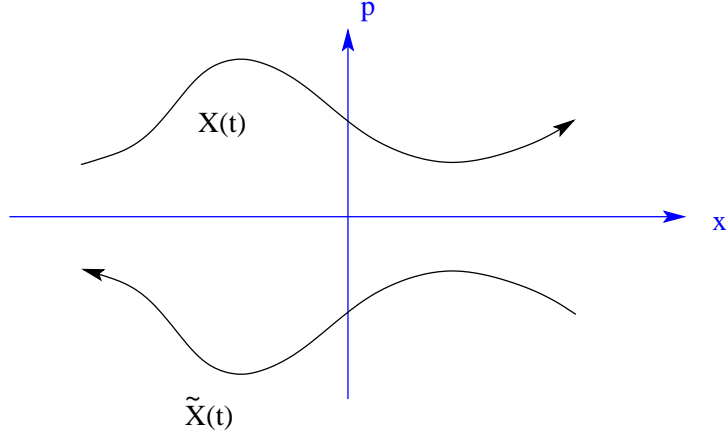


Figure 1.2: The figure shows a typical forward trajectory $X(t)$ in phase space and its corresponding reverse trajectory $\tilde{X}(t)$. The momentum coordinates (p) are inverted in the case of the reverse trajectory, while the position coordinates (x) remain the same.

Since we are considering the initial states of the system to be at thermal equilibrium for either process, we have $p_1(\tilde{x}_\tau) = p_1(x_\tau)$ (the Hamiltonian being assumed to be time-reversal invariant), and the above ratio gives the Crooks work theorem in the trajectory picture:

$$\frac{P[X]}{\tilde{P}[\tilde{X}]} = e^{\beta(W - \Delta F)}. \quad (1.24)$$

The detailed derivation for a system following overdamped Markov dynamics has been given in appendix A. This theorem physically means that ratio of the probability density of observing a trajectory X for a system driven by the protocol $\lambda(t)$ (forward process), to the probability density of observing the trajectory \tilde{X} under the protocol $\lambda(\tau - t)$ (reverse process), is given by the exponential of the dissipated work along the forward process. The work theorem in terms of probability densities for the work done on the system in forward and reverse processes can

be readily obtained from the above relation (see appendix A):

$$\frac{P(W)}{\tilde{P}(-W)} = e^{\beta(W-\Delta F)}. \quad (1.25)$$

The Jarzynski equality can be easily obtained from the Crooks fluctuation theorem (1.23) by simple cross multiplication and integration over W :

$$\begin{aligned} \langle e^{-\beta W} \rangle &= \int dW P(W) e^{-\beta W} = e^{-\beta \Delta F} \int dW \tilde{P}(-W) \\ &= e^{-\beta \Delta F}. \end{aligned} \quad (1.26)$$

Since ΔF is a constant, $e^{-\beta \Delta F}$ has been taken out of the integral. The final step uses the normalization condition $\int dW \tilde{P}(-W) = 1$. Thus, from repeated measurements of the nonequilibrium work and subsequent averaging over all the realizations, one can obtain the value of the equilibrium free energy change of the system. This has been verified experimentally [2]. Further, application of the Jensen's inequality⁷ (for exponential functions, this inequality is given by $\langle e^y \rangle \geq e^{\langle y \rangle}$) to the relation (1.26), we get the generalized maximum work theorem for mesoscopic systems:

$$\langle W \rangle \geq \Delta F. \quad (1.27)$$

Interestingly, the Jarzynski equality implies that the information about equilibrium free energy is encoded in the work done along a nonequilibrium process.

1.3.2 The Integral Fluctuation Theorem (IFT) for total entropy

The entropy of a system is in general considered to be an ensemble property. However, the entropy of a system along a single trajectory can be defined. These definitions have been stated in equations (1.16)–(1.19).

To discuss the approach of Seifert, we define the quantity R as the ratio between the uncon-

⁷Using the inequality [45] $e^y \geq 1 + y$, we get $\langle e^y \rangle = \langle e^{y - \langle y \rangle + \langle y \rangle} \rangle = e^{\langle y \rangle} \langle e^{y - \langle y \rangle} \rangle \geq e^{\langle y \rangle} \langle 1 + y - \langle y \rangle \rangle = e^{\langle y \rangle}$, which is the Jensen's inequality for the exponential function.

ditional probability densities of the forward and the backward paths [28, 29]:

$$R \equiv \ln \frac{P[X]}{\tilde{P}[\tilde{X}]} = \ln \left\{ \frac{P[X|x_0]p_0(x_0)}{\tilde{P}[\tilde{X}|\tilde{x}_\tau]p_1(\tilde{x}_\tau)} \right\} = \Delta s_m + \ln \frac{p_0(x_0)}{p_1(\tilde{x}_\tau)} \quad (1.28)$$

In the last step, we have used the Crooks fluctuation theorem for dissipated heat, eq. (1.23), keeping in mind that βQ is simply the change in the entropy Δs_m of the heat bath. In this case, we do not consider equilibration of the system at the beginning of either the forward or the reverse protocols, so that $p_0(x_0)$ and $p_1(x_\tau)$ are in general nonequilibrium distributions. The following general identity can be easily derived [28]:

$$\langle e^{-R} \rangle \equiv \int \mathcal{D}[X] P[X|x_0] p_0(x_0) e^{-R} = \int \mathcal{D}[X] \tilde{P}[\tilde{X}|\tilde{x}_\tau] p_1(\tilde{x}_\tau) = 1. \quad (1.29)$$

Here, $\mathcal{D}[X]$ is the measure of integration over all trajectories. In the discrete-time picture, when the path is given by $\{x_0, x_1, \dots, x_\tau\}$, we have $\mathcal{D}[X] = dx_0 dx_1 \dots dx_\tau$. Also, the Jacobian between any x_t and its time-reversed state \tilde{x}_t is identically equal to one, so that we have $\mathcal{D}[X] = \mathcal{D}[\tilde{X}]$. $p_0(x_0)$ and $p_1(x_\tau)$ can be chosen to be any hypothetical normalized probability distributions of the system states. If $p_1(x_\tau)$ is the solution of the Fokker-Planck equation for the forward process, then the second term in eq. (1.28) becomes the change in entropy Δs of the system, and R is then the total entropy change of the system: $\Delta s_{tot} = \Delta s_m + \Delta s$. In this case, we can write equation (1.28) as

$$\frac{P[X]}{\tilde{P}[\tilde{X}]} = e^{\Delta s_{tot}}. \quad (1.30)$$

We then have the integral fluctuation theorem (IFT) for total entropy change:

$$\langle e^{-\Delta s_{tot}} \rangle = 1. \quad (1.31)$$

Application of Jensen's inequality to this IFT immediately leads us to the second law of ther-

modynamics that holds for the average change in total entropy:

$$\langle \Delta s_{tot} \rangle \geq 0. \quad (1.32)$$

1.3.3 The Detailed Fluctuation Theorem (DFT)

The detailed fluctuation theorem (DFT) for total entropy holds only if the system stays throughout in the same steady state or is in equilibrium at the initial and final times. The reason for this constraint is that, in general the change in system entropy does not switch its sign in the reverse path [27]. The theorem reads (see appendix A for the steps in the derivation)

$$\frac{P(\Delta s_{tot})}{P(-\Delta s_{tot})} = e^{\Delta s_{tot}}. \quad (1.33)$$

Note that the tilde symbol to denote the reverse process has been done away with, in accordance with the fact that the steady state distributions are characterized by a constant value of the external protocol in either process.

1.4 Fluctuation theorems for systems making transition between steady states

The second law simply states that the total entropy change of the system and environment never decreases with time. However, while maintaining a steady state (for example, in the presence of a time-independent non-conservative force), heat is naturally dissipated into the environment and as a result the total entropy keeps increasing. Hence, the lower bound (namely, zero) for the change in total entropy loses its significance. Keeping this in mind, Oono and Paniconi [46] had proposed the division of the total dissipated heat into two separate parts: one is called the *housekeeping heat* Q_{hk} that is required to maintain a particular steady state corresponding to a fixed value of the external drive. The other was called the *excess heat* Q_{ex} that is dissipated over and above the housekeeping heat in presence of a time-dependent perturbation or during

relaxation to a steady state, and is obtained by subtracting the contribution of the housekeeping heat from the total heat dissipated during the process: $Q_{ex} = Q - Q_{hk}$.

We would restrict ourselves to overdamped systems in this section. Interestingly, in this case, both the housekeeping heat and the excess heat can be shown to follow separate fluctuation theorems (the case of underdamped systems has been analyzed in [50], where it has been shown that the housekeeping heat does not follow a fluctuation theorem in general for such systems. Nevertheless, the Hatano-Sasa identity, eq. (1.37) below, is always obeyed), and the second law takes the form [47]

$$\beta \langle Q_{ex} \rangle + \langle \Delta s \rangle \geq 0. \quad (1.34)$$

The system has been assumed to be initially in a steady state, and also that it relaxes to a steady state corresponding to the final protocol value at the end of the process. Defining the steady-state probability density as $\rho_{ss}(x; \lambda) = e^{-\phi(x; \lambda)}$, where $\phi(x; \lambda)$ is an effective potential, the expressions for the housekeeping and the excess heat for an overdamped system are given respectively by

$$Q_{hk} = \gamma \int dt \dot{x} v_{ss}; \quad Q_{ex} = -k_B T \int dt \dot{x} \frac{\partial \phi}{\partial x}. \quad (1.35)$$

The local velocity v_{ss} is obtained by dividing the steady-state probability current j_{ss} (obtained from the corresponding Fokker-Planck equation [48]) by the steady-state probability density $\rho_{ss}(x, \lambda)$ [47]:

$$v_{ss} \equiv \frac{j_{ss}}{\rho_{ss}(x, \lambda)}. \quad (1.36)$$

We define the total change in the effective potential to be $\Delta \phi = \phi(x_\tau; \lambda_\tau) - \phi(x_0; \lambda_0)$, when the process is being carried out from time $t = 0$ to $t = \tau$. The Hatano-Sasa fluctuation relation for the excess heat is given by

$$\langle e^{-\beta Q_{ex} - \Delta \phi} \rangle = 1. \quad (1.37)$$

The application of the Jensen's inequality to the above relation gives the modified second law, eq. (1.34), provided the system is allowed to relax to the corresponding steady state at the final

value of the protocol, so that $\Delta s = \Delta\phi = -\ln \frac{\rho_{ss}(x;\lambda(t))}{\rho_{ss}(x_0;\lambda(0))}$. The adiabatic entropy is defined in terms of Q_{hk} as

$$\Delta s_a = \frac{Q_{hk}}{T}. \quad (1.38)$$

The nonadiabatic entropy is given by

$$\Delta s_{na} = \frac{Q_{ex}}{T} + \Delta\phi = k_B T \int dt \dot{\lambda} \frac{\partial\phi}{\partial\lambda}. \quad (1.39)$$

The quantity Δs_{na} is called the nonadiabatic entropy, because $\langle \dot{s}_{na} \rangle$ vanishes for a system undergoing an adiabatic transition between two steady states [47,49]. In an adiabatic transition, the system remains in the steady state corresponding to the instantaneous parameter value, when the parameter is changed slowly enough during the process. The total entropy can then be written as

$$\Delta s_{tot} = \Delta s_m + \Delta s = \Delta s_a + \Delta s_{na}. \quad (1.40)$$

1.5 The dual trajectory formalism

Let us consider an overdamped system in a nonequilibrium steady state (the analysis for underdamped systems can be found in [50]). In this case, the detailed balance condition does not hold, but there exists a counterpart to this condition, which also involves the transition probabilities in the so-called *dual dynamics* [47,49,51,52] (denoted by the symbol \dagger):

$$\rho_{ss}(x_i; \lambda_i) p(x_{i+1}|x_i; \lambda_i) = \rho_{ss}(x_{i+1}; \lambda_i) p^\dagger(x_i|x_{i+1}; \lambda_i). \quad (1.41)$$

Here, $p(x_{i+1}|x_i; \lambda_i)$ is the transition probability of the system from state x_i to state x_{i+1} when the value of the external protocol is λ_i during this transition. Similarly, $p^\dagger(x_i|x_{i+1}; \lambda_i)$ is the transition probability of the system from state x_{i+1} to state x_i when the value of the external protocol is λ_i , in the dual dynamics.

Under the dual dynamics, if the system is allowed to relax to a steady state with a fixed

value of λ , then one would find that the functional form of the steady state density remains the same as in the original dynamics, while the probability current changes sign [51, 52]. For a system at equilibrium, the dual transition probabilities are simply the same as those in the original dynamics.

One can now obtain an elegant expression for the excess heat [47, 51]:

$$\beta Q_{ex} = \ln \prod_{i=1}^{N-1} \frac{p(x_{i+1}|x_i; \lambda_i)}{p^\dagger(x_i|x_{i+1}; \lambda_i)} \equiv \ln \frac{P[X|x_0]}{\tilde{P}^\dagger[\tilde{X}|x_\tau]}. \quad (1.42)$$

Note that the denominator consists of path probability densities obtained after switching over to the dual dynamics and thereafter applying the time-reversed protocol.

In a similar way, the housekeeping heat can be shown to be given by [51]

$$\beta Q_{hk} = \ln \prod_{i=1}^{N-1} \frac{p(x_{i+1}|x_i; \lambda_i)}{p^\dagger(x_{i+1}|x_i; \lambda_i)} \equiv \ln \frac{P[X|x_0]}{P^\dagger[X|x_0]} = \ln \frac{P[X]}{P^\dagger[X]}. \quad (1.43)$$

Here we have the same forward trajectory both in the numerator as well as in the denominator, weighted in two different dynamics. The last step follows from the fact that the initial distribution, $\rho_{ss}(x_0)$, is the same for both the processes. More detailed derivations of the above relations are given in appendix B.

1.6 Stochastic resonance

The phenomenon of stochastic resonance (SR) [53] was first introduced by Robert Benzi in his seminal paper [54] in 1981, where he had pointed out that the frequency of occurrence of ice ages on earth can be explained using this phenomenon.

The usual mechanical resonance is the property of a system to absorb a large energy from an external periodic force, when the frequency of this force equals the natural frequency of the system. An example is a swing, which after reaching a highest point has got all its kinetic energy converted to potential energy, and then begins the process of transferring potential to kinetic energy. Now suppose that this transfer of energies is boosted by applying a push at this

highest point in the appropriate direction. Intuition correctly tells us that this will cause the swing to reach a higher point on the opposite side. If this external driving continues, then the amplitude will become higher and higher, thus causing the swing to resonate mechanically.

The phenomenon of SR is different from mechanical resonance in the sense that it depends on the presence of a noisy (thermal noise in our case) environment. The system is considered to be a two-state one, whose “natural frequency” is the (average) frequency with which it can cross the energy barrier and switch its state. A simple model to see this is the double-well potential $V(x)$ in which the system is confined and is kept in contact with a thermal bath at temperature T . If a feeble periodic signal is applied to this potential, it will alternately rock the left and the right wells in every cycle. We will consider the barrier height ΔV in-between the wells to be high enough to stop the particle from moving from one well to another in absence of thermal noise. This is known as *subthreshold* driving. The barrier crossing rate (Kramers escape rate) for the particle in the unperturbed well will be given by [48]

$$r_K = \left(\frac{\gamma \sqrt{V''(x_{min}) \cdot |V''(x_{max})|}}{2\pi} \right) e^{-\beta \Delta V}. \quad (1.44)$$

Here, the double primed symbol implies double derivative with respect to x , $\pm x_{min}$ are the positions of the minima of the potential, x_{max} is the position of the potential maximum in-between the two minima, and γ is the friction coefficient. Figure 1.3 shows a typical bistable potential.

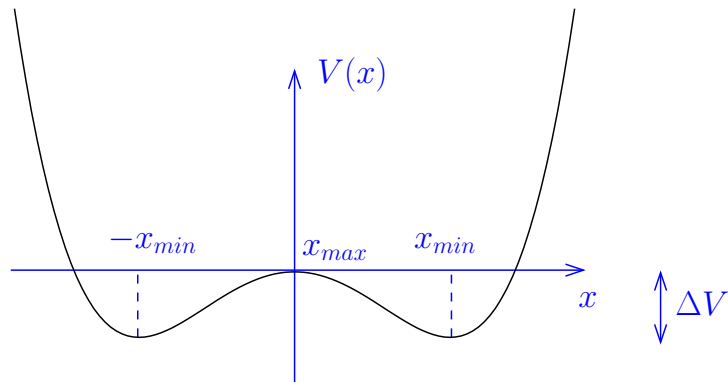


Figure 1.3: A typical bistable potential showing the positions of $\pm x_{min}$ and x_{max} , and the barrier height ΔV .

We would consider a particle following the overdamped Langevin equation, eq. (1.10). Let us suppose that the (feeble) input signal is of the form $f(t) = A \sin \omega t$. It has a half time period $\tau_\omega/2 = \pi/\omega$, which is in general different from the escape time $1/r_K$. By tuning either the bath temperature at a fixed frequency of the signal, or by keeping the former fixed and tuning the latter, the SR condition ($r_K = \frac{\pi}{\omega}$) can be satisfied. Under this condition, the synchronization between the particle hopping and external drive is illustrated in figure 1.4. In

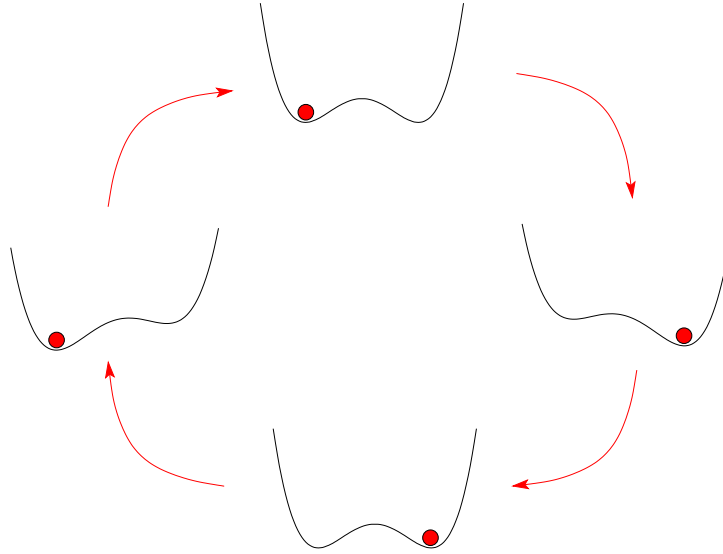


Figure 1.4: Schematic diagram for synchronization of particle hopping with the drive frequency at stochastic resonance.

such a situation, we find that almost every time the right well becomes lower, the particle hops into it and vice versa. How to quantify resonance has been an issue of a long-standing debate. It has been recently found that the absorbed input energy (or work done on the system) may be the appropriate quantifier [55].

1.7 Plan of the thesis

The plan of the thesis is as follows. In **chapter two**, the total entropy production fluctuations are studied in some exactly solvable models. For these systems, the detailed fluctuation theorem holds even in the transient state, provided initially that the system is prepared in thermal equilibrium. The nature of entropy production during the relaxation of a system to equilibrium

is analyzed. The averaged entropy production over a finite time interval gives a better bound for the average work performed on the system than that obtained from the well-known Jarzynski equality. Moreover, the average entropy production as a quantifier for information theoretic nature of irreversibility for finite time nonequilibrium processes is discussed.

In **chapter three**, we rederive the fluctuation theorems in the presence of feedback by assuming the known Jarzynski equality and detailed fluctuation theorems. We find that both the classical and quantum systems can be analyzed using a similar treatment in terms of state space trajectories. First, we briefly reproduce the already known work theorems for a classical system in order to show its equivalence with the quantum treatment. We then extend the treatment to arrive at new results, namely the generalizations of Seifert's entropy production theorem and the Hatano-Sasa fluctuation theorem, in the presence of feedback. We have also derived the extended version of the Tasaki-Crooks fluctuation theorem for a quantum particle in the presence of multiple loop feedback. For deriving the extended quantum fluctuation theorems, we have considered open systems. No assumption is made on the nature of environment and the strength of system-bath coupling. However, it is assumed that the measurement process involves classical errors.

In **chapter four**, we turn our attention to the *efficacy parameter* that quantifies how efficient a given feedback algorithm is. In presence of feedback, the forms of the conventional fluctuation theorems get modified. The modified form involves correction terms that depend on the rules of using feedback in order to generate the exact time-reversed/conjugate protocols. We show that this can be done in a large number of ways, and in each case we would get a different expression for the correction term. This would in turn lead to several lower bounds on the mean work performed on the system, or on the entropy changes. Here we analyze a form of the extended fluctuation theorems involving the efficacy parameter, and find that this form gives rise to a lower bound for the mean work that retains a consistent physical meaning regardless of the design of feedback along the conjugate process. This is opposed to the case of the usual form of the modified fluctuation theorems, that is found in literature.

In **chapter five**, we analyze the other important phenomenon that takes place in nature under

the influence of noise, namely stochastic resonance. We investigate the total entropy production of a Brownian particle in a driven bistable system. This system exhibits the phenomenon of stochastic resonance. We show that in the time-periodic steady state, the probability density function for the total entropy production satisfies Seifert's integral and detailed fluctuation theorems over finite time trajectories.

In **chapter six**, we study the fluctuations of work done and dissipated heat of a Brownian particle in a symmetric double well system. The system is driven by two periodic input signals that rock the potential simultaneously. Confinement in one preferred well can be achieved by modulating the relative phase between the drives. We show that in the presence of pumping the stochastic resonance signal is enhanced when analyzed in terms of the average work done on the system per cycle. This is in contrast to the case when pumping is achieved by applying an external static bias, which degrades the resonance. We analyze the nature of work and heat fluctuations and show that the steady state fluctuation theorem holds in this system.

Chapter seven concludes the thesis by briefly summarizing the results obtained in the previous chapters.

Chapter 2

Entropy production theorems and some consequences

2.1 Introduction

In the field of nonequilibrium thermodynamics of small systems, the fluctuation theorems (FTs) [4, 27–43] provide exact equalities valid in a system driven out of equilibrium, independent of the nature of driving. FTs make quantitative predictions for observing events that violate the second law within a short time for small systems by comparing the probabilities of entropy generating trajectories to those of entropy annihilating trajectories. They play an important role in allowing us to obtain results generalizing Onsager Reciprocity relations to the nonlinear response coefficients in nonequilibrium state [56].

The total entropy production is shown to obey the integral fluctuation theorem (IFT) [28, 29] for any initial condition and drive, over an arbitrary finite time interval, i.e., transient case (see last chapter). In [28, 29], it is also shown that in the nonequilibrium steady state over a finite time interval, a stronger fluctuation theorem, namely the detailed fluctuation theorem (DFT) holds. Originally DFT was found in simulations of two-dimensional sheared fluids [30] for entropy production in the medium in the steady state, but in the long-time limit. This was proved in various contexts, e.g. (i) using chaotic hypothesis by Gallavotti and Cohen [32], (ii)

using stochastic dynamics by Kurchan [43] as well as by Lebowitz and Spohn [57], and (iii) for Hamiltonian systems by Jarzynski [58].

In this chapter, we obtain the total entropy production (Δs_{tot}) distribution function, $P(\Delta s_{tot})$, for different classes of solvable models [59]. In particular, we consider (i) a Brownian particle in a harmonic trap subjected to an external time-dependent force, and (ii) a Brownian particle in a harmonic trap, the centre of which is dragged with an arbitrary time-dependent protocol.

In these models, we show that the DFT is valid *even in the transient case*, provided the initial distribution of the state variable is a canonical one. If the initial distribution is other than canonical, DFT in transient case does not hold, as expected. To illustrate this, we have analyzed the total entropy production for a system initially prepared in nonequilibrium state which relaxes to equilibrium. Finally we briefly discuss the important consequences of entropy production fluctuation theorem, namely, (i) it gives a new bound for the average work done during a nonequilibrium process over a finite time, generalizing the earlier known concept of free energy to a time-dependent nonequilibrium state. This bound is shown to be better than that obtained from the Jarzynski equality; (ii) average total entropy production over a finite time quantifies irreversibility in an information theoretic framework via the concept of relative entropy. This is distinct from the recently studied measure [60–64].

2.2 The model

2.2.1 Case I: A particle in a harmonic trap subjected to an external time-dependent force

We consider a Brownian particle in a harmonic potential and in contact with a heat bath at temperature T . The system is then subjected to a general driving force $f(t)$. The potential is given by $V_0(x) = \frac{1}{2}kx^2$. The particle dynamics is governed by the Langevin equation in the overdamped limit:

$$\gamma\dot{x} = -kx + f(t) + \xi(t), \quad (2.1)$$

where γ is the friction coefficient, k is the spring constant and $\xi(t)$ is the Gaussian white noise with the properties $\langle \xi(t) \rangle = 0$ and $\langle \xi(t)\xi(t') \rangle = 2T\gamma\delta(t - t')$. The magnitude of the strength of white noise ensures that the system reaches equilibrium in the absence of time-dependent fields.

Such a system can be experimentally realized by using a colloidal particle in a laser trap. The setup is similar to the one used in [16, 65], where the authors had modulated a bistable potential sinusoidally. In the present case, to modulate the trap, the trap position as well as the intensity of the laser have to be varied simultaneously. The former adjustment changes the position of the potential, while the latter changes its depth. A superposition of these two modulations, carried out in an appropriate manner, can reproduce the action of an arbitrary force on the bare potential.

Using the method of stochastic energetics (or the energy balance) [23, 66], the values of physical quantities such as injected work or thermodynamic work (W), change in internal energy (ΔU) and heat (Q) dissipated to the bath can be calculated for a given stochastic trajectory $X(t)$ over a finite time duration t . Using the expression for the internal energy $U(x, t) = \frac{1}{2}kx^2 - xf(t)$, we get (see chapter 1, sect. 1.1)

$$W = \int_0^t \frac{\partial U(x, t')}{\partial t'} dt' = - \int_0^t x(t') \dot{f}(t') dt', \quad (2.2a)$$

$$\Delta U = U(x(t), t) - U(x_0, 0) = \frac{1}{2}kx^2 - xf(t) - \frac{1}{2}kx_0^2, \quad (2.2b)$$

and

$$Q = - \int \frac{\partial U(x, t')}{\partial x} \dot{x}(t') dt' = \int (-kx(t') + f(t')) \dot{x}(t') dt'. \quad (2.2c)$$

Also, from the first law of thermodynamics, we have

$$Q = W - \Delta U. \quad (2.2d)$$

The particle trajectory extends from initial time $t = 0$ to final time t , x_0 in equation (2.2b) is the initial position of the particle. For simplicity, we have assumed that $f(0) = 0$.

Initially the system is prepared in thermal equilibrium. The distribution function is given by

$$p_0(x_0) = \sqrt{\frac{k}{2\pi T}} \exp\left(-\frac{kx_0^2}{2T}\right). \quad (2.3)$$

The Boltzmann constant k_B has been absorbed in T . The evolved distribution function $p_1(x, t)$, subjected to the initial condition $p_0(x_0)$, is obtained by solving the corresponding Fokker Planck equation, and is given by

$$p_1(x, t) = \sqrt{\frac{k}{2\pi T}} \exp\left(-\frac{k(x - \langle x \rangle)^2}{2T}\right), \quad (2.4)$$

where

$$\langle x \rangle = \frac{1}{\gamma} \int_0^t e^{-k(t-t')/\gamma} f(t') dt'. \quad (2.5)$$

A change in the medium entropy (Δs_m) over a time interval is given by

$$\Delta s_m = \frac{Q}{T}. \quad (2.6)$$

We now use the definition for the realization dependent entropy $s(t)$ of the particle [28, 29], namely $s(t) = -\ln p(x(t), t)$. We then get the change in system entropy for any trajectory of duration t as (see chapter 1, sect. 1.2)

$$\Delta s = -\ln \left[\frac{p_1(x, t)}{p_0(x_0)} \right], \quad (2.7)$$

where $p_0(x_0)$ and $p_1(x, t)$ are the probability densities of the particle positions at initial time $t = 0$ and final time t respectively. Thus for a given trajectory $x(t)$, the system entropy $s(t)$ depends on the initial probability density and hence contains the information about the whole ensemble. The total entropy change over time duration t is given by

$$\Delta s_{tot} = \Delta s_m + \Delta s. \quad (2.8)$$

Using the above definition of total entropy production, Seifert [28, 29] has derived the IFT, i.e.,

$$\langle e^{-\Delta s_{tot}} \rangle = 1, \quad (2.9)$$

where angular brackets denote average over the statistical ensemble of realizations, or over the ensemble of finite time trajectories.

In nonequilibrium steady state, where the system is characterized by time-independent stationary distribution, a stronger fluctuation theorem (DFT) valid over arbitrary finite time interval holds [28, 29]:

$$\frac{P(\Delta s_{tot})}{P(-\Delta s_{tot})} = e^{\Delta s_{tot}}. \quad (2.10)$$

The above theorem holds even under more general situation, i.e. when system is subjected to periodic driving: $f(x, \tau) = f(x, \tau + \tau_p)$, where τ_p is the period. The additional requirement is that the system has to settle into a time-periodic state: $P(x, \tau) = P(x, \tau + \tau_p)$, and trajectory length t is an integral multiple of τ_p .

As a side remark, we would like to state that if the distribution $P(\Delta s_{tot})$ is a Gaussian and satisfies IFT, then it naturally satisfies DFT, even if system is in a transient state. This happens to be the case in our present problem only under the condition that the system is being prepared initially in equilibrium, as shown below.

Using (2.2d), (2.6), (2.7) and (2.8), the total entropy becomes

$$\Delta s_{tot} = \frac{W - \Delta U}{T} - \ln \frac{p_1(x, t)}{p_0(x_0)}. \quad (2.11)$$

Substituting for ΔU from equation (2.2b), and using (2.3) and (2.4), we get

$$\Delta s_{tot} = \frac{1}{T} \left(W + \frac{1}{2} k \langle x \rangle^2 + x f(t) - k x \langle x \rangle \right). \quad (2.12)$$

The work W is a linear functional of $x(t)$, and from the above equation, we observe that Δs_{tot} is linear in x , while x is itself a linear functional of Gaussian random variable $\xi(t)$:

$$x(t) = x_0 e^{-kt/\gamma} + \frac{1}{\gamma} \int_0^t e^{-k(t-t')/\gamma} [f(t') + \xi(t')] dt'. \quad (2.13)$$

From the above fact it follows that $P(\Delta_{S_{tot}})$ is a Gaussian function. It is therefore sufficient to calculate the mean ($\langle \Delta_{S_{tot}} \rangle$) and variance ($\sigma^2 \equiv \langle \Delta_{S_{tot}}^2 \rangle - \langle \Delta_{S_{tot}} \rangle^2$) to get the distribution, which is of the form

$$P(\Delta_{S_{tot}}) = \frac{1}{\sqrt{2\pi\sigma^2}} \exp\left(-\frac{(\Delta_{S_{tot}} - \langle \Delta_{S_{tot}} \rangle)^2}{2\sigma^2}\right), \quad (2.14)$$

where

$$\langle \Delta_{S_{tot}} \rangle = \frac{1}{T} \left(\langle W \rangle - \frac{1}{2} k \langle x \rangle^2 + \langle x \rangle f \right). \quad (2.15)$$

The formal expression of $\langle W \rangle$ is given by

$$\langle W \rangle = - \int_0^t \langle x(t') \rangle \dot{f}(t') dt \quad (2.16)$$

where $\langle x \rangle$ is given by (2.5). The variance σ^2 for total entropy is given by

$$\begin{aligned} \sigma^2 &= \frac{1}{T} \left(\frac{\langle W^2 \rangle - \langle W \rangle^2}{T} + \frac{f^2(t)}{k} + k \langle x \rangle^2 - 2 \langle x \rangle f(t) \right) \\ &\quad + \frac{1}{T^2} (\langle Wx \rangle - \langle W \rangle \langle x \rangle) (2f(t) - 2k \langle x \rangle) \end{aligned} \quad (2.17a)$$

$$\begin{aligned} &= \frac{1}{T} \left(2 \langle W \rangle + \frac{2f^2(t)}{k} + k \langle x \rangle^2 - 2 \langle x \rangle f(t) \right) \\ &\quad + \frac{1}{T^2} (\langle Wx \rangle - \langle W \rangle \langle x \rangle) (2f(t) - 2k \langle x \rangle). \end{aligned} \quad (2.17b)$$

To arrive at (2.17b), we have used the fact that $\langle W^2 \rangle - \langle W \rangle^2 = 2T \left(\langle W \rangle + \frac{f^2(t)}{2k} \right)$ which has been proved in appendix C. Also in the same appendix, we have shown that the cross-correlation is given by

$$\langle Wx \rangle - \langle W \rangle \langle x \rangle = \frac{T}{k} [k \langle x(t) \rangle - f(t)]. \quad (2.18)$$

Using equation (2.18) in (2.17b), it follows that

$$\sigma^2 = 2\langle\Delta_{S_{tot}}\rangle. \quad (2.19)$$

The Gaussian distribution of $P(\Delta_{S_{tot}})$ along with the above obtained condition for variance implies validity of the detailed fluctuation theorem for general protocol $f(t)$. Needless to say, this theorem in the considered linear system is valid in the transient case *only when* the initial distribution for the state variable is a canonical distribution. Further, DFT also implies IFT (but the converse is not true).

Special case: sinusoidal perturbation

For this case, we consider $f(t)$ to be a sinusoidal oscillating drive, i.e., $f(t) = A \sin \omega t$.

Using equation (2.15), we then obtain

$$\begin{aligned} \langle\Delta_{S_{tot}}\rangle &= \frac{1}{T} \left[\langle W \rangle - \frac{1}{2} k \langle x \rangle^2 + A \langle x \rangle \sin \omega t \right] \\ &= \frac{A^2 \gamma \omega}{4T(k^2 + \gamma^2 \omega^2)} \left[2\omega \{ k^2 t + (-2 - e^{-2kt/\gamma}) k \gamma + t \gamma^2 \omega^2 \} \right. \\ &\quad \left. + 8e^{-kt/\gamma} k \gamma \omega \cos \omega t - 2k \gamma \omega \cos 2\omega t + (k^2 - \gamma^2 \omega^2) \sin 2\omega t \right]. \end{aligned} \quad (2.20)$$

The variance is $\sigma^2 = 2\langle\Delta_{S_{tot}}\rangle$, and distribution $P(\Delta_{S_{tot}})$ is Gaussian as mentioned earlier. For this case, if the initial distribution is not canonical, then $P(\Delta_{S_{tot}})$ is not a Gaussian. This is shown in figure 2.1 where we have plotted $P(\Delta_{S_{tot}})$ for the above protocol obtained numerically for various times as mentioned in the figure caption.

The initial distribution being a Gaussian with $p_0(x_0) = \sqrt{\frac{k}{2\pi\sigma_x^2}} \exp\left(-\frac{kx_0^2}{2\sigma_x^2}\right)$, where the condition $\sigma_x^2 \neq T$, represents an athermal distribution. In the inset, we have plotted $P(\Delta_{S_{tot}})$ for same parameters used for the main figure for thermal initial distribution: $\sigma_x^2 = T = 0.1$ (for this case, distributions for $\Delta_{S_{tot}}$ are Gaussian). All quantities are in dimensionless units and values of physical parameters are mentioned in figure caption. We clearly notice that the

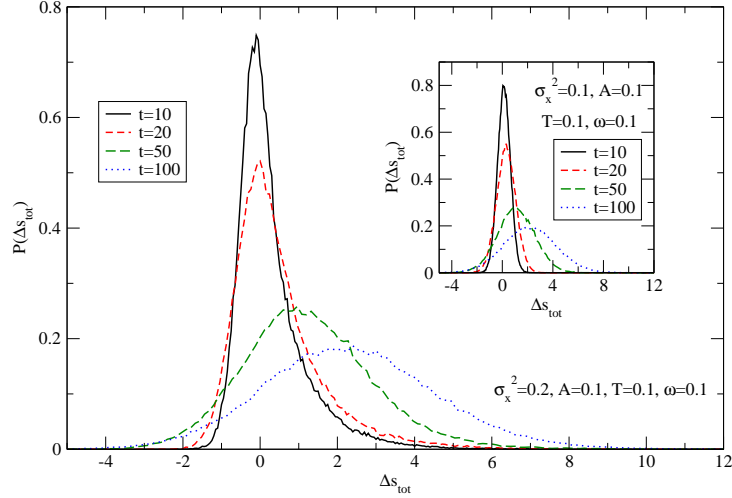


Figure 2.1: In the figure, we have plotted $P(\Delta s_{tot})$ vs Δs_{tot} for various observation times, when the initial distribution is athermal ($\sigma_x^2 = 0.2$). For thermal distribution, $\sigma_x^2 = 0.1$. The observation times are $t = 10$ (solid line), $t = 20$ (dashed line), $t = 50$ (bigger dashed line) and $t = 100$ (dotted line). The inset shows total entropy distributions for same observation time values, when the the initial distribution is thermal. For this case, all distributions are Gaussian. For both cases, $A = 0.1$, $k = 0.1$ and $\omega = 0.1$.

distributions $P(\Delta s_{tot})$ in the main figure are non-Gaussian. The observed values of $\langle e^{-\Delta s_{tot}} \rangle$ from our simulation equal 1.005, 1.006, 0.995 and 1.011 for $t = 10, 20, 50$ and 100 respectively in the athermal case. All these values are close to unity within our numerical accuracy, clearly validating IFT. For numerical simulations, we have used Heun's scheme. This gives a global error in the dynamics of the order of h^2 , where h is the time step taken in the simulation (for details, refer to [67]). To minimize the error in calculating $\langle e^{-\Delta s_{tot}} \rangle$, we have taken large number of realizations (more than 10^5), depending on parameters. Our estimated error bars are found to be around 10^{-4} . Moreover, these values act as a check on our numerical simulations [59, 68–70]. As the observation time of trajectory increases, weight on the negative side of $P(\Delta s_{tot})$ decreases, i.e., the number of trajectories for which $\Delta s_{tot} < 0$ decreases (see figure 2.1). This is expected as we go to macroscopic scale in time. The distributions that were asymmetric at short time scales tend closer to being a Gaussian distribution with non-zero positive $\langle \Delta s_{tot} \rangle$. The central Gaussian region increases with the time of observation. The presence of non-Gaussian tails (large deviation functions associated with the probability of extreme events) at large values of Δs_{tot} becomes very difficult to detect numerically. However,

they are not ruled out. For large times, $\sigma^2 \approx 2\langle\Delta s_{tot}\rangle$, suggesting validity of DFT only in the time asymptotic regime. Similar observations have been made in regard to work and heat distributions for a driven Brownian particle [59, 68–71].

The Fourier transform of the distribution $P(\Delta s_{tot})$ can be obtained analytically for a given initial athermal Gaussian distribution of the particle position in presence of a drive. This can be obtained following exactly the same procedure of Zon et al [40] for heat fluctuations. However, later we consider a simpler case of a system relaxing to equilibrium in absence of protocol (case-III).

2.2.2 Case II: $P(\Delta s_{tot})$ for particle in a dragged harmonic oscillator

For this case, the effective potential $U(x, t)$ for the Brownian particle is given by

$$U(x, t) = \frac{1}{2}k \left(x - \frac{f(t)}{k} \right)^2. \quad (2.21)$$

The centre of the harmonic oscillator is moved with a time-dependent protocol $f(t)/k$. The special case of this model is when $f(t)/k = ut$ (centre of the oscillator is moved uniformly with velocity u). This model has been extensively studied both experimentally [72] and theoretically [39, 40, 73–75] in regard to analysis of Jarzynski non-equilibrium work relation [33] and related issues.

The expression for work is given by

$$W(t) \equiv \int_0^t \frac{\partial U}{\partial t'} dt' = - \int_0^t x(t') \dot{f}(t') dt' + \frac{f^2(t)}{2k}. \quad (2.22)$$

By taking canonical initial condition for $p_0(x_0)$, given in equation (2.3), the probability density at time t is given by

$$p_1(x, t) = \sqrt{\frac{k}{2\pi T}} \exp\left(-\frac{k(x - \langle x \rangle)^2}{2T}\right). \quad (2.23)$$

where

$$\langle x \rangle = \frac{1}{\gamma} \int_0^t e^{-k(t-t')/\gamma} f(t') dt'. \quad (2.24)$$

The change in internal energy during a time t is

$$\Delta U = \frac{1}{2}k \left(x - \frac{f(t)}{k} \right)^2 - \frac{1}{2}kx_0^2. \quad (2.25)$$

For simplicity, we have set $f(0) = 0$. The expression for $\Delta_{s_{tot}}$ reduces to

$$\Delta_{s_{tot}} = \frac{W}{T} - \frac{f^2}{2kT} + \frac{xf}{T} + \frac{k\langle x \rangle^2}{2T} - \frac{kx\langle x \rangle}{T}. \quad (2.26)$$

From equation (2.26), it follows that $P(\Delta_{s_{tot}})$ is a Gaussian. Carrying out exactly the similar analysis as before (i.e., for case I), after tedious but straightforward algebra, we finally obtain the expressions for mean and variance:

$$\langle \Delta_{s_{tot}} \rangle = \frac{\langle W \rangle}{T} - \frac{f^2}{2kT} - \frac{k\langle x \rangle^2}{2T} + \frac{f\langle x \rangle}{T} \quad (2.27)$$

and

$$\sigma^2 = \frac{2\langle W \rangle}{T} - \frac{f^2}{kT} - \frac{k\langle x \rangle^2}{T} + \frac{2f\langle x \rangle}{T} = 2\langle \Delta_{s_{tot}} \rangle, \quad (2.28)$$

where $\langle W \rangle = \int_0^t \langle x(t') \rangle \dot{f}(t') dt'$, and $\langle x \rangle$ is given in equation (2.24). The condition (2.28) along with $P(\Delta_{s_{tot}})$ being Gaussian implies validity of both DFT and IFT for $\Delta_{s_{tot}}$.

Special case: The dragging force is linear

We consider $\frac{f(t)}{k} = ut$, i.e., centre of the harmonic trap is being dragged uniformly with velocity u . To obtain $P(\Delta_{s_{tot}})$, we need the expression for $\langle \Delta_{s_{tot}} \rangle$ only:

$$\langle \Delta_{s_{tot}} \rangle = \frac{u^2\gamma t}{T} - \frac{u^2\gamma^2}{2kT} (1 - e^{-kt/\gamma}) (3 - e^{-kt/\gamma}). \quad (2.29)$$

The above expression can be shown to be positive for all times, as it must be.

2.2.3 Case III: Entropy production with athermal initial condition: a case study for a relaxation dynamics

In this subsection, we study a system relaxing towards equilibrium. If initially the system is prepared in a nonequilibrium state, then in absence of any time-dependent perturbation or protocol, it will relax to a unique equilibrium state. The statistics of total entropy production is analyzed. Our system consists of an overdamped Brownian particle in a harmonic oscillator ($V_0(x) = \frac{1}{2}kx^2$) and the temperature of the surrounding medium is T . The initial distribution of the particle is taken to be

$$p_0(x_0) = \sqrt{\frac{k}{2\pi\sigma_x^2}} \exp\left(-\frac{kx_0^2}{2\sigma_x^2}\right) \quad (2.30)$$

Note that when $\sigma_x^2 \neq T$, it represents athermal initial distribution. Since no protocol is being applied, the thermodynamic work done on the system is identically zero. As time progresses, the distribution evolves with probability density given by

$$p_1(x, t) = \sqrt{\frac{1}{2\pi\langle x^2 \rangle}} \exp\left(-\frac{x^2}{2\langle x^2 \rangle}\right), \quad (2.31)$$

where $\langle x^2(t) \rangle$ is the variance in x at time t , which is equal to $\langle x^2(t) \rangle = \frac{T}{k} + \frac{\sigma_x^2 - T}{k} e^{-2kt/\gamma}$. The distribution $P(x, t)$ relaxes to equilibrium distribution as time $t \rightarrow \infty$. Using equation (2.11), (2.30) and (2.31), we get

$$\Delta S_{tot} = -\frac{\Delta U}{T} - \frac{1}{2} \ln\left(\frac{\sigma_x^2}{k\langle x^2 \rangle}\right) - \left(-\frac{x^2}{2\langle x^2 \rangle} + \frac{kx_0^2}{2\sigma_x^2}\right).$$

Now, considering the fact that $\Delta U = \frac{1}{2}k(x^2 - x_0^2)$, we arrive at

$$\Delta S_{tot} = \frac{k}{2} \left(\frac{\sigma_x^2 - T}{T\sigma_x^2}\right) x_0^2 + \frac{1}{2} \left(\frac{T - k\langle x^2 \rangle}{T\langle x^2 \rangle}\right) x^2 - \frac{1}{2} \ln\left(\frac{\sigma_x^2}{k\langle x^2 \rangle}\right)$$

This can be written in a simplified form,

$$\Delta S_{tot} = \frac{1}{2}\alpha x_0^2 + \frac{1}{2}\beta x^2 + \kappa, \quad (2.32)$$

where $\alpha = k \left(\frac{\sigma_x^2 - T}{T\sigma_x^2} \right)$; $\beta = \left(\frac{T - k\langle x^2 \rangle}{T\langle x^2 \rangle} \right)$ and $\kappa = -\frac{1}{2} \ln \left(\frac{\sigma_x^2}{k\langle x^2 \rangle} \right)$.

The total entropy production is a quadratic function of x and x_0 and hence $P(\Delta S_{tot})$ is not Gaussian. To obtain $P(\Delta S_{tot})$, we have to know the joint distribution of x_0 and x , namely $P(x_0, x, t)$ which in our problem can be obtained readily and is given by

$$p(x_0, x, t) = \frac{1}{2\pi\sqrt{\det \mathbf{A}}} \exp[(\mathbf{a} - \langle \mathbf{a} \rangle)^\dagger \cdot \mathbf{A}^{-1} \cdot (\mathbf{a} - \langle \mathbf{a} \rangle)] \quad (2.33)$$

where

$$\mathbf{a} = \begin{pmatrix} x_0 \\ x \end{pmatrix}, \quad (2.34)$$

x_0 and x being respectively the initial and final positions of the particle. The matrix \mathbf{A} is defined through

$$\begin{aligned} \mathbf{A} &\equiv \langle (\mathbf{a} - \langle \mathbf{a} \rangle) \cdot (\mathbf{a} - \langle \mathbf{a} \rangle)^\dagger \rangle = \langle \mathbf{a} \cdot \mathbf{a}^\dagger \rangle \\ &= \left\langle \begin{pmatrix} x_0 \\ x \end{pmatrix} \begin{pmatrix} x_0 & x \end{pmatrix} \right\rangle = \begin{pmatrix} \langle x_0^2 \rangle & \langle x x_0 \rangle \\ \langle x x_0 \rangle & \langle x^2 \rangle \end{pmatrix} \\ &= \begin{pmatrix} \frac{\sigma_x^2}{k} & \frac{\sigma_x^2}{k} e^{-kt/\gamma} \\ \frac{\sigma_x^2}{k} e^{-kt/\gamma} & \frac{T}{k} + \left(\frac{\sigma_x^2 - T}{k} \right) e^{-2kt/\gamma} \end{pmatrix}. \end{aligned} \quad (2.35)$$

With the help of the distribution given in (2.33), one can write, using equation (2.32),

$$\begin{aligned} P(\Delta S_{tot}, t) &= \int_{-\infty}^{\infty} dx dx_0 P(x_0, x, t) \\ &\times \delta \left[\Delta S_{tot} - \left(\frac{\alpha}{2} x_0^2 + \frac{\beta}{2} x^2 + \kappa \right) \right]. \end{aligned} \quad (2.36)$$

The evaluation of $P(\Delta_{s_{tot}})$ is a difficult task. However, the Fourier transform $\hat{P}(R, t) \equiv \int e^{iR\Delta_{s_{tot}}} P(\Delta_{s_{tot}}) d\Delta_{s_{tot}}$ of $P(\Delta_{s_{tot}})$ can be obtained easily. To this end we can carry out the analysis similar to that for heat distribution in a driven harmonic oscillator by Zon et al [40].

Finally we get

$$\hat{P}(R, t) = \frac{e^{iR\kappa}}{\sqrt{\det(\mathbf{I} - i\mathbf{R}\mathbf{A}\mathbf{.B})}}. \quad (2.37)$$

The details of this derivation are given in appendix C.3. Substituting $R = i$ in the above equation, and we get $\hat{P}(R = i, t) = \langle e^{-\Delta_{s_{tot}}} \rangle = 1$, consistent with the IFT (see appendix C.3 for details). From equation (2.37), we also note that $\hat{P}(R, t) \neq \hat{P}(i - R, t)$, indicating that DFT is not valid for this linear problem in the presence of athermal initial distribution. From above equation, we can also obtain average entropy production given by

$$\begin{aligned} \langle \Delta_{s_{tot}} \rangle &= \frac{1}{i} \frac{\partial}{\partial R} \hat{P}(R, t) \Big|_{R=0} \\ &= \frac{\sigma_x^2 - T}{2T} (1 - e^{-2kt/\gamma}) - \frac{1}{2} \ln \left[\frac{\sigma_x^2}{T + e^{-2kt/\gamma}(\sigma_x^2 - T)} \right]. \end{aligned} \quad (2.38)$$

Similarly, higher moments can also be obtained with the use of this characteristic function. One can invert the characteristic function to obtain $P(\Delta_{s_{tot}})$ using integral tables. However, the expression is complicated and unilluminating. From the Fourier transform, it is obvious that $P(\Delta_{s_{tot}})$ is non-Gaussian.

In figure 2.2, we have plotted $P(\Delta_{s_{tot}})$ versus $\Delta_{s_{tot}}$ over a fixed time interval (see figure caption) for two different cases for which initial width of the distribution σ_x^2 equals 0.05 and 0.2. The temperature of the bath is 0.1. The distribution $P(\Delta_{s_{tot}})$ in both cases are asymmetric. For the case $\sigma_x^2 = 0.2$, the distribution is peaked around the negative value of $\Delta_{s_{tot}}$. However, it exhibits a long tail making sure that $\langle \Delta_{s_{tot}} \rangle$ is always positive. Since initial width of the distribution is larger than the thermal distribution, change in the entropy of the system during the relaxation process is negative and it dominates the total entropy production. Hence we obtain peak in $P(\Delta_{s_{tot}})$ in the negative side of $\Delta_{s_{tot}}$. For the case $\sigma_x^2 = 0.05$, change in the entropy of the system is positive. Hence peak in $P(\Delta_{s_{tot}})$ is in the positive region. In both

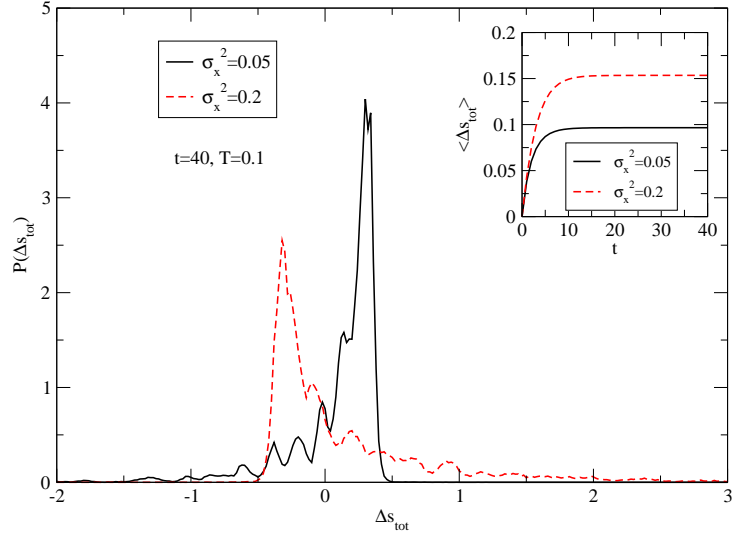


Figure 2.2: The figure shows plots of $P(\Delta s_{tot})$ vs Δs_{tot} during relaxation to equilibrium (external protocol is absent). The initial distributions are athermal with $\sigma_x^2 = 0.05$ (solid line) and $\sigma_x^2 = 0.2$ (dashed line). The spring constant is $k = 0.1$ and observation time was $t = 40$, by which the system has reached equilibrium (see inset). The inset shows plots average entropy versus observation time for the same initial distributions.

cases, we obtain $\langle e^{-\Delta s_{tot}} \rangle$ equal to unity within our numerical accuracy: 0.978 ($\sigma_x^2 = 0.2$) and 1.001 ($\sigma_x^2 = 0.05$), consistent with IFT. In the inset, we have plotted $\langle \Delta s_{tot} \rangle$ as a function of time for the above cases. $\langle \Delta s_{tot} \rangle$ is a monotonically increasing function of time and saturates asymptotically when equilibrium is reached. It may be noted that equilibrium is characterized by zero total entropy production, change in the entropy of bath at any instant being compensated by equal and opposite change in entropy of the system.

2.3 Some relations resulting from the average entropy production fluctuations over finite time

We now discuss some related offshoots of the total entropy production. These give a better bound for the average work done over a finite time and provide a different quantifier for the footprints of irreversibility. The Jarzynski non-equilibrium work relation [33] relates work done over a finite time in a non-equilibrium state to the equilibrium free energy differences,

namely,

$$\langle e^{-\beta W} \rangle = e^{-\beta \Delta F}. \quad (2.39)$$

Here the angular brackets denote an average over a statistical ensemble of realizations of a given thermodynamic process. The finite time thermodynamic process involves changing the time dependent thermodynamic parameter $\lambda(t)$ of the system from initial value $\lambda(0) = A$ to a final value $\lambda(\tau) = B$. $\lambda(t)$ can be an arbitrary function of time. Initially the system is prepared in equilibrium state corresponding to parameter A , and work W is evaluated over a time τ . At the end of the period τ , the system in general will not be at equilibrium corresponding to parameter B , yet from this non-equilibrium work, one can determine the difference in equilibrium free energies, ΔF , between the states described by A and B , using equation (2.39). From the same equation, using Jensen's inequality, it follows that

$$\langle W \rangle \geq \Delta F = F_B - F_A. \quad (2.40)$$

This result is consistent with the Clausius inequality, which is written in the form of work and energy, instead of the usual heat and entropy. Using Jensen's inequality and the integral fluctuation theorem of entropy production, namely equation (2.9), it follows that the average total entropy production over a time τ , $\langle \Delta s_{tot} \rangle \geq 0$. Using equation (2.2d), this can be rewritten as

$$\langle \Delta s_{tot} \rangle = \frac{1}{T} \langle W - \Delta U + T \Delta s \rangle \geq 0 \Rightarrow \langle W \rangle \geq \langle \Delta U - T \Delta s \rangle, \quad (2.41)$$

where ΔU and Δs are the changes in internal energy and in system entropy respectively. The time-dependent free energy in a nonequilibrium state can be defined as [76]:

$$F(x, t) = U(x, t) - T s(x, t) = U(x, t) + T \ln p(x, t), \quad (2.42)$$

which is in general a fluctuating quantity. Since free energy depends on entropy, it contains the information of the whole ensemble. In equilibrium, the expectation value of this free energy reduces to the Helmholtz free energy. Using (2.41) and the given definition of nonequilibrium

free energy described above, it follows that

$$\langle W \rangle \geq \langle \Delta F(\tau) \rangle, \quad (2.43)$$

where $\Delta F(\tau) = F_2(\tau) - F_1(0)$.

If initially the system is prepared in equilibrium with parameter A , F_1 equals equilibrium free energy F_A . $F_2(\tau)$ is determined by the probability distribution at the end point of the protocol at which the system is out of equilibrium with system parameter at $\lambda = B$, i.e. $F_2(\tau) \equiv U(x, \tau) + T \ln p_1(x, \tau)$. Now in the following, we show that

$$\langle \Delta F(\tau) \rangle \geq \Delta F = F_B - F_A, \quad (2.44)$$

thus giving a better bound for the average work done over a finite time. To this end, consider a situation at which initially the system is prepared in equilibrium with parameter $\lambda = A$ (corresponding to free energy F_A) and is allowed to evolve with the time-dependent protocol $\lambda(t)$ up to time τ at which $\lambda = B$. Beyond τ , the system is allowed to relax to equilibrium by keeping λ fixed at B . At the end of the entire process, the total change in equilibrium free energy equals $F_B - F_A$. The free energy being a state function, one can rewrite it as

$$\begin{aligned} F_B - F_A &= \langle F_B - F_2(\tau) + F_2(\tau) - F_A \rangle \\ &= F_B - \langle F_2(\tau) \rangle + \langle \Delta F(\tau) \rangle. \end{aligned} \quad (2.45)$$

Here, $\langle \Delta F(\tau) \rangle$ is the average change in the nonequilibrium free energy, $\langle F_2(\tau) \rangle - F_A$, during the process up to time τ , whereas $F_B - \langle F_2(\tau) \rangle$ is the change in the free energy during the relaxation period when the protocol is held fixed. One can readily show that [76] during the relaxation process towards equilibrium, the average (or expectation value) of free energy always decreases, i.e., $\langle F_B - F_2(\tau) \rangle$ is negative. From this and equation (2.45), it follows that $\langle \Delta F(\tau) \rangle \geq F_B - F_A$. Thus we get a better bound for the average work done than that obtained from the Jarzynski identity [33].

To illustrate this, in figure 2.3 we have plotted $\langle W \rangle$, $\langle \Delta F(\tau) \rangle$ and ΔF for a driven harmonic oscillator $U(x) = \frac{1}{2}kx^2$ with force $f(t) = A \sin \omega t$ as a function of the amplitude of driving A . For this graph, system parameter $f(t)$ changes from $f(0) = 0$ to $f(\tau) = A$ ($\Delta F = F_B - F_A = \frac{-A^2}{2k}$), i.e., for a time variation from $t = 0$ to $t = \tau = \frac{\pi}{2\omega}$. We observe from the figure that $\langle \Delta F(\tau) \rangle$ is indeed a better bound. The analytical results for this model are presented in appendices C.4 and C.5.

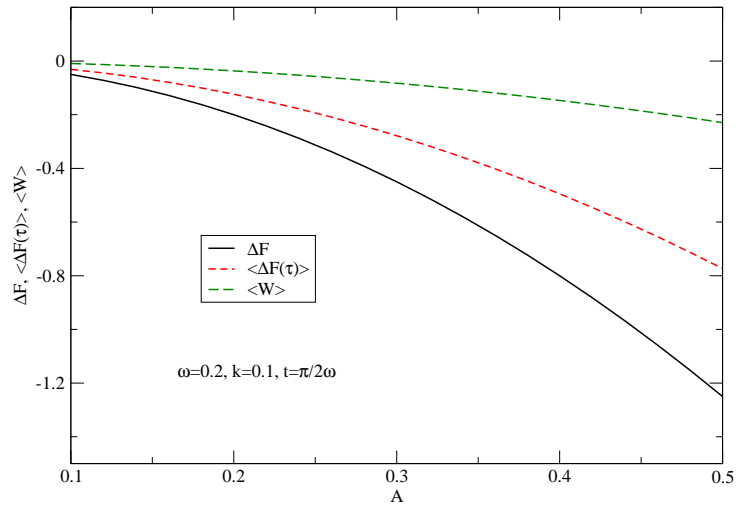


Figure 2.3: Plots for ΔF , $\langle \Delta F(\tau) \rangle$ and $\langle W \rangle$ as functions of the driving amplitude A , with the parameter values set at $\omega = 0.2$, $k = 0.1$ and $\tau = \pi/2\omega$.

Some remarks, however, are in order. The realizations for which $W < \Delta F$ need not correspond to $\Delta s_{tot} < 0$, and vice versa. This implies that the trajectories which violate the inequality $\Delta s_{tot} \geq 0$, do not necessarily violate the inequality $W \geq \Delta F$, although both the inequalities are closely related to the second law [77] that is valid on average. Equation (2.43) can be treated as a generalization of maximum work theorem¹ to nonequilibrium processes.

Dissipation is related to our ability to distinguish the arrow of time. Hence the dissipated work $\langle W_d \rangle = \langle W \rangle - \Delta F$ is recently identified as the measure of irreversibility. Moreover, it turns out that the relative entropy of microscopic trajectories $D_1(P||\tilde{P})$ in full path space between forward (P) and reverse (\tilde{P}) processes is indeed equal to dissipative work,

¹This theorem states that work extracted from a system is maximum for a reversible process. In our notation, since W is the work done *on* the system, the theorem implies that W is minimum for a reversible process.

$$\langle W_d \rangle = D_1(P||\tilde{P}). \quad (2.46)$$

Hence $D_1(P||\tilde{P})$ works as a measure of irreversibility or indistinguishability between forward and backward evolutions. Here, forward evolution corresponds to the system being prepared initially at equilibrium in the state with control parameter $\lambda(0) = A$ evolved up to time τ at which the control parameter is $\lambda(\tau) = B$. During the backward evolution, the system is prepared in equilibrium with control parameter B and the time-reversed protocol is applied from B to A . For details, see [60–63]. Separately, it can also be shown by using Crooks identity [42, 61].

$$\langle W_d \rangle = D(P(W)||\tilde{P}(-W)) \quad (2.47)$$

Here $D(P(W)||\tilde{P}(-W))$ is the relative entropy between the two probability distributions $P(W)$ and $\tilde{P}(-W)$ which are the work distributions for the same thermodynamic process for forward and backward evolutions respectively. This brings us to an important conclusion that dissipation can be revealed by any finite set of variables which contain information about the work or from the dynamics of those variables which couple to the control parameter λ . Thus one can identify few dynamical variables in which traces of the dissipation reside. This is unlike $D(P||\tilde{P})$, which requires information about entire set of microscopic system variables during their evolution.

We note that $\langle \Delta_{stot} \rangle$ can be taken as the measure of irreversibility as it also represents the relative probability $D_2(P||\tilde{P})$ between forward and time-reversed backward protocols [27–29]:

$$\langle \Delta_{stot} \rangle = D_2(P||\tilde{P}) = \int \mathcal{D}[X] p(x_0) P[X|x_0] \ln \left(\frac{p(x_0) P[X|x_0]}{p_1(\tilde{x}_\tau) \tilde{P}[\tilde{X}|\tilde{x}_\tau]} \right). \quad (2.48)$$

where $P[X|x_0]$ and $\tilde{P}[\tilde{X}|\tilde{x}_\tau]$ are the shorthand notations for the probabilities of traversing the entire forward path from $t = 0$ to $t = \tau$ described by $X(t)$ and that of traversing the reverse path described by $\tilde{X}(\tau - t)$. For details, see references [27–29]. Here, the forward evolution

corresponds to the system being prepared initially in any arbitrary state and evolved up to time τ along a prescribed protocol. At the end of the protocol, the system is in a state $p_1(x, \tau)$ determined by the initial condition and the dynamics. During the backward process, the system is assumed to be in the *same* state corresponding to the end point of forward evolution $p_1(x, \tau)$ and protocol is time-reversed, thereby evolving the system along the backward trajectory. Unlike for work (equation (2.47)), there is no Crooks'-like identity for the total entropy production between forward and reverse process (except in the stationary state). Hence it is not possible to describe the measure of irreversibility or dissipation in terms of the relative entropy between probability distribution of Δs_{tot} for forward and backward processes. Thus, the information of irreversibility is contained in all the microscopic variables associated with the system. This can also be noticed from the fact that the definition of total entropy production, involves the probability density of all the system variables. Moreover, this probability density contains the information about the initial and final ensembles of the system variables.

Identification of $\langle \Delta s_{tot} \rangle$ as a measure of irreversibility, is tantamount to identifying average dissipative work over a finite time process $\langle W - \Delta F(\tau) \rangle \equiv \langle W_d(\tau) \rangle$ as a measure of irreversibility, where $\langle \Delta F(\tau) \rangle$ is the nonequilibrium change in average free energy over a finite time as mentioned before. Needless to say, for this measure $\langle W_d(\tau) \rangle$, the system need not be in equilibrium at the beginning of the forward process which is a necessary condition for earlier defined measure for irreversibility [60–63].

2.4 Conclusion

In conclusion, we have shown that in a class of solvable linear models, Δs_{tot} satisfies DFT even in the transient regime provided the system is initially prepared in an equilibrium state. For athermal initial condition, the nature of total entropy production is analyzed during a relaxation process. The bound on average entropy production over a finite time process leads to a better bound for the average work done over the same finite time interval. Some points have been raised if one assigns meaning to the average entropy production as a measure of irreversibility.

This measure implies the generalization of Clausius' statement to nonequilibrium finite time processes, namely $\langle W_d(\tau) \rangle = \langle W - \Delta F(\tau) \rangle \geq 0$.

Chapter 3

Fluctuation theorems in presence of information gain and feedback

3.1 Introduction

One of the major breakthroughs in the field of fluctuation theorems has been the Jarzynski Equality [33], which has already been stated in the previous chapters. A direct outcome of this equality is the second law of thermodynamics, which states that the average work done on a system that is initially in equilibrium with a thermal reservoir, cannot be less than the change in free energy during the process: $\langle W \rangle \geq \Delta F$. A further generalization of the Jarzynski Equality is the Crooks' Work Theorem [42].

The above theorems are valid for what are known as *open-loop* feedback, i.e., when the protocol for the entire process is predetermined. In contrast, in a *closed-loop* feedback, a system observable is measured along the forward trajectory, and the protocol is changed depending on the outcomes of these measurements¹. These systems have recently attracted much interest, because they can enhance the efficiency of a process [21, 79, 82–89]. For such feedback-controlled systems, the fluctuation theorems need modifications so as to account for the infor-

¹Perhaps the simplest example of such a feedback driven process is the Szilard engine [78, 79], which consists of a single particle in a box, into which a movable partition is inserted. Now the position of the particle is measured, and depending on which side of the partition it is present, the partition is moved so as to extract work from the system. The AFM cantilever, is another example [81].

mation gained through measurement. Sagawa and Ueda have derived these extended relations for both the classical [82] and the quantum [21] cases. In the original papers, a single measurement (at some instant $t = t_m$) was considered. Subsequently, in a detailed review [83], the authors have derived the relations in the classical case, when multiple measurements are being performed.

In this work, we rederive the results for the classical systems, assuming the known fluctuation theorems in their integral as well as detailed form [84]. The same treatment goes through for deriving the generalized Hatano-Sasa identity, which provides equalities for a driven system from one steady state to another. We also extend the same treatment to the quantum case, and show that no matter how many intermediate projective measurements and subsequent feedbacks are performed, the extended Tasaki-Crooks fluctuation theorem remains unaffected. Although we have considered non-degenerate states for the quantum system, it is easy to extend the treatment to the degenerate case. The efficacy parameters for classical and quantum systems are also obtained.

3.2 The System

We have a Brownian particle that is initially prepared in canonical equilibrium with a heat bath at temperature T . Now, we apply an external drive $\lambda_0(t)$ from time $t_0 = 0$ up to $t = t_1$. At t_1 , we measure the state of the system and find it to be m_1 (see figure 3.1). Then, we modify our protocol from $\lambda_0(t)$ to $\lambda_{m_1}(t)$ and evolve the system up to time t_2 , where we perform a second measurement with outcome m_2 . Subsequently the protocol is changed to $\lambda_{m_2}(t)$, and so on up to the final form of the protocol $\lambda_{m_N}(t)$, which ends at $t = \tau$ (total time of observation). However, the time instants at which such measurements are taken need not be equispaced. We assume that there can be a measurement error with probability $p(m_k|x_k)$, where m_k is the measurement outcome at time t_k , when the system's actual state is x_k . Obviously, the value of ΔF will be different for different protocols.

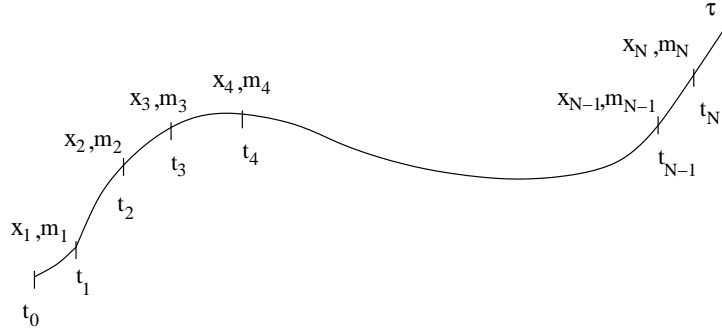


Figure 3.1: A typical phase space trajectory $x(t)$ vs t . The actual and the measured states at time t_k are x_k and m_k , respectively.

3.3 Rederivation of previous results

3.3.1 Extended Jarzynski equality

The results of this section have already been derived in [79]. The result for a single measurement has been derived in [82]. We briefly outline the derivation in a simpler way, assuming the already known fluctuation theorems in their integral as well as detailed forms. This would be helpful in bringing out the similarity between the classical and quantum approach. For a *given* set of observed values $M \equiv \{m_1, m_2, \dots, m_N\}$, which we would call the *measurement trajectory*, we have a given protocol $\Lambda_M(t) \equiv \{\lambda_0(t), \lambda_{m_1}(t), \lambda_{m_2}(t), \dots, \lambda_{m_N}(t)\}$. Here, the notation implies that the functional form of the protocol is $\lambda_0(t)$ from time $t = 0$ to $t = t_1$, then it is $\lambda_{m_1}(t)$ from $t = t_1$ to $t = t_2$, and so on, up to the final form $\lambda_{m_N}(t)$ from $t = t_N$ to $t = \tau$. This protocol depends on all the measured values $\{m_k\}$, as explained above². For such a given protocol, the Jarzynski Equality must be satisfied. The Jarzynski Equality, $\langle e^{-\beta(W-\Delta F)} \rangle = 1$, can be explicitly written as

$$\int \mathcal{D}[X] p_{eq}(x_0) P_{\Lambda_M}[X|x_0] \exp \{-\beta W[X, M] + \beta \Delta F(\lambda_{m_N}(\tau))\} = 1, \quad (3.1)$$

where $p_{eq}(x_0)$ is the equilibrium distribution of the system at the beginning of the protocol, $P_{\Lambda_M}[X|x_0]$ is the path probability for this fixed protocol, and the work W is a functional of the

²In other words, we assume that the measurement trajectory M is in one-to-one correspondence with the functional form of the full protocol, namely $\Lambda_M(t)$.

path. $\mathcal{D}[X]$ is a measure for the functional integral over all possible phase space trajectories. Since we are initially beginning with a predetermined protocol $\lambda_0(t)$, the value of ΔF depends only on the value of the protocol at the final time, i.e., on $\lambda_{m_N}(\tau)$.

Now we average over all possible protocols (i.e., over all possible measurement trajectories), and readily arrive at

$$\int \mathcal{D}[M] P[M] \int \mathcal{D}[X] p_{eq}(x_0) P_{\Lambda_M}[X|x_0] \exp \{-\beta W[X, M] + \beta \Delta F(\lambda_{m_N}(\tau))\} = 1. \quad (3.2)$$

Here, $D[M] \equiv dm_1 dm_2 \cdots dm_N$, and $P[M]$ is the joint probability of a set of measured values. The *mutual information*, which would soon appear in our derivation, is defined as [79]

$$I \equiv \ln \left[\frac{p(m_1|x_1) p(m_2|x_2) \cdots p(m_N|x_N)}{P[M]} \right]. \quad (3.3)$$

The mutual information essentially provides a measure of the information contained in the measurement outcomes about the actual values of the observables being measured, when the measuring device is in general subject to measurement errors.

The path probability $P_{\Lambda_M}[X]$ for a fixed protocol $\Lambda_M(t)$ (i.e., for a fixed measurement trajectory M) is given by

$$P_{\Lambda_M}[X] = p_{eq}(x_0) P_{\lambda_0}[x_0 \rightarrow x_1] P_{\lambda_{m_1}}[x_1 \rightarrow x_2] \cdots P_{\lambda_{m_N}}[x_N \rightarrow x_\tau]. \quad (3.4)$$

The notation $P_{\lambda_{m_k}}[x_k \rightarrow x_{k+1}]$ represents the probability of the path from x_k to x_{k+1} , under the protocol $\lambda_{m_k}(t)$.

The joint probability for obtaining a phase space trajectory X and the corresponding measurement trajectory M , in presence of feedback, will be given by

$$P[X, M] = p_{eq}(x_0) P_{\lambda_0}[x_0 \rightarrow x_1] p(m_1|x_1) P_{\lambda_{m_1}}[x_1 \rightarrow x_2] \\ \times p(m_2|x_2) P_{\lambda_{m_2}}[x_2 \rightarrow x_3] \cdots p(m_N|x_N) P_{\lambda_{m_N}}[x_N \rightarrow x_\tau].$$

$$= P_{\Lambda_M}[X] p(m_1|x_1) p(m_2|x_2) \cdots p(m_N|x_N), \quad (3.5)$$

on using eq. (3.4). Using eqs. (3.3) and (3.5), we have

$$P_{\Lambda_M}[X]P[M] = P[X, M]e^{-I}. \quad (3.6)$$

Using (3.6) in (3.2), and using the relation $P_{\Lambda_M}[X|x_0]p_{eq}(x_0) = P_{\Lambda_M}[X]$, we get

$$\begin{aligned} \int \mathcal{D}[X]\mathcal{D}[M] P[M]P_{\Lambda_M}[X] e^{-\beta(W-\Delta F)} &= 1 \\ \Rightarrow \int \mathcal{D}[X]\mathcal{D}[M] P[X, M] e^{-\beta(W-\Delta F)-I} &= 1. \end{aligned}$$

To keep the notations simple, the arguments of W , ΔF and I have been omitted. The above relation is then the generalized Jarzynski equality:

$$\langle e^{-\beta(W-\Delta F)-I} \rangle = 1. \quad (3.7)$$

The Jensen's inequality leads to the second law of thermodynamics which is generalized due to information gain, namely, $\langle W \rangle \geq \langle \Delta F \rangle - k_B T \langle I \rangle$. Since $\langle I \rangle \geq 0$ (being a relative entropy³) [80], work extracted from the system can be made more than that in the reversible case, even though the system is in contact with a single bath, by using feedback controlled drive.

3.3.2 Detailed Fluctuation Theorem

The probability of forward path is given by (3.5). To generate a reverse trajectory, we first select one of the measurement trajectories M (with probability $P[M]$), among all the possible measurement trajectories generated in the forward process. We then begin with the system

³This is clear from eq. (3.6). We find that

$$\langle I \rangle = \int \mathcal{D}[X]\mathcal{D}[M] P[X, M] \ln \frac{P[X, M]}{P_{\Lambda_M}[X]P[M]} = D(P[X, M] || P_{\Lambda_M}[X]P[M]),$$

$D(p(x)||q(x))$ being the relative entropy between the two probability densities $p(x)$ and $q(x)$.

being at canonical equilibrium at the final value of the forward protocol $\lambda_{m_N}(\tau)$, and *blindly* run the full forward protocol in reverse, i.e., $\Lambda_M(t) \rightarrow \tilde{\Lambda}_M(t) \equiv \Lambda_M(\tau - t)$. We will use the notation $\tilde{t} \equiv \tau - t$ to denote the time elapsed along the reverse process. The time-reversal of the forward protocol is shown in figure 3.2.

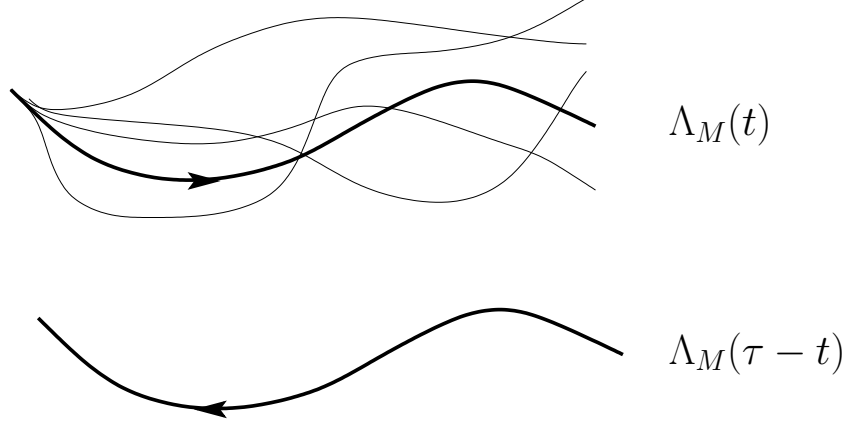


Figure 3.2: The figure at the top shows several protocols generated in the forward process, as a function of time. To generate the reverse process, we choose one of these protocols, say the bold one with functional form $\Lambda_M(t)$, and time reverse it, as shown in the lower figure.

It may be noted that, had we used feedback in the reverse process just as it had been used along the forward process, then in the time interval from \tilde{t}_{i+1} to \tilde{t}_i , we should have the protocol $\lambda_{m_i}(\tau - t)$, ending at time \tilde{t}_i where the measured outcome should be m_i . Since m_i is the *cause* and the protocol $\lambda_{m_i}(\tau - t)$ is its *effect*, the above procedure of implementing the protocol first and then measuring the outcome that determines it, would be an acausal one [79]. Thus, no feedback is performed during the reverse process in order to respect causality⁴.

In the present case, the probability of a reverse trajectory simply becomes

$$\tilde{P}[\tilde{X}; M] = P[M]P_{\tilde{\Lambda}_M}[\tilde{X}]. \quad (3.8)$$

$\tilde{P}[\tilde{X}; M]$ should not be confused with the joint probability $P_{\tilde{\Lambda}_M}[\tilde{X}, \tilde{M}]$, that we would use later (see eq. (3.12)). The former represents the probability of the reverse path with the particular protocol corresponding to the fixed measurement trajectory M , namely $P_{\tilde{\Lambda}_M}[\tilde{X}]$,

⁴In the next chapter, we will see that even the reverse process can be generated by using feedback, albeit by a different algorithm, without breaking the causality.

multiplied by the probability $P[M]$ of choosing this particular measurement trajectory. On the other hand, the latter represents the following: suppose we are using the reverse protocol $\tilde{\Lambda}_M(\tau - t)$ to generate the reverse process. Now we perform measurements along the reverse process as well, at the time instants $\tilde{t}_N, \tilde{t}_{N-1}$, and so on, up to \tilde{t}_1 . The joint probability of a trajectory \tilde{X} along with the measured outcomes \tilde{M} in this process, will be denoted by $P[\tilde{X}, \tilde{M}]$.

Now we take the ratio of eqs. (3.5) and (3.8), and use eq. (3.6) to get

$$\frac{P[X, M]}{\tilde{P}[\tilde{X}; M]} = \frac{P_{\Lambda_M}[X]P[M] e^I}{P_{\tilde{\Lambda}_M}[\tilde{X}]P[M]} = e^{\beta(W - \Delta F) + I}, \quad (3.9)$$

where we have used the known Crooks' work theorem (for a predetermined protocol) [27, 42],

$$\frac{P_{\Lambda_M}[X]}{P_{\tilde{\Lambda}_M}[\tilde{X}]} = e^{\beta(W - \Delta F)}. \quad (3.10)$$

Here, $P_{\tilde{\Lambda}_M}[\tilde{X}]$ is the probability density for the time-reversed phase space trajectory \tilde{X} under the time-reversed protocol $\tilde{\Lambda}_M$. Eq. (3.9) is the generalized Crooks theorem in the presence of feedback.

3.3.3 The generalized Jarzynski equality and the efficacy parameter

The Jarzynski equality can also be extended to a different form in the presence of information:

$$\langle e^{-\beta(W - \Delta F)} \rangle = \gamma, \quad (3.11)$$

where γ is the efficacy parameter [82, 83]. Note that the right hand side would be equal to one in absence of any feedback. The efficacy parameter γ defines how efficient our feedback control is. This is because if dissipated work along a process is less, then eq. (3.11) says that γ is more and hence the process is more efficient.

Following similar mathematical treatment as in the derivation of extended Jarzynski equal-

ity, and using the definition of dissipated work, $W_d = W - \Delta F$, we have

$$\begin{aligned}
\gamma &= \int \mathcal{D}[X] \mathcal{D}[M] P[X, M] e^{-\beta W_d[X, M]} \\
&= \int \mathcal{D}[X] \mathcal{D}[M] \tilde{P}[\tilde{X}; M] e^{I[X, M]} \\
&= \int \mathcal{D}[X] \mathcal{D}[M] P_{\tilde{\Lambda}_M}[\tilde{X}] p(m_0|x_0) p(m_1|x_1) \cdots p(m_N|x_N) \\
&= \int \mathcal{D}[X] \mathcal{D}[M] P_{\tilde{\Lambda}_M}[\tilde{X}] p(\tilde{m}_0|\tilde{x}_0) p(\tilde{m}_1|\tilde{x}_1) \cdots p(\tilde{m}_N|\tilde{x}_N) \\
&= \int \mathcal{D}[\tilde{X}] \mathcal{D}[M] P_{\tilde{\Lambda}_M}[\tilde{X}, \tilde{M}] = \int \mathcal{D}[M] P_{\tilde{\Lambda}_M}[\tilde{M}]. \tag{3.12}
\end{aligned}$$

In the second step we have used eq. (3.9), while in the third step the definition of $I[X, M]$ (eq. (3.3)) has been used. In the fourth step, the time-reversal symmetry of the measurements [82], i.e., the relation $p(\tilde{m}_k|\tilde{x}_k) = p(m_k|x_k)$, has been assumed. $P_{\tilde{\Lambda}_M}[\tilde{X}, \tilde{M}]$ is the joint probability of obtaining both the backward trajectory \tilde{X} and the set of measured outcomes \tilde{M} in the reverse process under the protocol $\tilde{\Lambda}_M$ (see the discussion below eq. (3.8)). Physically, this means that γ also describes the sum of the probabilities of observing time-reversed outcomes in the time-reversed protocols. Note that the integral over $P_{\tilde{\Lambda}_M}[\tilde{M}]$ is not equal to unity, because the reverse protocol $\tilde{\Lambda}_M$ is itself dependent on M , and hence the probability function depends on the forward measurements as well.

Experimental relevance: Some of the results in this section, including the computation of efficacy parameter, have recently been verified experimentally [92]. The setup consists of a dimeric particle pinned at a single point, undergoing rotational Brownian motion inside a buffer solution, and subjected to electric fields generated by quadrant electrodes. The particle essentially experiences a potential resembling a spiral staircase. Although it diffuses by jumping either upwards or downwards along the staircase, its downward jumps are more probable. The feedback is designed such that, whenever it jumps upwards, a barrier is introduced so as to block its subsequent downward jumps. This leads to a net increase in its free energy at the end of the process, which is more than the work done on the system.

3.4 Modification in Seifert's and Hatano-Sasa identities

Now we derive other identities which are straightforward generalizations of their earlier counterparts, in the presence of information. The mathematics involved is the same as in sections 3.3.1 and 3.3.2. For a predetermined protocol, if the probability distribution of the initial states for the forward path (denoted by $p_0(x_0)$) are arbitrary rather than being the Boltzmann distribution, and that of the reverse path is the final distribution of states (denoted by $p_\tau(x_\tau)$) attained in the forward process, we obtain the Seifert's theorem in lieu of the Jarzynski equality [28,29]:

$$\langle e^{-\Delta s_{tot}} \rangle = 1. \quad (3.13)$$

Here, $\Delta s_{tot} = \Delta s_m + \Delta s$ is the change in the total entropy of bath and system. The path-dependent medium entropy change is given by $\Delta s_m = Q/T$, where Q is the heat dissipated into the bath. Δs is the change in the system entropy given by $\Delta s = \ln[p_0(x_0)/p_\tau(x_\tau)]$. Eq. (3.13) can be explicitly written as (see the discussion before eq. (3.1))

$$\int \mathcal{D}[X] p_0(x_0) P_{\Lambda_M}[X|x_0] \exp \{-\Delta s_{tot}[X, M]\} = 1, \quad (3.14)$$

Averaging over different sets of protocols determined by the different measurement trajectories, we get

$$\int \mathcal{D}[M] P[M] \int \mathcal{D}[X] p_0(x_0) P_{\Lambda_M}[X|x_0] e^{-\Delta s_{tot}[X, M]} = 1. \quad (3.15)$$

Proceeding exactly in the same way as in section 3.3.1 (eqns. (3.2)–(3.7)), we readily get

$$\langle e^{-\Delta s_{tot} - I} \rangle = 1. \quad (3.16)$$

Eq. (3.16) is the generalization of the entropy production theorem and it gives the modified

second law in the presence of feedback:

$$\langle \Delta s_{tot} \rangle \geq -\langle I \rangle. \quad (3.17)$$

Thus with the help of information (feedback), the lower limit of change in average total entropy change can be made less than zero, by an amount given by the average mutual information gained.

The Hatano-Sasa identity [47] can also be similarly generalized:

$$\left\langle \exp \left[- \int_0^\tau dt \dot{\lambda} \frac{\partial \phi(x; \lambda)}{\partial \lambda} - I \right] \right\rangle = 1, \quad (3.18)$$

where $\phi(x; \lambda) \equiv -\ln \rho_{ss}(x; \lambda)$, the negative logarithm of the nonequilibrium steady state distribution corresponding to parameter value λ . The derivation (3.18) is simple and similar to the earlier derivations (see sections 3.3.1 and 3.3.2), and hence is not reproduced here.

In terms of the excess heat Q_{ex} , which is the heat dissipated in addition to the housekeeping heat, when the system moves from one steady state to another, the above equality (eq. (3.18)) can be rewritten in the following form (for details see [47]):

$$\langle \exp[-\beta Q_{ex} - \Delta \phi - I] \rangle = 1. \quad (3.19)$$

Using the Jensen's inequality, the generalized second law for transitions between nonequilibrium steady states follows, namely,

$$T \langle \Delta s \rangle \geq -\langle Q_{ex} \rangle - k_B T \langle I \rangle, \quad (3.20)$$

where Δs is the change in system entropy defined by $\Delta s \equiv -\ln \frac{\rho_{ss}(x, \lambda_\tau)}{\rho_{ss}(x, \lambda_0)} = \Delta \phi$.

3.5 Quantum case

Now we extend the above treatment to the case of a quantum open system. Hänggi et al. have shown [20] that for a closed quantum system, the fluctuation theorems remain unaffected even if projective measurements are performed in-between. This happens in spite of the fact that the probabilities of the forward and backward paths (by “path” we mean here a collection of the successive eigenstates to which the system collapses each time a projective measurement is performed) do change in general. Taking cue from this result, we proceed as follows. The supersystem consisting of the bath and the system evolve under the total Hamiltonian

$$H(t) = H_S(t) + H_{SB} + H_B. \quad (3.21)$$

The bath Hamiltonian H_B and the interaction Hamiltonian H_{SB} have been assumed to be time-independent, whereas the system Hamiltonian $H_S(t)$ depends explicitly on time through a time-dependent external drive $\lambda(t)$. We first prepare the supersystem at canonical equilibrium at temperature T . At initial time $t_0 = 0$, we measure the total Hamiltonian, and the collapsed eigenstate is $|k_0\rangle$. The notation means that the total system has collapsed to the k_0^{th} eigenstate (of the corresponding measured operator, which is $H(0)$ at $t = 0$) when measured at time $t = 0$. The supersystem consisting of the bath and the system is described by the density matrix

$$\rho(0) \equiv \frac{e^{-\beta H(0)}}{Y(0)} \Rightarrow \rho_{k_0 k_0} = \frac{e^{-\beta E_{k_0}}}{Y(0)}. \quad (3.22)$$

In the above relation, $\rho_{k_0 k_0}$ are the diagonal elements of the initial density matrix of the supersystem, and $Y(0)$ is the partition function for the entire supersystem:

$$Y(0) = \text{Tr} e^{-\beta H(0)}. \quad (3.23)$$

We then evolve the system up to time t_1 under a predetermined protocol $\lambda_0(t)$, and at t_1 we measure some observable M of the system. Let the outcome be m_1 , whereas the actual col-

lapsed state is $|k_1\rangle$ corresponding to eigenvalue M_{k_1} . This outcome is obtained with probability $p(m_1|k_1)$, which is an assumed classical error involved in the measurement. Now we introduce the feedback by modifying the original protocol to $\lambda_{m_1}(t)$, and then continue up to t_2 , where we perform the measurement to get outcome m_2 , the actual state being $|k_2\rangle$. Subsequently our protocol becomes $\lambda_{m_2}(t)$, and so on. Thus the probability of getting the set of eigenstates $K \equiv \{|k_0\rangle, |k_1\rangle, \dots, |k_\tau\rangle\}$ with the measurement trajectory $\{m_k\} \equiv M$ is given by

$$P[K, M] = \rho_{k_0 k_0} |\langle k_1 | U_{\lambda_0}(t_1, 0) | k_0 \rangle|^2 p(m_1 | k_1) |\langle k_2 | U_{\lambda_{m_1}}(t_2, t_1) | k_1 \rangle|^2 \dots p(m_N | k_N) |\langle k_\tau | U_{\lambda_{m_N}}(\tau, t_N) | k_N \rangle|^2. \quad (3.24)$$

Here, $U_{\lambda_{m_i}}(t_{i+1}, t_i)$ is the unitary evolution operator from time t_i to time t_{i+1} . The reverse process is generated by starting with the supersystem in canonical equilibrium with protocol value $\lambda_{m_N}(\tau)$, and blindly reversing one of the chosen protocols of the forward process. Now we need to perform measurements along the reverse process as well, simply to ensure that the state *does* collapse to specific eigenstates and we do obtain an unambiguous reverse trajectory in each experiment. However, in order to respect causality [79], we do not perform feedback using these measurements during the reverse process. The probability for a trajectory that starts from initial collapsed energy eigenstate $|k_\tau\rangle$ and follows the exact sequence of collapsed states as the forward process, is given by

$$\tilde{P}[\tilde{K}; M] = |\langle k_0 | \Theta^\dagger U_{\tilde{\lambda}_0}(\tilde{0}, \tilde{t}_1) \Theta | k_1 \rangle|^2 |\langle k_1 | \Theta^\dagger U_{\tilde{\lambda}_{m_1}}(\tilde{t}_1, \tilde{t}_2) \Theta | k_2 \rangle|^2 \dots |\langle k_N | \Theta^\dagger U_{\tilde{\lambda}_0}(\tilde{t}_N, \tilde{\tau}) \Theta | k_\tau \rangle|^2 \rho_{k_\tau k_\tau} P[M]. \quad (3.25)$$

Here, Θ is a time-reversal operator [20], and $|\langle k_n | \Theta^\dagger U_{\tilde{\lambda}_{m_n}}(\tilde{t}_n, \tilde{t}_{n+1}) \Theta | k_{n+1} \rangle|^2$ is the probability of transition from the time-reversed state $\Theta | k_{n+1} \rangle$ to $\Theta | k_n \rangle$ under the unitary evolution with the reverse protocol: $U_{\tilde{\lambda}_{m_n}}(\tilde{t}_n, \tilde{t}_{n+1}) = U_{\lambda_{m_n}}(\tau - t_n, \tau - t_{n+1})$. The tilde symbol implies time calculated along the reverse trajectory: $\tilde{t} \equiv \tau - t$. $\rho_{k_\tau k_\tau}$ is the diagonal element of the density

matrix when the system is at canonical equilibrium at the beginning of the reverse process:

$$\rho_{k_\tau k_\tau} = \frac{e^{-\beta E_{k_\tau}}}{Y(\tau)}. \quad (3.26)$$

Now we have,

$$\begin{aligned} \Theta^\dagger U_{\tilde{\lambda}_{m_n}}(\tilde{t}_n, \tilde{t}_{n+1}) \Theta &= \Theta^\dagger T \exp \left[-\frac{i}{\hbar} \int_{\tilde{t}_{n+1}}^{\tilde{t}_n} H_{\tilde{\lambda}_{m_n}}(t) dt \right] \Theta \\ &= T \exp \left[+\frac{i}{\hbar} \int_{\tilde{t}_{n+1}}^{\tilde{t}_n} H_{\tilde{\lambda}_{m_n}}(t) dt \right] \\ &= T \exp \left[-\frac{i}{\hbar} \int_{t_{n+1}}^{t_n} H_{\tilde{\lambda}_{m_n}}(\tau - t) dt \right] \\ &= T \exp \left[-\frac{i}{\hbar} \int_{t_{n+1}}^{t_n} H_{\lambda_{m_n}}(t) dt \right] \\ &= U_{\lambda_{m_n}}(t_n, t_{n+1}) = U_{\lambda_{m_n}}^\dagger(t_{n+1}, t_n). \end{aligned} \quad (3.27)$$

Here, T is the time-ordering operator. In the third step, the variable of integration has been changed from t to $\tau - t$. In the next step, we have used the relation $H_{\tilde{\lambda}_{m_n}}(\tau - t) = H_{\lambda_{m_n}}(t)$, which follows from the fact that $\tilde{\lambda}_{m_n}(\tau - t) = \lambda_{m_n}(t)$. Accordingly,

$$\langle k_n | \Theta^\dagger U_{\tilde{\lambda}_{m_n}}(\tilde{t}_n, \tilde{t}_{n+1}) \Theta | k_{n+1} \rangle = \langle k_n | U_{\lambda_{m_n}}^\dagger(t_{n+1}, t_n) | k_{n+1} \rangle = \langle k_{n+1} | U_{\lambda_{m_n}}(t_{n+1}, t_n) | k_n \rangle^\dagger. \quad (3.28)$$

Thus, while dividing eq. (3.24) by (3.25), all the modulus squared terms cancel, and we have,

$$\begin{aligned} \frac{P[K, M]}{\tilde{P}[\tilde{K}; M]} &= \frac{\rho_{k_0 k_0}}{\rho_{k_\tau k_\tau}} \frac{p(m_1 | k_1) \cdots p(m_N | k_N)}{P[M]} \\ &= \frac{Y(\tau)}{Y(0)} e^{\beta W + I}, \end{aligned} \quad (3.29)$$

where $W \equiv E_{k_\tau} - E_{k_0}$ is the work done by the external drive on the system. This follows from the fact that the external forces act only on the system S . In the final step, eqs. (3.22), (3.26)

and (3.3) have been invoked.

Now we follow [19] and define the equilibrium free energy of the system, $F_S(t)$, as the thermodynamic free energy of the open system, which is the difference between the total free energy $F(t)$ of the supersystem and the bare bath free energy F_B :

$$F_S(t) \equiv F(t) - F_B. \quad (3.30)$$

Here, t specifies the values of the external parameters in the course of the protocol at time t . From the above equation, the partition function for the open system is given by [19, 90]

$$Z_S(t) = \frac{Y(t)}{Z_B} = \frac{\text{Tr}_{S,B} e^{-\beta H(t)}}{\text{Tr}_B e^{-\beta H_B}}, \quad (3.31)$$

where S and B represent system and bath variables, respectively. Since Z_B is independent of time, using (3.31) in (3.29), we have

$$\frac{P[K, M]}{\tilde{P}[\tilde{K}; M]} = \frac{Z_S(\tau)}{Z_S(0)} e^{\beta W + I} = e^{\beta(W - \Delta F_S) + I}. \quad (3.32)$$

The above relation is the extended form of the Tasaki-Crooks detailed fluctuation theorem for open quantum systems in presence of feedback where the measurement process involves classical errors.

From (3.32), the quantum Jarzynski Equality follows:

$$\sum_K \int \mathcal{D}[M] P[K, M] e^{-\beta(W - \Delta F_S) - I} = \sum_K \int \mathcal{D}[M] \tilde{P}[\tilde{K}; M] = 1,$$

i.e.,

$$\langle e^{-\beta(W - \Delta F_S) - I} \rangle = 1. \quad (3.33)$$

The summation extends over all possible intermediate collapsed states $\{|k_1\rangle, |k_2\rangle, \dots, |k_N\rangle\}$. This is valid for open quantum system and is independent of the coupling strength and the nature of the bath.

The quantum efficacy parameter is defined as $\langle e^{-\beta(W-\Delta F_S)} \rangle \equiv \gamma$, and the calculation of γ is exactly in the spirit of section 3.3.3, except that $\int \mathcal{D}[X]$ is replaced by \sum_K , i.e., summation over all possible eigenstates. Finally we get the same result, namely,

$$\gamma = \int \mathcal{D}[M] P_{\tilde{\Lambda}_M}[\tilde{M}]. \quad (3.34)$$

3.6 Conclusion

In conclusion, we have rederived several extended fluctuation theorems in the presence of feedback, and have also derived some new ones. To this end, we have used several equalities given by the already known fluctuation theorems. We have also extended the quantum fluctuation theorems for open systems, following the earlier treatment [19, 20]. No assumption is made on the strength of the system-bath coupling and the nature of the environment. However, we have assumed that the measurement process leading to information gain involves classical errors.

Chapter 4

Universal interpretation of efficacy parameter in perturbed nonequilibrium systems

4.1 Introduction

We have discussed about several fluctuation theorems in the foregoing chapters. In this chapter, we will write the fluctuation theorems in the following general form:

$$\frac{P(\Sigma_t)}{P^T(\Sigma_t^T)} = e^{\Sigma_t}, \quad (4.1)$$

where P^T is the functional form of the probability density along a process which is related to the forward process through a conjugate transformation T (not to be confused with temperature). This transformation is not necessarily time-reversal. As before, Σ_t is some observable that is to be measured (up to time t , say) and is in general a path function. $P(\Sigma_t)$ is the probability density of this observable along the forward process, which in turn is parametrized by an externally controlled time-dependent protocol $\lambda(t)$. In the previous chapters, T was simply the time-reversal operator that changes the signs of the velocities. However, there have been

fluctuation theorems in which T is not so. It may include the dual transformation or may be a combination of both the dual transformation and time-reversal, as will be discussed later. The argument Σ_t^T in eq. (4.1) is the value assumed by the observable along the conjugate phase space trajectory.

In this chapter, we will study the extended forms of these relations in feedback-controlled processes, when feedback is applied along the reverse process as well [91] (still respecting the causality of the process, as will be elaborated later). This is contrast to the last chapter, where the reverse process was generated by blindly reversing the forward protocol.

In chapter 3, we had found that in the presence of feedback, the form of the second law needs to be modified to:

$$\langle \Sigma_t \rangle \geq -\langle I \rangle; \quad \langle I \rangle \geq 0. \quad (4.2)$$

Here, the mutual information is defined as [21, 79, 82–84, 86]

$$I \equiv \ln \frac{p(m_0|x_0)p(m_1|x_1) \cdots P(m_N|x_N)}{P(m_0, m_1, \cdots, m_N)}, \quad (4.3)$$

where the presence of measurement errors is assumed (see chapter 3). In the arguments of the conditional probability $p(m_i|x_i)$, m_i is the outcome when a measurement is performed at time t_i , while x_i is the actual value of the observable. The entire sequence of measurement outcomes¹ is given by $M \equiv \{m_0, m_1, \cdots, m_N\}$, which are measured at time instants $\{t_0 = 0, t_1, \cdots, t_N\}$. The phase space trajectory will be denoted by $X \equiv \{x_0, x_1, \cdots, x_\tau\}$, where $\tau = t_{N+1}$. The sequence of protocols used will then be $\Lambda_M(t) \equiv \{\lambda_{m_0}(t), \lambda_{m_1}(t), \cdots, \lambda_{m_N}(t)\}$, the subscripts denoting the measurement outcomes on which the functional form of the protocol depends. Here, $\lambda_{m_0}(t)$ is the protocol in the time interval between t_0 and t_1 , $\lambda_{m_1}(t)$ is the protocol in the time interval between t_1 and t_2 , etc.

The Jarzynski equality [33, 34] has two different generalized forms in the presence of feedback. The more commonly used form of the extended Jarzynski Equality (EJE) is [21, 79, 82–

¹This time we would measure at the initial time $t = 0$ as well, unlike in the previous chapter.

84, 86]

$$\langle e^{-\beta W_d[X, M] - I[X, M]} \rangle = 1. \quad (4.4)$$

W_d is the dissipated work defined through $W_d = W - \Delta F$, where ΔF is the difference between free energies at the end and at the beginning of a particular protocol. It is a functional of both the phase space path X as well as of the measurement trajectory M . Note that the value of ΔF itself changes, depending the form of the protocol.

In eq. (4.4), the reverse trajectories are generated by simply reversing the sequence of one of the forward protocols. As we will show, $I[X, M]$ will in general be replaced by a different physical quantity $\phi[X, M]$, if we choose to use feedback along the reverse process as well, i.e.,

$$\langle e^{-\beta W_d[X, M] - \phi[X, M]} \rangle = 1. \quad (4.5)$$

Other than eq. (4.4), there is yet another form of the extended Jarzynski Equality that has been introduced in the literature [82, 83]:

$$\langle e^{-\beta W_d[X, M]} \rangle = \gamma. \quad (4.6)$$

The *efficacy parameter* γ depends on the feedback control algorithm used along the forward process, and determines the extent to which the feedback is efficient (i.e., more work can be extracted from the system). We will find that γ can be shown to be equal to the sum of probabilities for observing the time-reversed measurements along the time-reversed trajectories. If $\gamma = 1$, then we would have the Jarzynski equality in absence of feedback. The efficacy parameter has been measured experimentally [92] and equations (4.4) and (4.6) have been verified. Using the Jensen's inequality, we have the dissipated work bounded from below through the relation

$$\langle W_d[X, M] \rangle \geq -\ln \gamma. \quad (4.7)$$

Thus, $\gamma > 1$ implies that work can be extracted, on average, from the system, even in the presence of a single heat bath.

Although this inequality looks similar to the one stated in eq. (4.2), it may seem to be a trivial statement because it is a simple consequence of the definition of γ . However, the fact that this definition lends a very clear physical meaning to the efficacy parameter and that this meaning can be exploited to experimentally measure γ (without using the definition eq. (4.6)) underlines the importance of the relations (4.6) and (4.7). We explicitly show that γ retains the simple meaning even when we extend eq. (4.6) to driven systems making transitions among nonequilibrium steady states under arbitrary feedback-controlled protocols.

4.2 Extended Jarzynski Equality

4.2.1 Blind time-reversal of protocol

As shown in [21, 79, 82–84, 86], in presence of information gain and of feedback applied *only* along the forward trajectory, the Jarzynski Equality gets modified to eq. (4.4). This relation is easily derived from the detailed fluctuation theorem, in the case when the reverse protocol is the blind time-reversal of the corresponding protocol along the forward process (see chapter 3). Then the ratio of the forward and reverse trajectories become [79, 84, 86]

$$\begin{aligned} \frac{P[X, M]}{\tilde{P}[\tilde{X}; M]} &= \frac{P_{\Lambda_M}[X]}{P_{\tilde{\Lambda}_M}[\tilde{X}]} \times \frac{p(m_0|x_0)p(m_1|x_1) \cdots P(m_N|x_N)}{P(m_0, m_1, \cdots, m_N)}, \\ &= e^{\beta W_d[X, M] + I[X, M]}. \end{aligned} \quad (4.8)$$

In the above equation, \tilde{X} is the time-reversed trajectory $(\tilde{x}_\tau, \tilde{x}_N, \cdots, \tilde{x}_0)$, $P_{\Lambda_M}[X]$ is the probability density of phase space trajectories when the forward protocol is given by Λ_M (corresponding to the measurement trajectory M); $P[X, M]$ and $\tilde{P}[\tilde{X}; M]$ are the probabilities of the forward and reverse processes, as has been explained in chapter 3. A simple cross-multiplication followed by integration over X and M will give rise to the modified Jarzynski Equality, eq. (4.4).

4.2.2 Using feedback to generate reverse process

The reverse process can also be defined by designing a suitable feedback procedure to generate the time-reversed protocol, which does not violate causality [93]. The feedback procedure is as follows: we first measure system observable at time² $t = \tau$. Let the measurement outcome be \tilde{m}'_τ (say), which is the time-reversed value of m'_τ (which in turn can be equal to any of the possible measurement outcomes). Then the protocol $\lambda_{m'_\tau}(\tau - t)$ is applied, till we reach the time instant $t = t_N$. At t_N , we measure the outcome to be \tilde{m}'_N , and apply the protocol $\lambda_{m'_N}(\tau - t)$, and so on.

Now, suppose that the chosen forward protocol corresponds to the measurement outcomes $\{m_0, m_1, \dots, m_N\}$ at times $\{t_0 = 0, t_1, \dots, t_N\}$, respectively. By using the above algorithm, we will get the exact time-reversed protocol only if the measurement outcomes along the reverse process are $\{\tilde{m}_N, \tilde{m}_{N-1}, \dots, \tilde{m}_0\}$ at the time instants $\{t_{N+1} = \tau, t_N, \dots, t_1\}$, respectively. This means that, we need to have, $\tilde{m}'_\tau = \tilde{m}_N$, $\tilde{m}'_N = \tilde{m}_{N-1}$, and so on. Correspondingly, the protocols applied are $\lambda_{m_N}(\tau - t)$, $\lambda_{m_{N-1}}(\tau - t)$, etc. Any other sequence of obtained measured outcomes along the reverse process, would correspond to the reversal of a different forward protocol. The procedure has been schematically represented in figure 4.1 for an overdamped system, where $\tilde{x}_i = x_i$ and $\tilde{m}_i = m_i$.

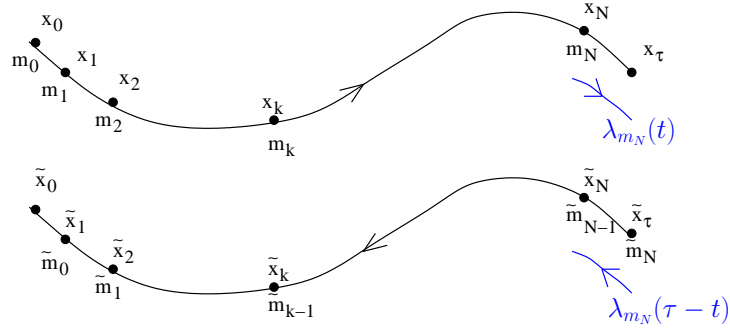


Figure 4.1: The above figure shows the forward (upper curve) and reverse (lower curve) phase space trajectories for an overdamped system. The reverse protocol has been generated using feedback during the reverse process. The reversal of $\lambda_{m_N}(t)$ to $\lambda_{m_N}(\tau - t)$ has been indicated in the time interval from t_N to τ .

²For clarity, for the time being, let us use the forward time to describe the time instants in both the forward and the reverse processes.

In this process, i.e., changing the protocol according to measurement outcome \tilde{m}_{k-1} at time $t = t_k$, the reverse protocol is exactly reproduced without ever violating causality. This is because nowhere are we implementing a protocol and then measuring the outcome that should determine this protocol (as would have been the case if the measurements were not made at the shifted time instants).

The joint probability density for a forward phase space trajectory X and corresponding measurement trajectory M in presence of feedback is given by [84]

$$P[X, M] = p(x_0)p(m_0|x_0)P_{\lambda_{m_0}}[x_0 \rightarrow x_1]p(m_1|x_1)P_{\lambda_{m_1}}[x_1 \rightarrow x_2] \cdots p(m_N|x_N)P_{\lambda_{m_N}}[x_N \rightarrow x_\tau]. \quad (4.9)$$

The probability for the reverse trajectory in presence of feedback becomes

$$\tilde{P}[\tilde{X}; M] = p(\tilde{x}_\tau)p(\tilde{m}_N|\tilde{x}_\tau)P_{\tilde{\lambda}_{m_N}}[\tilde{x}_\tau \rightarrow \tilde{x}_N] p(\tilde{m}_{N-1}|\tilde{x}_N)P_{\tilde{\lambda}_{m_{N-1}}}[\tilde{x}_N \rightarrow \tilde{x}_{N-1}] \cdots p(\tilde{m}_0|\tilde{x}_1)\tilde{P}_{\tilde{\lambda}_{m_0}}[\tilde{x}_1 \rightarrow \tilde{x}_0]. \quad (4.10)$$

Here, the notation $\tilde{\lambda}_{m_k}(t) \equiv \lambda_{m_k}(\tau - t)$, has been used. $p(\tilde{m}_{k-1}|\tilde{x}_k)$ gives the error probability of obtaining the outcome \tilde{m}_{k-1} , when the actual state is \tilde{x}_k .

This gives the new extended Crooks relation

$$\frac{P[X, M]}{\tilde{P}[\tilde{X}; M]} = e^{\beta W_d[X] + \Delta s_p[X, M]}, \quad (4.11)$$

We assume time-reversibility of measurements, $p(\tilde{m}'_i|\tilde{x}_i) = p(m'_i|x_i)$, that is, $p(\tilde{m}_{i-1}|\tilde{x}_i) = p(m_{i-1}|x_i)$. Then we have,

$$\Delta s_p[X, M] \equiv \ln \frac{p(m_0|x_0)p(m_1|x_1) \cdots p(m_N|x_N)}{p(m_N|x_\tau)p(m_{N-1}|x_N) \cdots p(m_0|x_1)}. \quad (4.12)$$

Here, Δs_p represents a disorder parameter, but is not the mutual information (see eq. (4.3)) as defined in [82]. Of course, equations (4.8) and (4.11) contain different information as well as

provide different bounds for the average total entropy change for the system.

4.2.3 The general case

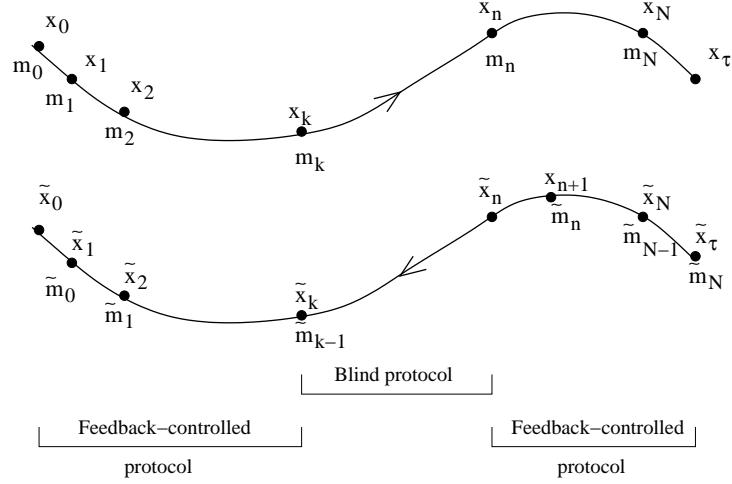


Figure 4.2: The figure shows the representative plot of the phase space trajectory in a simple case for the most general form of feedback that can be considered during the reverse process (the lower curve) corresponding to the forward process (the upper curve). First, from $t = \tau$ to $t = t_n$, we have the feedback-controlled reverse protocol, while from $t = t_n$ to $t = t_k$ we have used the blindly time-reversed protocol. In the final part, up to $t = 0$, we revert to the feedback-controlled reverse protocol.

The general form of the probability density for a forward trajectory in presence of feedback is given by [84] equation (4.9).

The general protocol to generate the reverse process would be to use both the protocols described in sections 4.2.1 and 4.2.2 at random during the reverse process. Let us take one simple case when, along the reverse process, up to time $t = t_n$, we use the feedback-controlled protocol of section 4.2.2. Then from time $t = t_n$ to $t = t_k$, we use the blindly applied reverse protocol of section 4.2.1. Finally, from $t = t_k$ to $t = 0$, we once again use the feedback-controlled reverse protocol (see figure 4.2, where the forward and reverse trajectories are shown for an overdamped system). Here, k and n can be any two integers chosen at random from the set $\{1, 2, \dots, N\}$, with $n > k$. In this case, the reverse process becomes,

$$\begin{aligned}
\tilde{P}[\tilde{X}; M] &= \{p(\tilde{x}_\tau)p(\tilde{m}_N|\tilde{x}_\tau)P_{\tilde{\lambda}_{m_N}}[\tilde{x}_\tau \rightarrow \tilde{x}_N]p(\tilde{m}_{N-1}|\tilde{x}_N)P_{\tilde{\lambda}_{m_{N-1}}}[\tilde{x}_N \rightarrow \tilde{x}_{N-1}] \\
&\quad \cdots p(\tilde{m}_n|\tilde{x}_{n+1})P_{\tilde{\lambda}_{m_n}}[\tilde{x}_{n+1} \rightarrow \tilde{x}_n]\} \times \{p(m_{n-1}, \dots, m_k)\tilde{P}[\tilde{x}_n \rightarrow \tilde{x}_k]\} \\
&\quad \times \{p(\tilde{m}_{k-1}|\tilde{x}_k)P_{\tilde{\lambda}_{m_{k-1}}}[\tilde{x}_k \rightarrow \tilde{x}_{k-1}] \cdots p(\tilde{m}_0|\tilde{x}_1)P_{\tilde{\lambda}_{m_0}}[\tilde{x}_1 \rightarrow \tilde{x}_0]\}. \quad (4.13)
\end{aligned}$$

Each of the three parts in the reverse process (time intervals τ to t_n , t_n to t_k , and t_k to 0) have been enclosed within separate pairs of braces $\{\}$ for clarity. Therefore, we arrive at (once again using the time-reversibility of measurements to do away with the tilde symbols)

$$\begin{aligned}
\frac{P[X, M]}{\tilde{P}[\tilde{X}; M]} &= \frac{P_{\Lambda_M}[X]}{P_{\tilde{\Lambda}_M}[\tilde{X}]} \times \frac{p(m_0|x_0) \cdots p(m_{k-1}|x_{k-1})}{p(m_0|x_1) \cdots p(m_{k-1}|x_k)} \times \frac{p(m_k|x_k) \cdots p(m_{n-1}|x_{n-1})}{p(m_k, \dots, m_{n-1})} \\
&\quad \times \frac{p(m_n|x_n) \cdots p(m_N|x_N)}{p(m_n|x_{n+1}) \cdots p(m_N|x_\tau)} \\
&= \exp [\beta W_d + \Delta s_p^1 + I^1 + \Delta s_p^2], \quad (4.14)
\end{aligned}$$

where

$$I^1 = \ln \frac{p(m_k|x_k) \cdots p(m_{n-1}|x_{n-1})}{p(m_k, \dots, m_{n-1})}; \quad (4.15)$$

$$\Delta s_p^1 = \ln \frac{p(m_0|x_0) \cdots p(m_{k-1}|x_{k-1})}{p(m_0|x_1) \cdots p(m_{k-1}|x_k)}; \quad (4.16)$$

$$\Delta s_p^2 = \ln \frac{p(m_n|x_n) \cdots p(m_N|x_N)}{p(m_n|x_{n+1}) \cdots p(m_N|x_\tau)}. \quad (4.17)$$

We are thus led to a different extended detailed fluctuation theorem where disorder parameters Δs_p^1 , I^1 and Δs_p^2 are different as they contain different information about the feedback process. Thus, it is clear that the $\phi[X, M]$ in eq. (4.5) does not have a unique interpretation, but depends on the manner of feedback along the backward process. From eq. (4.14), one can obtain the related integral fluctuation theorem, namely

$$\langle \exp[-\beta W_d - I^1 - \Delta s_p^1 - \Delta s_p^2] \rangle = 1. \quad (4.18)$$

All the three results derived above, eqs. (4.8), (4.11) and (4.14), can be written in compact form as

$$\frac{P[X, M]}{\tilde{P}[\tilde{X}; M]} = e^{\beta W_d + \phi[X, M]}. \quad (4.19)$$

In eq. (4.8), $\phi[X, M]$ simply equals $I[X, M]$. In eq. (4.11), it is equal to $\Delta s_p[X, M]$. In eq. (4.14), $\phi[X, M] = I^1[X, M] + \Delta s_p^1[X, M] + \Delta s_p^2[X, M]$.

In principle, for different feedback protocols, $\phi[X, M]$ will be different, and terms like Δs_p^1 , Δs_p^2 , etc. become difficult to interpret physically. This problem also gets reflected in the extended forms of the Jarzynski equality. We next turn our attention to the efficacy parameter.

4.3 Efficacy parameter in presence of general feedback

In absence of feedback, the Jarzynski equality is given by [27, 33, 34, 42]

$$\langle e^{-\beta W_d[X]} \rangle = 1. \quad (4.20)$$

In presence of feedback, the right hand side of the above relation will in general not be unity. The efficacy parameter for the feedback in this case (when system is initially at thermal equilibrium with the medium) is defined as

$$\gamma = \langle e^{-\beta W_d[X]} \rangle. \quad (4.21)$$

It can be readily seen that lesser the amount of dissipated work, more is the magnitude of the efficacy parameter, as is desirable for a quantity that measures the efficiency of feedback. Now we use the general case for obtaining the reverse trajectories, namely the case 4.2.3.

Therefore, we get

$$\begin{aligned} \gamma &= \int \mathcal{D}[X] \mathcal{D}[M] P[X, M] e^{-\beta W_d[X, M]} \\ &= \int \mathcal{D}[X] \mathcal{D}[M] \tilde{P}[\tilde{X}; M] e^{\Delta s_p^1 + I^1 + \Delta s_p^2} \end{aligned}$$

$$\begin{aligned}
&= \int \mathcal{D}[X] \mathcal{D}[M] P_{\tilde{\Lambda}_M}[\tilde{X}] p(m_0|x_0) p(m_1|x_1) \cdots p(m_N|x_N) \\
&= \int \mathcal{D}[\tilde{X}] \mathcal{D}[\tilde{M}] P_{\tilde{\Lambda}_M}[\tilde{X}] p(\tilde{m}_0|\tilde{x}_0) p(\tilde{m}_1|\tilde{x}_1) \cdots p(\tilde{m}_N|\tilde{x}_N) \\
&= \int \mathcal{D}[\tilde{X}] \mathcal{D}[\tilde{M}] P_{\tilde{\Lambda}_M}[\tilde{X}, \tilde{M}] = \int \mathcal{D}[\tilde{M}] P_{\tilde{\Lambda}_M}[\tilde{M}], \tag{4.22}
\end{aligned}$$

where we have used the detailed fluctuation theorem (4.14), and the definitions (4.16), (4.15) and (4.17). $\mathcal{D}[X]$ is the measure for the functional integral over all possible phase space trajectories while $\mathcal{D}[M]$ is that for the integral over all possible measurement trajectories. The time-reversibility of measurements has been assumed: $p(m_i|x_i) = \tilde{p}(\tilde{m}_i|\tilde{x}_i)$ [82]. The physical meaning of $P_{\tilde{\Lambda}_M}[\tilde{X}, \tilde{M}]$ has been clarified in chapter 3. The same chapter also explains why the final integral, $\int \mathcal{D}[\tilde{M}] P_{\tilde{\Lambda}_M}[\tilde{M}]$, is not unity.

In more general cases, when the two different algorithms (those of sections 4.2.1 and 4.2.2) are applied at various time intervals to generate the reverse protocol, we need to use the following algebra in the integrand:

$$\begin{aligned}
\tilde{P}[\tilde{X}; M] e^{\phi[X, M]} &= \tilde{P}[\tilde{X}; M] \exp\left(\sum_i \Delta s_p^i + \sum_j I^j\right) \\
&= P_{\tilde{\Lambda}_M}[\tilde{X}] p(m_0|x_0) \cdots p(m_N|x_N) \\
&= P_{\tilde{\Lambda}_M}[\tilde{X}] \tilde{p}(\tilde{m}_0|\tilde{x}_0) \cdots \tilde{p}(\tilde{m}_N|\tilde{x}_N) \\
&= P_{\tilde{\Lambda}_M}[\tilde{X}, \tilde{M}]. \tag{4.23}
\end{aligned}$$

Here, the summations \sum_i and \sum_j run over all the time intervals in which the reverse protocols have been executed by using feedback and by blind time-reversal, respectively. We find that although the form of $\tilde{P}[\tilde{X}; M]$ contains detailed information about the actual feedback procedure used along the backward process, when it is multiplied by the factor $e^{\phi[X, M]}$, we obtain $P_{\tilde{\Lambda}_M}[\tilde{X}, \tilde{M}]$, whose form does not contain any such information. This is the reason behind the fact that the efficacy parameter retains the same physical meaning in each case, namely, it is the *total probability to observe the time-reversed outcomes for the measurements performed along the reverse process* [21, 82–84].

This derivation of γ (eq. (4.22)) for the general case is our central result. It simply shows that it retains the same meaning as for the specific case considered in the earlier literature [79, 82–88].

The results in this chapter can be verified, using the same setup as mentioned in chapter 3.

4.4 The three detailed fluctuation theorems

We will be generalizing our treatment to the other detailed fluctuation theorems, which involve the non-adiabatic entropy production and adiabatic entropy production. The total entropy change by definition is the sum of entropy changes in the system (Δs) and in the medium (Δs_m): $\Delta s_{tot} = \Delta s + \Delta s_m$. Recently it has been observed that while generalizing the second law for systems making transitions between steady states, the total entropy production can also be split into two distinct parts such that each part, interestingly, follows a detailed fluctuation theorem [49, 51, 94, 95]:

$$\Delta s_{tot} = \Delta s_{na} + \Delta s_a. \quad (4.24)$$

The averages of all these three quantities are always non-negative, thereby providing a new twist to the second law. Δs_a is related to the housekeeping heat Q_{hk} , while Δs_{na} is the sum of the entropy change of the system and the entropy produced due to excess heat Q_{ex} [49, 51, 94, 95]. They are known as the adiabatic and the nonadiabatic entropy productions, respectively, as has been discussed in the introduction (see section 1.4).

In the case of adiabatic and non-adiabatic entropy productions, the concept of dual dynamics is very helpful. Under the dual dynamics, if the system is allowed to reach the corresponding steady state, then the steady-state distribution ρ_{SS} retains the same form as in the original dynamics, but the probability current reverses its sign [51, 52]. Hatano and Sasa had shown that the physical meaning of the nonadiabatic entropy becomes clear in the dual dynamics formalism [47]. These detailed fluctuation theorems are taken up in the following discussion.

4.4.1 Total entropy

Suppose that the initial state of the system for the forward process is not necessarily at thermal equilibrium with the bath, and the initial distribution for the reverse process is the final distribution attained in the forward process. Then in absence of feedback, the following ratio is obtained between the forward and the reverse trajectories [5, 28, 29]:

$$\frac{P[X]}{\tilde{P}[\tilde{X}]} = e^{\Delta_{stot}[X]}, \quad (4.25)$$

from which the following integral fluctuation theorem can be obtained:

$$\langle e^{-\Delta_{stot}[X]} \rangle = 1. \quad (4.26)$$

In presence of feedback, the right hand side will in general be different from unity. For this general case, instead of eq. (4.19), we would get the following ratio between the forward and reverse paths:

$$\frac{P[X, M]}{\tilde{P}[\tilde{X}; M]} = e^{\Delta_{stot}[X, M] + \phi[X, M]}. \quad (4.27)$$

We now consider the case with general reverse protocol. We define the efficacy parameter as

$$\gamma_{tot} = \langle e^{-\Delta_{stot}[X, M]} \rangle \quad (4.28)$$

Proceeding in exactly the same way as before (see eqs. (4.22) and (4.23)), we find

$$\begin{aligned} \gamma_{tot} &= \int \mathcal{D}[X] \mathcal{D}[M] P[X, M] e^{-\Delta_{stot}[X, M]} \\ &= \int \mathcal{D}[X] \mathcal{D}[M] \tilde{P}[\tilde{X}; M] e^{\phi[X, M]} \\ &= \int \mathcal{D}[\tilde{M}] P_{\tilde{\Lambda}_M}[\tilde{M}]. \end{aligned} \quad (4.29)$$

Thus, γ_{tot} retains the same physical meaning as γ for the Jarzynski equality, although here we do not have the constraint of sampling the initial state of the system from the equilibrium

distribution.

4.4.2 Nonadiabatic entropy

For transitions between nonequilibrium steady states, we have the following detailed fluctuation theorem in absence of feedback [47, 50, 51, 94]:

$$\frac{P[X]}{\tilde{P}^\dagger[\tilde{X}]} = e^{\Delta s_{na}[X]}. \quad (4.30)$$

The superscript \dagger implies that keeping the functional form of the protocol same, we are switching to the dual dynamics. The tilde symbol over P implies that the protocol for the forward process has been time-reversed after the system has been allowed to follow the dual dynamics. In other words, $\tilde{P}^\dagger[\tilde{X}]$ is the probability density for a trajectory along the process generated, in presence of dual dynamics, by the time-reversed protocol. Similar to the above cases, in presence of feedback, we have [84, 87]

$$\frac{P[X, M]}{\tilde{P}^\dagger[\tilde{X}; M]} = e^{\Delta s_{na}[X, M] + \phi[X, M]}, \quad (4.31)$$

where the form of $\phi[X, M]$ depends on the way in which feedback is applied in the reverse process, as given in section 2. The efficacy parameter in this case is given by

$$\begin{aligned} \gamma_{na} &= \langle e^{-\Delta s_{na}[X, M]} \rangle = \int \mathcal{D}[X] \mathcal{D}[M] P[X, M] e^{-\Delta s_{na}[X, M]} \\ &= \int \mathcal{D}[X] \mathcal{D}[M] \tilde{P}^\dagger[\tilde{X}; M] e^{\phi[X, M]} \\ &= \int \mathcal{D}[X] \mathcal{D}[M] P_{\tilde{\Lambda}_M}^\dagger[\tilde{X}] p(m_0|x_0) \cdots p(m_N|x_N) \\ &= \int \mathcal{D}[X] \mathcal{D}[M] P_{\tilde{\Lambda}_M}^\dagger[\tilde{X}, \tilde{M}] = \int \mathcal{D}[\tilde{M}] P_{\tilde{\Lambda}_M}^\dagger[\tilde{M}]. \end{aligned} \quad (4.32)$$

In the third step, we have used the algebra that has already been shown in the case of the most general protocol (section 4.3) for extended Jarzynski equality, which results in

$$\begin{aligned}\tilde{P}^\dagger[\tilde{X}; M]e^{\phi[X, M]} &= P_{\tilde{\Lambda}_M}[\tilde{X}] \exp\left(\sum_i \Delta s_p^i + \sum_j I^j\right) \\ &= P_{\tilde{\Lambda}_M}^\dagger[\tilde{X}, \tilde{M}].\end{aligned}\tag{4.33}$$

We have assumed that the measurement errors do not change on changing the dynamics, which is quite reasonable assumption, because it is a property of the measuring device. Thus, γ_{na} is the net probability for obtaining the time-reversed outcomes along the time-reversed process in dual dynamics.

4.4.3 Adiabatic entropy

The DFT for adiabatic entropy production³ is given by [51, 94]

$$\frac{P[X]}{P^\dagger[X]} = e^{\Delta s_a[X]}.\tag{4.34}$$

$P^\dagger[X]$ is the probability density for the path followed by the system in phase space, when the system is evolving under the dual dynamics. In presence of feedback, we then have,

$$\frac{P[X, M]}{P^\dagger[X; M]} = e^{\Delta s_a[X, M] + \phi[X, M]}.\tag{4.35}$$

Since both the processes considered are forward processes (in two different dynamics), there is no need to perform measurements and feedbacks at shifted times in order to respect causality. The denominator can therefore only consist of the following options:

(1) The same feedback procedure is used to generate the forward process in the dual dynamics as well, in which case we have $\phi[X, M] = 0$ (since the error probabilities in the numerator cancel with those in the denominator). Once again, measurement errors are assumed to be

³In this subsection, we will deal only with overdamped systems, where $\tilde{x} = x$ and $\tilde{m} = m$. For underdamped systems, this fluctuation theorem is in general not valid [50].

independent of the dynamics followed by the system.

(2) One of the forward protocols in the original dynamics is recorded, and this protocol is blindly executed in presence of the dual dynamics, in which case we simply have $\phi[X, M] = I[X, M]$.

(3) We use the above two procedures at random while generating the forward trajectories in presence of dual dynamics, which is the most general case. In this case, however, $\phi[X, M] = \sum_j I^j$, i.e., the summation over Δs_p^i will be absent, because the latter quantity never appears in this case.

The efficacy parameter is

$$\gamma_a \equiv \langle e^{-\Delta s_a[X, M]} \rangle, \quad (4.36)$$

which leads to

$$\begin{aligned} \gamma_a &= \int \mathcal{D}[X] \mathcal{D}[M] P[X, M] e^{-\Delta s_a[X, M]} \\ &= \int \mathcal{D}[X] \mathcal{D}[M] P^\dagger[X; M] e^{\sum_j I^j} = \int \mathcal{D}[M] P_{\Lambda_M}^\dagger[M]. \end{aligned} \quad (4.37)$$

Therefore, γ_a is the total probability for observing the same outcomes as the initial process with the same protocols, if the system follows the dual dynamics.

We thus find that the physical meaning of efficacy parameter can be very generally stated as follows: it is the total probability to observe the measured outcomes conjugate to those along the forward protocol, for the intermediate measurements along the process with the corresponding conjugate dynamics. Since the efficacy parameters are experimentally measurable, they would provide more meaningful forms of the extended fluctuation relations. Further, they would provide universal bounds for $\langle W_d \rangle$, $\langle \Delta s_a \rangle$, $\langle \Delta s_{na} \rangle$, $\langle \Delta s_{tot} \rangle$, and these bounds are in fact independent of whether or not feedback is performed along the conjugate process in the actual protocol.

For the other extended relations and bounds stated in section 4.2, the expressions would depend sensitively on whether and how the feedback is performed along the conjugate dynamics,

namely, the extended integral fluctuation theorems can be stated as

$$\left\langle \exp \left(-\Delta s_k - \sum_i \Delta s_p^i - \sum_j I^j \right) \right\rangle = 1 \quad (4.38)$$

for $k = 1, 2, 3, 4$ representing W_d , Δs_{tot} , Δs_{na} and Δs_a , respectively (keeping in mind that $\Delta s_p^i = 0$ for all i , in the case of Δs_a). This would lead to the bounds

$$\langle \Delta s_k \rangle \geq - \left\langle \sum_i \Delta s_p^i \right\rangle - \left\langle \sum_j I^j \right\rangle. \quad (4.39)$$

As a consequence, arbitrary number of modified relations and corresponding bounds can be computed for this latter case, which can cause confusion. The efficacy parameter, on the other hand, is a more suitable experimentally measurable quantity that can characterize not only the performance of the system, but can also act as a useful parameter to define the extended fluctuation relations.

4.5 Conclusion

In this chapter, we have shown that out of the two known forms of the modified fluctuation theorems in presence of feedback, one of the forms is heavily dependent on the way feedback is applied along the conjugate process, and thereby leads to arbitrary number of extended relations for work done on the system or for the relevant entropy changes (total entropy, nonadiabatic and adiabatic entropies) taking place. The bounds obtained from these relations, therefore, also have this arbitrariness. On the other hand, the second form, namely the fluctuation theorem expressed in terms of the efficacy parameter, provides a relation for work and entropy changes that carries a clear and consistent physical meaning, irrespective of the manner of application of feedback along the conjugate process. This consistency is robust even when the conjugate process is not the time-reversed process. This study would hopefully help in simpler experimental verification of the extended fluctuation theorems.

Chapter 5

Total entropy production fluctuation theorems in a nonequilibrium time-periodic steady state

5.1 Introduction

The fluctuation theorems reveal rigorous relations for properties of distribution functions of physical variables such as work, heat and entropy production for systems driven away from equilibrium, where Einstein's and Onsager's relations no longer hold.

In the present work, we probe numerically the entropy production fluctuation theorems (the IFT and the DFT) in the case of a Brownian particle placed in a double well potential and subjected to an external harmonic drive [96]. In the absence of drive, the particle hops between the two wells with Kramer's escape rate $r_K = \tau_0^{-1} e^{-\Delta V/k_B T}$ [97] where τ_0 is a characteristic time (see chapter 1 for the explicit expression for τ_0 in an overdamped system), ΔV is the energy barrier height between the two symmetric wells and T is the temperature of the bath. The random hops of the Brownian particle between the two wells get synchronized with the external drive if r_K matches twice the frequency of the external drive. This optimization condition can be achieved by tuning the noise intensity, and is called *stochastic resonance* (SR) [53, 54, 98].

Noise plays a constructive role in this case and SR finds applications in almost all areas of natural sciences. To characterize this resonance behaviour, different quantifiers have been introduced in the literature [53, 55, 65, 98–102]. The average work injected into the system (or the average thermodynamic work done on the system) per cycle characterizes SR as a bona fide resonance [55, 98, 102]. Recently work and heat fluctuation theorems have been analyzed in a symmetric double well system exhibiting SR in presence of external subthreshold harmonic [68, 69] and biharmonic [70] drives. Theoretical [68, 69] and experimental [15, 16] studies reveal the validity of the steady state fluctuation theorem (SSFT) for heat and work integrated over finite time intervals. In the following, we extend the study to fluctuation theorems for total entropy production and associated probability density functions.

5.2 The Model

The overdamped dynamics for the position (x) of the particle is given by a Langevin equation in a dimensionless form, namely

$$\gamma \frac{dx}{dt} = -\frac{\partial U(x, t)}{\partial x} + \xi(t), \quad (5.1)$$

where $\xi(t)$ is the Gaussian white noise with $\langle \xi(t) \rangle = 0$ and $\langle \xi(t)\xi(t') \rangle = 2D\delta(t-t')$, where the noise strength $D = \gamma k_B T$, k_B being the Boltzmann constant. The potential $U(x, t)$ can be split into two parts: a static potential $V(x) = -\frac{1}{2}x^2 + \frac{1}{4}x^4$, and the potential due to external harmonic perturbation $V_1(x, t) = -xA \sin \omega t$. A and ω are amplitude and frequency of the external drive, respectively.

The static double well potential $V(x)$ has a barrier height $\Delta V = 0.25$ (see figure 5.1) between two symmetrically placed wells (or minima) located at $x_m = \pm 1$. We have restricted our analysis to subthreshold forcings, $A|x_m| < \Delta V$. The total potential $U(x, t) = V(x) + V_1(x, t)$. Using the method of stochastic energetics [23] for a given particle trajectory $X(t)$ over a finite time duration τ , the physical quantities such as injected work or thermodynamic work (W), change in internal energy (ΔU) and heat (Q) dissipated to the bath are given by (see

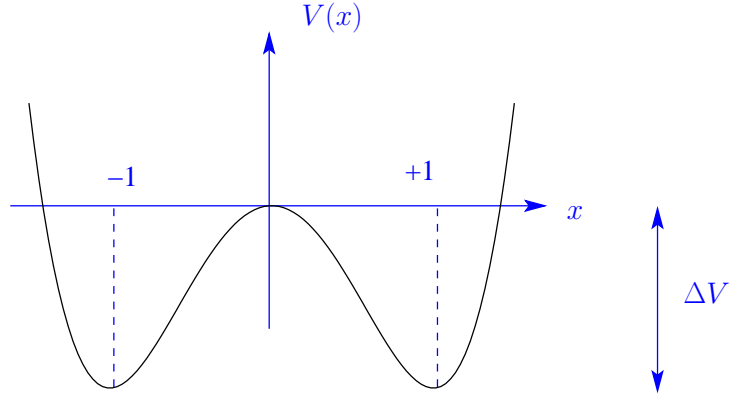


Figure 5.1: The double-well potential used in this chapter. Here, ΔV is the barrier height between the two wells, while the minima of the two wells are located at $x_m = \pm 1$.

chapter 1, sect. 1.1)

$$W = \int_{t_0}^{t_0+\tau} \frac{\partial U(x, t)}{\partial t} dt, \quad (5.2a)$$

$$\Delta U = U(x(t_0 + \tau), t_0 + \tau) - U(x(t_0), t_0), \quad \text{and} \quad (5.2b)$$

$$Q = W - \Delta U. \quad (5.2c)$$

Equation (5.2c) is a statement of the first law of thermodynamics. The particle trajectory extends from initial time t_0 to final time $t_0 + \tau$. W , ΔU and Q are all stochastic quantities and we have evaluated them numerically by solving Langevin equation using Heun's method [67–69] (see appendix D).

A change in the medium entropy (Δs_m) over a time interval τ is given by $\Delta s_m = Q/T$. As explained in sect. 1.2 of chapter 1, the change in the system entropy for any trajectory of duration τ is given by

$$\Delta s = -\ln \left[\frac{p_1(x(t_0 + \tau), t_0 + \tau)}{p_0(x(t_0), t_0)} \right], \quad (5.3)$$

where $p_0(x(t_0), t_0)$ and $p_1(x(t_0 + \tau), t_0 + \tau)$ are the probability densities of the particle positions at initial time t_0 and final time $t_0 + \tau$ respectively.

The total entropy change over time duration τ is given by

$$\Delta s_{tot} = \Delta s_m + \Delta s. \quad (5.4)$$

Using the above definition of total entropy production, Seifert has derived the IFT [28, 29] (see chapter 1), i.e.,

$$\langle e^{-\Delta s_{tot}} \rangle = 1, \quad (5.5)$$

where angular brackets denote average over the statistical ensemble of realizations, i.e., over the ensemble of finite time trajectories. This identity is very general and holds at any time interval and for arbitrary initial conditions.

In the presence of external periodic perturbations, the system relaxes to a time-periodic steady state. In this state, a stronger detailed fluctuation theorem holds [27–29]:

$$\frac{P(\Delta s_{tot})}{P(-\Delta s_{tot})} = e^{\Delta s_{tot}}, \quad (5.6)$$

where Δs_{tot} is evaluated over time intervals $\tau = nT_1$, n being an integer, and T_1 being the period of the external drive. $P(\Delta s_{tot})$ (or $P(-\Delta s_{tot})$) is the probability that the trajectory produces (or consumes) entropy with the magnitude Δs_{tot} .

To calculate the total entropy production, we evolve the Langevin system under the time-periodic force over many realizations of noise. Ignoring transients, we first find out probability density function $p(x, t)$ in the time asymptotic regime. In this case, $p(x, t)$ is a periodic function in t with the period equal to that of the external drive. The heat dissipated is calculated over a period (or over a number of periods) using (5.2c). Thereby we obtain the change in the medium entropy ($\Delta s_m = Q/T$). Knowing the end-points of each trajectory, and the time-periodic $p(x, t)$, the change in system entropy Δs is calculated (equation (5.3)). Thus we obtain for each trajectory the total entropy production ($\Delta s_{tot} = \Delta s_m + \Delta s$). To calculate the averages of the physical quantities or the probability distribution, Δs_{tot} is obtained for more than 10^5 realizations. In the following we present the results where all the physical parameters are taken in dimensionless form.

5.3 Results and Discussions

The work W_p calculated over a period¹ chosen at random varies from realization to realization and is a random quantity. So are internal energy change ΔU_p and dissipated heat Q_p . However, all these quantities satisfy equation 5.2c for each period chosen at random. The averages of physical quantities ($\langle \cdot \cdot \cdot \rangle$) are calculated over 10^5 realizations.

In figure 5.2, we have plotted the average work done (or injected work) $\langle W_p \rangle$ over a single period of the external drive in nonequilibrium time-periodic state, as a function of noise strength D for $A = 0.1$ (subthreshold driving). The internal energy U being a state variable, $\langle U_p \rangle$ is periodic in time and hence $\langle \Delta U_p \rangle = 0$. From equation (5.2c) we find that the average heat dissipated over a period $\langle Q_p \rangle$ equals the average work $\langle W_p \rangle$ done over a period. In the same figure, average total entropy production over a single period, $\langle \Delta s_{tot,p} \rangle$, as a function of D has also been plotted. Since entropy of system is a state variable, $\langle \Delta s_p \rangle = 0$, and we have $\langle \Delta s_{tot,p} \rangle = \langle \Delta s_{m,p} \rangle = \langle \frac{Q_p}{T} \rangle$.

We observe from figure 5.2 that the average work or heat exhibits a well-known SR peak (around $D = 0.12$) consistent with the condition (at low frequency of drive) of matching between Kramer's rate and frequency of drive, which has been studied in earlier results [55, 102]. However, peak in the $\langle \Delta s_{tot,p} \rangle$ is not at the same D at which SR condition is satisfied. It is expected that at resonance, system will absorb maximum energy from the medium and being in a stationary state, will release this same energy back to the medium.

The peak for $\langle \Delta s_{tot,p} \rangle$ not being at the same temperature as that for $\langle Q_p \rangle$ or $\langle W_p \rangle$ is understandable as $\langle \Delta s_{tot,p} \rangle = \langle \Delta s_{m,p} \rangle = \langle Q_p/T \rangle$, i.e., peak in $\langle Q_p \rangle$ versus T will be shifted if we plot $\langle Q_p/T \rangle$ versus T . Similar observations are noted in the nature of directed current in ratchet systems [103]. In these periodic systems, unidirectional currents can be obtained in a nonequilibrium state in the absence of obvious bias. The average current exhibits a resonance peak as a function of temperature. Even though currents in these systems are generated at the expense of entropy, the value of D at which entropy production shows a peak is not the same

¹We would be using the subscript p to denote the quantities measured over a single period, in this chapter as well as in the next. This is done to differentiate it from the quantities measured over n periods (say), where the measured quantities will carry the subscript np .

as that at which current shows a peak.

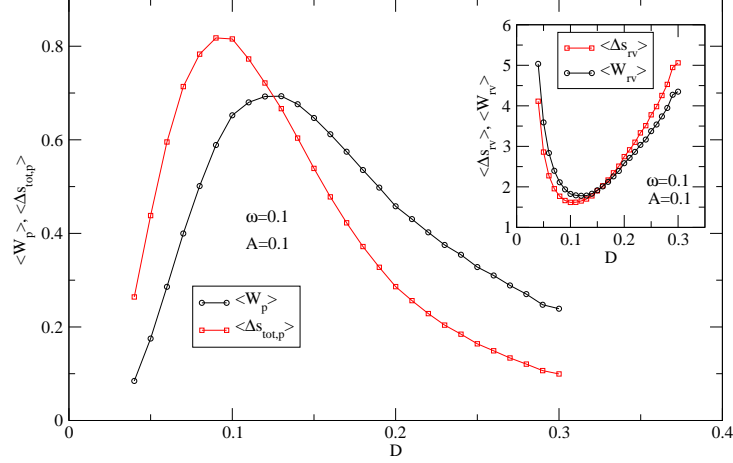


Figure 5.2: Variation of $\langle W_p \rangle (= \langle Q_p \rangle)$ and $\langle \Delta s_{tot,p} \rangle$ with D , for $A = 0.1$, $\omega = 0.1$. The curve of $\langle W_p \rangle$ versus D has been scaled by a factor of 8 for easy comparison. Inset shows the corresponding relative variances as a function of D .

In the inset of figure 5.2, we have plotted the relative variance of work $\left(\langle W_{rv} \rangle \equiv \frac{\sqrt{\langle W_p^2 \rangle - \langle W_p \rangle^2}}{\langle W_p \rangle} \right)$ and that of total entropy $\left(\langle \Delta s_{rv} \rangle \equiv \frac{\sqrt{\langle \Delta s_{tot,p}^2 \rangle - \langle \Delta s_{tot,p} \rangle^2}}{\langle \Delta s_{tot,p} \rangle} \right)$. $\langle W_{rv} \rangle$ exhibits a minimum around SR condition. However, $\langle \Delta s_{rv} \rangle$ shows a minimum around the same temperature at which $\langle \Delta s_{tot,p} \rangle$ shows a peak. Thus, unlike $\langle W_{rv} \rangle$ [17, 68, 69], $\langle \Delta s_{rv} \rangle$ cannot be used as a quantifier of SR. This is because the minimum in $\langle \Delta s_{rv} \rangle$ is correlated to the peak in $\langle \Delta s_{tot,p} \rangle$ as a function of D , which itself does not occur at the value of the D at which resonance condition is satisfied, as discussed earlier. It may be noted that relative variance of both work and total entropy production over single period are larger than 1, implying that these quantities are not self-averaging (i.e., fluctuation dominates the mean). However, when the observation time for the stochastic trajectory is increased to a large number (n) of periods, the relative variance, which scales as $n^{-1/2}$, becomes a self-averaging quantity, i.e., mean is larger than the dispersion [69].

In figure 5.3, we have plotted $\langle W_p \rangle$ and $\langle \Delta s_{tot,p} \rangle$ as a function of ω . The injected work $\langle W_p \rangle$, exhibits a peak as a function of ω , thus characterizing SR as a bona fide resonance [55, 98, 102]. It may be noted that the peak position for $\langle \Delta s_{tot,p} \rangle$, in this case, is at the same value as that for $\langle W_p \rangle$ or $\langle Q_p \rangle$, as expected. The inset shows the relative variances of $\Delta s_{tot,p}$

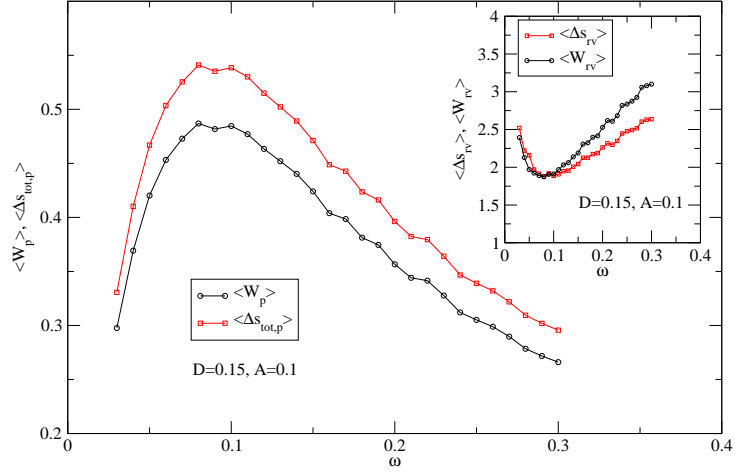


Figure 5.3: Variation of $\langle W_p \rangle = \langle Q_p \rangle$ and $\langle \Delta s_{tot,p} \rangle$ with ω , for $A = 0.1$, $D = 0.15$. The curve of $\langle W_p \rangle$ versus ω has been scaled by a factor of 6 for easy comparison. Inset shows the corresponding relative variances as a function of ω .

and W_p versus frequency of external drive ω , which in turn shows a minimum at the resonance condition.

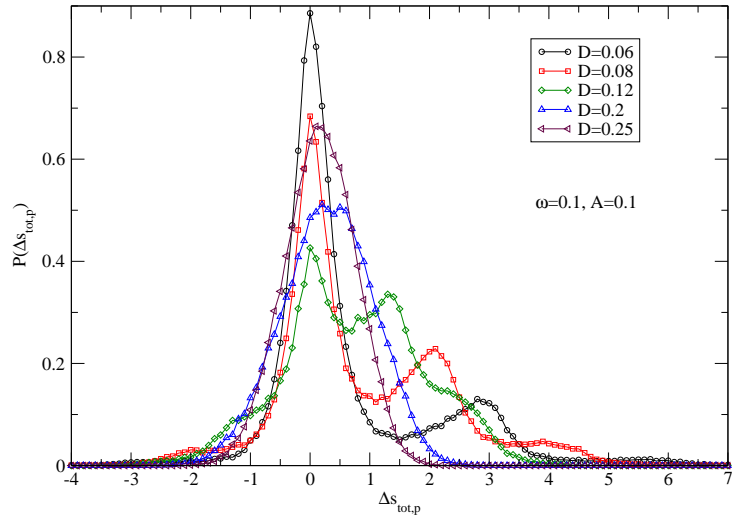


Figure 5.4: Plots of probability distribution functions of $\Delta s_{tot,p}$ for different values of noise strength D . The fixed parameters are: $A = 0.1$, $\omega = 0.1$.

In figure 5.4, we have plotted the probability distribution $P(\Delta s_{tot,p})$ versus $\Delta s_{tot,p}$, for different values of noise strength spanning a region of temperatures around that of SR ($D = 0.12$).

For low temperature side, $D = 0.06$, $P(\Delta_{S_{tot,p}})$ exhibits a double peak structure. The peak around zero can be attributed to the intrawell motion. The small peak at higher positive values of $\Delta_{S_{tot,p}}$ is caused by the occasional interwell transition which entails larger heat dissipation in the medium and contributes to the total entropy production via entropy produced in the bath, $\langle \Delta_{S_{m,p}} \rangle = \langle Q_p \rangle / T$. At very low temperature, $D = 0.02$, the interwell motion is subdominant (particle exhibits small oscillations about the minimum). $P(\Delta_{S_{tot,p}})$ exhibits a single peak around $\langle \Delta_{S_{tot,p}} \rangle$ and the distribution is closer to Gaussian, which is not shown in the graphs. As temperature is increased, due to the enhancement of interwell motion, peak at the right increases. These multi peaked distributions are asymmetric. The distributions extend to the negative side. Finite values of distributions in the negative side are necessary to satisfy fluctuation theorems. The contribution to the negative side comes from the trajectories which lead to transient violations of the second law. For higher values of temperature, $D = 0.25$ (and beyond), the peak structures merge and $P(\Delta_{S_{tot,p}})$ becomes closer to a Gaussian distribution. Similar observations have been made for distributions of work and heat in earlier literature [68, 69]. The observed values of $\langle e^{-\Delta_{S_{tot,p}}} \rangle$, from our simulations, are equal to 1.045, 1.017, 0.980, 1.024 and 1.032, for values of temperatures $D = 0.06, 0.08, 0.12, 0.2$ and 0.25 , respectively. All the values for $\langle e^{-\Delta_{S_{tot,p}}} \rangle$ are close to unity within our numerical accuracy, which is clearly consistent with IFT (equation (5.5)).

We have plotted $P(\Delta_{S_{tot,p}})$ and $P(-\Delta_{S_{tot,p}})e^{\Delta_{S_{tot,p}}}$ on the same graph for two values of D ($D = 0.08$ and 0.25) in figures 5.5(a) and (b) respectively, which abides by equation (5.6), namely the DFT. We would like to mention that the IFT and DFT are exact theorems for a driven Langevin system. Our results corresponding to figures 5.5(a) and (b) act as a check on the quality of our simulation.

In figure 5.6, we have plotted probability distributions of changes in total entropy $\Delta_{S_{tot,p}}$, medium entropy $\Delta_{S_{m,p}}$ and system entropy Δ_{S_p} over a single period for the parameter values $D = 0.08$, $\omega = 0.1$ and $A = 0.1$. System entropy $s_p(t)$ is a state function and its average value is a periodic function of time in the asymptotic regime. Thus average change in the system entropy over a period is zero. Moreover, $P(\Delta_{S_p})$ is a symmetric function of Δ_{S_p} . The medium

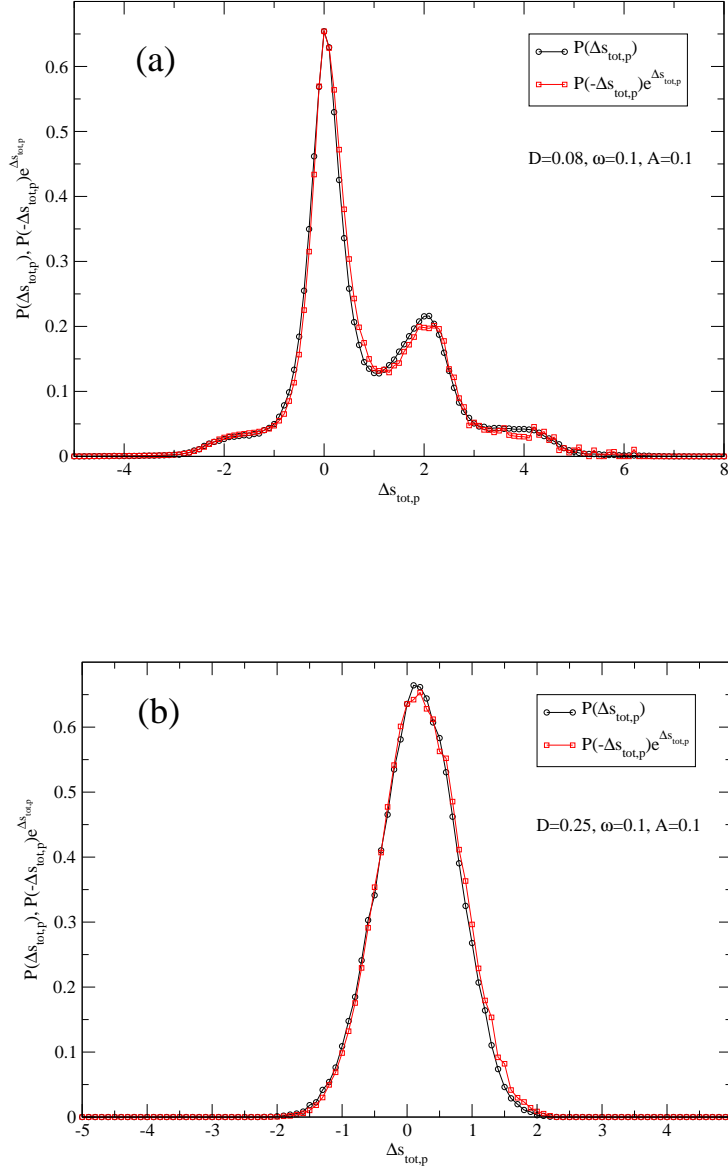


Figure 5.5: (a) Both $P(\Delta S_{tot,p})$ and $P(-\Delta S_{tot,p})e^{\Delta S_{tot,p}}$ have been plotted on the same graph for $D = 0.08$, $\omega = 0.1$ and $A = 0.1$. These curves match to a good accuracy, thereby providing a cross-verification for the validity of DFT. (b) Similar plots for $D = 0.25$. Other parameters are the same as in (a).

entropy is related to the heat dissipated along the trajectory ($\Delta S_{m,p} = Q_p/T$). The nature of $P(\Delta S_{m,p})$ is identical to that of heat distribution [69]. All these probabilities exhibit finite contribution to the negative side.

As the observation time of the trajectory increases, there will be decrease in the number of trajectories for which $\Delta S_{tot} < 0$. This is expected as we go to macroscopic scale in time.

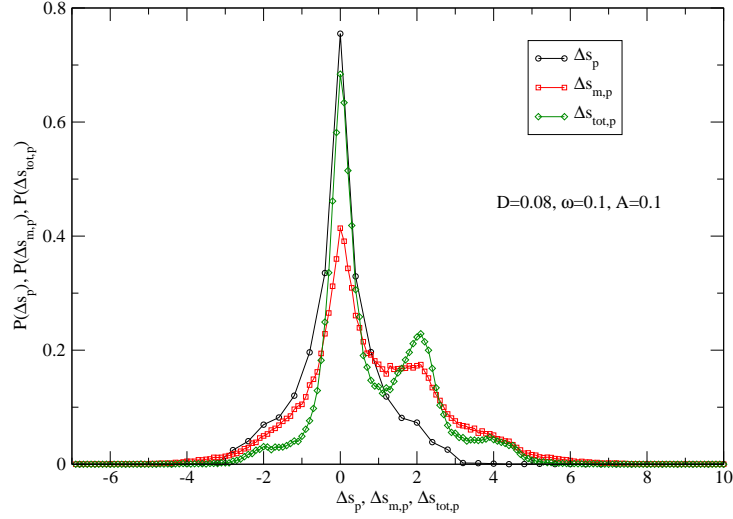


Figure 5.6: Plots showing distribution functions of $\Delta s_{tot,p}$, $\Delta s_{m,p}$ and of Δs_p , for $D = 0.08$, $\omega = 0.1$ and $A = 0.1$.

To this end we have plotted in figure 5.7(a) the $P(\Delta s_{tot,np})$ obtained over different numbers (n) of cycles (or for observation times $\tau = nT_1$, where T_1 is the period of external drive). For a fixed value of the parameters, $D = 0.12$, $A = 0.1$ and $\omega = 0.1$, and over single cycle, $P(\Delta s_{tot,p})$ exhibits multi-peaked structure which slowly disappears as we increase the period of observation. For larger periods, $P(\Delta s_{tot,np})$ tends closer to being a Gaussian distribution with a non-zero positive mean $\langle \Delta s_{tot} \rangle$. We also notice that as the number of periods increases, weight of the probability distributions to the negative side decreases.

In the inset of figure 5.7(a), we have plotted probability density of Δs_{tot} taken over 20 periods. The Gaussian fit is shown. The calculated values of variance, $\sigma^2 = 28.61$, and of the mean, $\langle \Delta s_{tot} \rangle = 14.18$, closely satisfy the condition $\sigma^2 = 2\langle \Delta s_{tot} \rangle$, thereby abiding by the fluctuation-dissipation relation (see equation (18) of [37]). If the distribution is a Gaussian and it satisfies the DFT, then the fluctuation-dissipation theorem $\sigma^2 = 2\langle \Delta s_{tot} \rangle$ must be satisfied [27, 37, 75]. The presence of non-Gaussian tails at large values of $\Delta s_{tot,np}$ are not ruled out (non-Gaussian nature of distribution). However, numerically it is difficult to detect them.

In figure 5.7(b), we have plotted the symmetry functions $\left(\ln \left[\frac{P(\Delta s_{tot,np})}{P(-\Delta s_{tot,np})} \right] \right)$ versus $\Delta s_{tot,np}$ for different periods. Irrespective of the number of periods, we find that slopes of all the curves

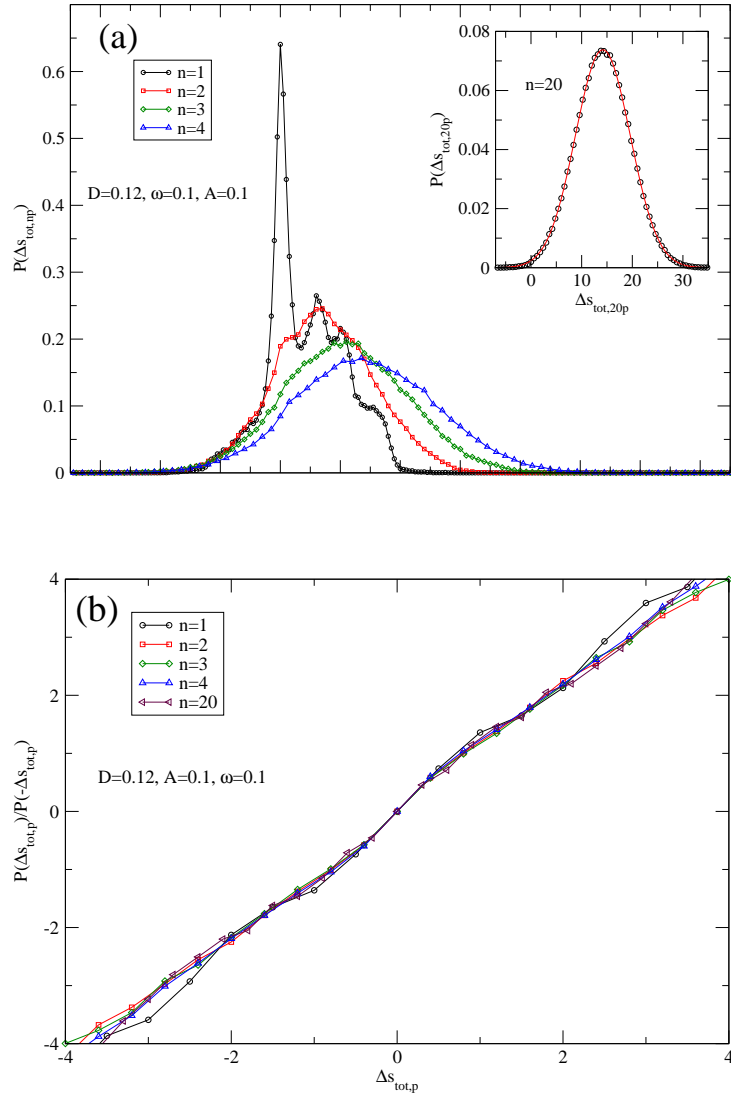


Figure 5.7: (a) Distributions of total entropy for different numbers of periods ($n = 1, 2, 3$ and 4). The inset shows data points for $n = 20$ and the corresponding Gaussian fit with $\sigma^2 = 28.61$ and $\langle \Delta S_{tot,20p} \rangle = 14.18$. Parameter values are: $A = 0.1$, $\omega = 0.1$ and $D = 0.12$. (b) Corresponding plots of symmetry functions of total entropy as a function of total entropy.

are equal to 1, which is consistent with DFT. The validity of DFT implies IFT, but not vice versa.

The medium entropy is extensive in time while the system entropy is not. Only over larger number of periods, the contribution to $\Delta S_{tot,np}$ from ΔS_{np} becomes very small as compared to $\Delta S_{m,np}$. This means that only over large time periods, $\Delta S_{m,np}$ obeys a DFT relation or steady state fluctuation theorem as noted in the earlier literature [16, 69] (see figure 5.8). Strictly speaking, this is valid if the system entropy is bounded. In this figure we have plotted symmetry

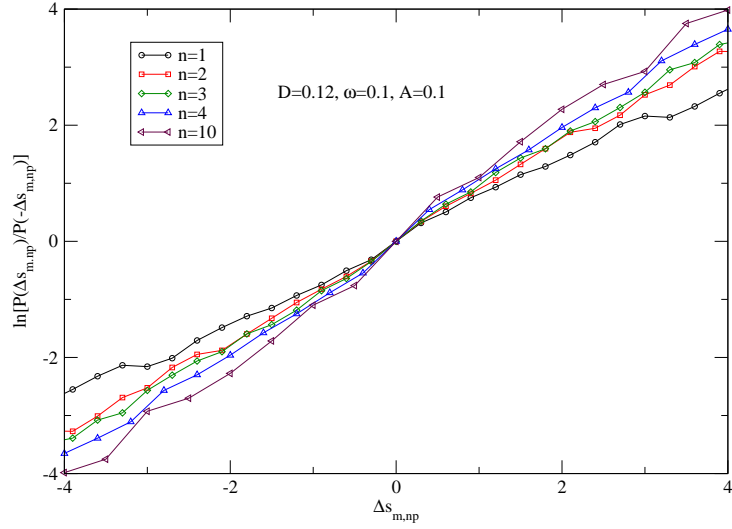


Figure 5.8: The figure gives the plots of symmetry functions of medium entropy as a function of the medium entropy, for different numbers of periods. Parameter values are: $A = 0.1$, $\omega = 0.1$ and $D = 0.12$.

functions for the medium entropy for different numbers of periods (n). As we increase n , the slope increases towards 1 and hence satisfies the DFT for large n . The value of n over which $\Delta s_{m,np}$ follows DFT depends sensitively on the physical parameters, unlike the DFT for $\Delta s_{tot,np}$.

All the results of this work can be tested experimentally by using the experimental setup in [16], and earlier in [65]. Here, the double-well potential was prepared by switching a laser trap very fast between two positions, compared to the relaxation time of the trapped particle. The sinusoidal modulation was achieved by changing the laser intensity harmonically. For other experimental setups that have been used to check for stochastic resonance, see the references cited in sec. II C of [53].

5.4 Conclusion

In conclusion, we have studied the entropy production of a Brownian particle in a driven double well system which exhibits stochastic resonance. Average total entropy production per cycle shows a peak as a function of noise strength. However, it is not directly correlated to stochastic

resonance condition. Moreover, as the period of observation increases, contribution of negative total entropy producing trajectories decreases. In this nonlinear system, we have verified the integral fluctuation theorem valid for time-periodic steady states. In this case, we obtain a rich structure for the probability distribution of trajectory dependent total entropy production.

Chapter 6

Energy fluctuations in a biharmonically driven nonlinear system

6.1 Introduction

In recent theoretical [68, 69] and experimental [7] studies, the distributions of dissipated heat and work done on the system have been explored in a system exhibiting stochastic resonance [68, 69]. The steady state fluctuation theorem (SSFT) holds in this system. Exploring the FTs in nonlinear systems by changing the symmetry of the driving force cycle has been suggested in [7]. To this end, we study the dynamics of a particle in a symmetric double well potential which is in contact with a thermal bath at temperature T . This system exhibits stochastic resonance (SR) under subthreshold external ac drive [54]. Because of its generic nature, this phenomenon boasts applications in almost all areas of natural science [53]. To characterize this resonance phenomenon, several different quantifiers have been introduced in the literature [53, 55, 65, 98–102]. One of the quantifiers, namely the input energy of the system or the work done on the system per cycle is known to characterize SR as a bona fide resonance [55, 68, 69, 102]. In this case, the resonance can be shown to occur both as a function of noise strength and driving frequency.

It is known that static asymmetry in the bistable potential weakens the magnitude of the

SR effect [53, 69]. Static tilt in the potential makes one potential well more stable than the other leading to more particle localization or pumping in one well (lower well) compared to the other. Moreover, due to asymmetry in the potential, escape rate of a particle from higher to lower well will be different from lower to higher well. These two different rates make synchronization difficult between the signal and the dynamics of the particle hopping, since the driving frequency cannot match both these hopping rates simultaneously.

In the present work, we study the SR for a particle in a symmetric double well potential, driven simultaneously by two periodic signals of frequencies ω and 2ω with a relative phase difference ϕ between them [104]. Such a force averaged over a period does not lead to a net bias and yet particle is preferentially pumped into one well depending on phase difference ϕ and other physical parameters [105–111]. This phenomenon is known as *harmonic mixing* [105–108]. Due to this statistical confinement of the particle, similar to the case of static tilt [53, 59], we expect to observe a reduced SR signal in this system. However, contrary to this expectation, we show that the resonance signal is enhanced in the presence of the biharmonic drive at frequency 2ω when analyzed in terms of the average input energy (or the average work done) per cycle, as a quantifier of SR. Using stochastic energetics [23, 28, 112] we also study the nature of fluctuations in the work done, dissipated heat and internal energy across SR. In some range of parameters, nature of hysteresis loops is analyzed. We show that the SSFT holds for work done and heat dissipated over a long time interval. These results can be tested experimentally, by using the setup discussed in chapter 5 (see [16] for details).

6.2 The Model: Brownian particle in a Rocked Double Well

Potential

We consider the stochastic dynamics of an overdamped Brownian particle in a double-well potential $V(x) = -\frac{x^2}{2} + \frac{x^4}{4}$ (see figure 5.1), rocked by a weak biharmonic (time-asymmetric) external field $F(t) = A \cos(\omega t) + B \cos(2\omega t + \phi)$. The potential $V(x)$ has two minima at $x = \pm 1$, separated by a central potential barrier of height $\Delta V = 0.25$. The overdamped

Langevin dynamics is given by [48],

$$\gamma \frac{dx}{dt} = -\frac{\partial U(x, t)}{\partial x} + \xi(t), \quad (6.1)$$

where $U(x, t) = V(x) - xF(t)$, γ is the friction coefficient, $\xi(t)$ is the Gaussian white noise with the properties $\langle \xi(t) \rangle = 0$ and $\langle \xi(t)\xi(t') \rangle = 2D\delta(t - t')$, where $D = \gamma k_B T$. The thermodynamic work done by an external drive over a period $\tau_\omega (= \frac{2\pi}{\omega})$ is given by [23]

$$\begin{aligned} W_p &= \int_{t_0}^{t_0+\tau_\omega} \frac{\partial U(x, t)}{\partial t} dt \\ &= \int_{t_0}^{t_0+\tau_\omega} x(t) [A\omega \sin \omega t + 2B\omega \sin(2\omega t + \phi)] dt. \end{aligned} \quad (6.2)$$

This work (or input energy) over a period equals the change in the internal energy $\Delta U_p = U(x(t_0 + \tau_\omega), t_0 + \tau_\omega) - U(x(t_0), t_0)$ plus the heat dissipated over a period Q_p , i.e.,

$$W_p = \Delta U_p + Q_p. \quad (6.3)$$

The above equation is the statement of the First law of thermodynamics and can readily be obtained using stochastic energetics [23]. The above model is solved numerically by using Heun's method [67] (all the physical quantities are in dimensionless units). We have ignored the initial transient regime up to time t_0 , after which the system settles into a time-periodic steady state. Then we have evaluated W_p , Q_p , and ΔU_p over many cycles ($\sim 10^5$) of a single long trajectory of the particle.

We note that all our results can be verified experimentally, using the setup used in [16].

6.3 Results and Discussions

6.3.1 SR as a function of noise strength

In figure 6.1, we have plotted the average work done over a single period $\langle W_p \rangle$ in the time asymptotic regime as a function of noise strength D for different values of biharmonic drive strength B (for $A=0.1$). Phase difference ϕ is taken to be zero. Other parameters are mentioned in the figure captions. For the case of $B = 0$ we have reproduced earlier results [55,68,69,102]. The average input energy ($\langle W_p \rangle$) shows a peak signifying SR as discussed extensively in earlier literature [55, 68, 69, 102]. The quantity $\langle W_p \rangle$ can also be identified as the average dissipated heat or hysteresis loss into the bath in a time periodic steady state. This follows from eq. (4) by noting that the internal energy being a state variable, ΔU_p averaged over a period is identically equal to zero. For different values of B , the system exhibits SR as a function of noise strength. The system in a steady state absorbs energy from the external drive and the same is dissipated as heat, on average, into the surrounding medium. It is expected that at the resonance the system will absorb maximum energy from the external drive. The input energy curves for higher values of B lie above those for the lower values of B . With increase in B , the peak position shifts towards higher values of D .

It is evident from the figure that in the presence of biharmonic drive enhancement of SR signal occurs even though there is more statistical confinement of the particle (as B increases) in one well as shown in figure 6.2. In this figure we have plotted average position ($\langle x \rangle$) over a single period in the time asymptotic regime as a function of B for fixed $D = 0.05$. The value of $\langle x \rangle$ not being zero signifies selective pumping or localization of particle from one well to another in the presence of biharmonic drive. Correspondingly, the probability density distribution of the particle averaged over a period shows a marked asymmetry even though the potential $V(x)$ is symmetric [107]. In the absence of second harmonic component i.e., $B = 0$, $\langle x \rangle = 0$ as expected. The pumping is very significant at low values of temperature. As we increase temperature, the effective pumping reduces. Around and beyond SR, pumping is quite small as shown in the inset of figure 6.2.

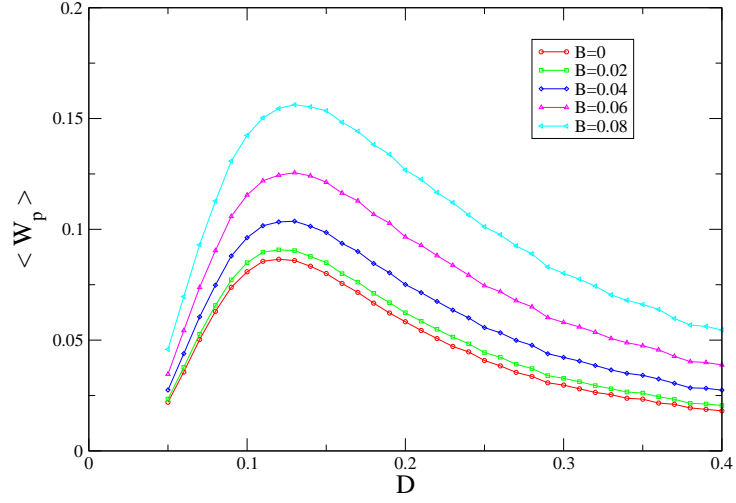


Figure 6.1: The input energy $\langle W_p \rangle$ as a function of D for different values of the strength of second harmonic (B). The parameters are: $\omega = 0.1$, $A = 0.1$, and $\phi = 0$.

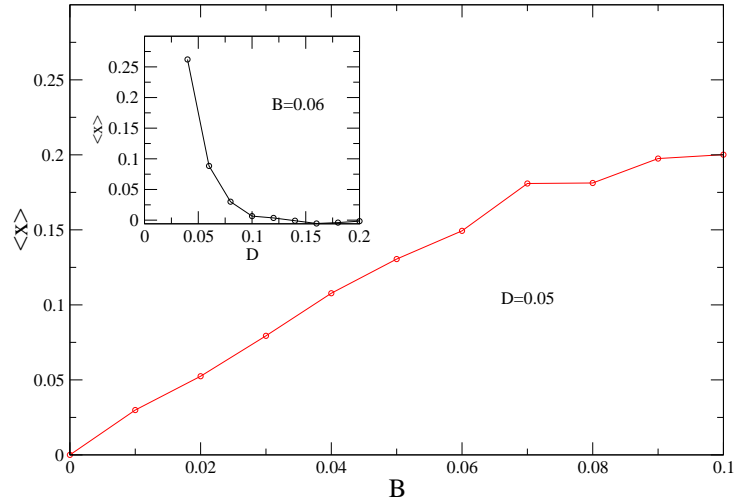


Figure 6.2: Particle mean position $\langle x \rangle$ as a function of B for $D = 0.05$. In the inset we have plotted $\langle x \rangle$ as a function D . Other parameters are: $B = 0.06$, $A = 0.1$, and $\omega = 0.1$.

Stochastic resonance being a synchronization phenomenon [99, 101] it is expected that particle hopping dynamics between the wells get synchronized with the input signal. We expect that the relative variance (RV) in physical quantities such as work $\left[= \frac{\sqrt{\langle W_p^2 \rangle - \langle W_p \rangle^2}}{\langle W_p \rangle} \right]$ and heat $\left[= \frac{\sqrt{\langle Q_p^2 \rangle - \langle Q_p \rangle^2}}{\langle Q_p \rangle} \right]$ also show minima at SR [7, 68, 69]. In figure 6.3 we have plotted relative variance (RV) as a function of D for various values of B . The parameters used are the same as in figure 6.1. For a given value of B the RV shows a minimum around the same value of D at

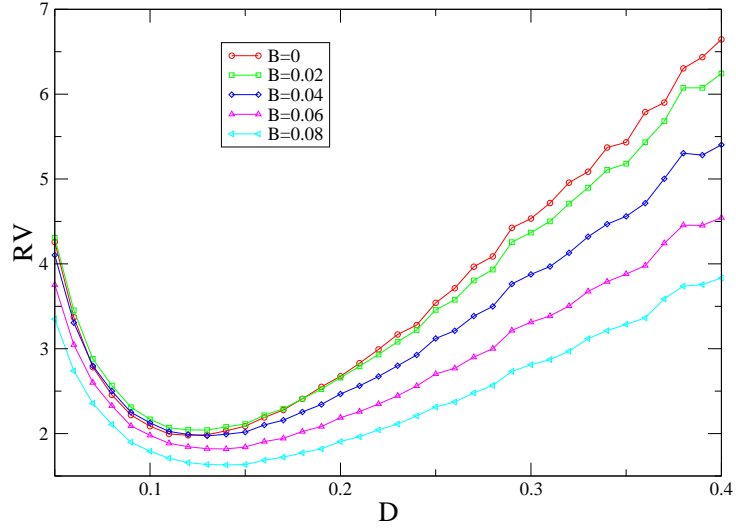


Figure 6.3: Relative variance (RV) of input energy versus D for different values of B . Other parameters are same as in figure 1.

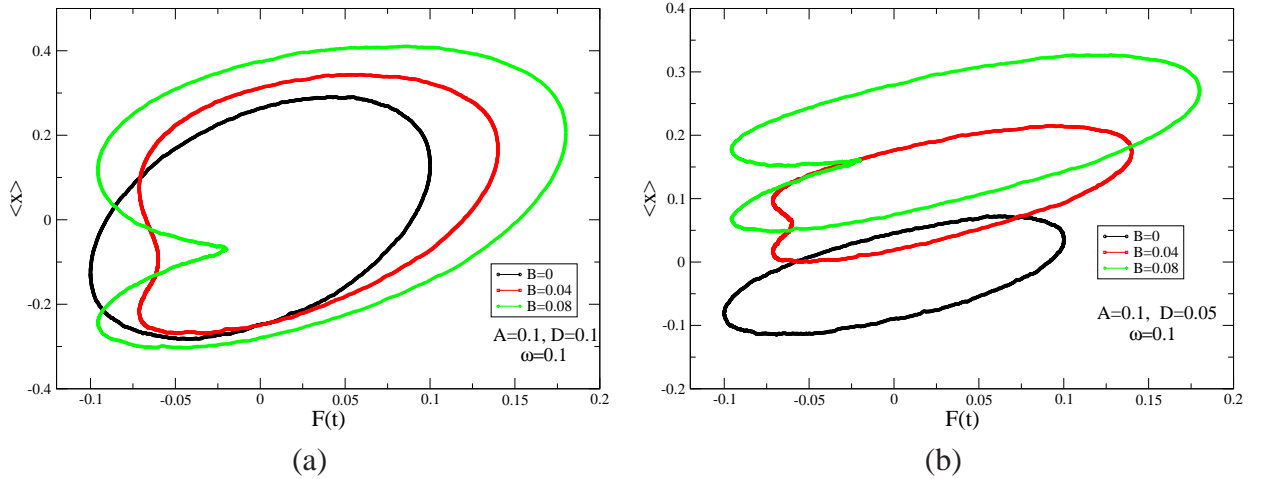


Figure 6.4: (a) Hysteresis loops ($\langle x \rangle$ vs F) for different values of B , and for $D = 0.1$. Other parameters are same in figure 1. (b) Hysteresis loops for different values of B at $D = 0.05$.

which $\langle W_p \rangle$ exhibits a maximum. As the amplitude of the biharmonic drive B increases, RV curves shift downwards. Higher the value of B , the lower is the value of RV at the resonance. These results are consistent with figure 6.1. In the parameter regime that we have considered, the RV is larger than one, i.e., variance in work is large compared to the mean. Hence in this regime, one should analyze full probability distribution as opposed to moments to get better understanding of the phenomenon.

Increasing the amplitude of biharmonic drive leads to more statistical confinement of particles (figure 6.2). This must be reflected in the nature of hysteresis loops [101, 109]. More

the pumping, more is the asymmetry in the hysteresis loops, as can be seen in figure 6.4(a) and (b). In these figures hysteresis loops are plotted for different values of D and B . The pumping of the particles also gets reflected in the shifting of figures in the vertical upward direction (as $\langle x \rangle > 0$). For the case when $B = 0$, there will be no pumping and as expected, the loop is symmetric.

6.3.2 SR in the presence of static tilt

Particle pumping in a preferential well can also be induced by applying a static tilt to the otherwise symmetric double well potential. For this we take potential to be $V_1(x) = -\frac{x^2}{2} + \frac{x^4}{4} - cx$. Depending on the value of c , the potential $V_1(x)$ becomes asymmetric and obviously more pumping results in the lower potential well. When this system is driven by external AC force $A \cos \omega t$ we show that SR signal weakens.

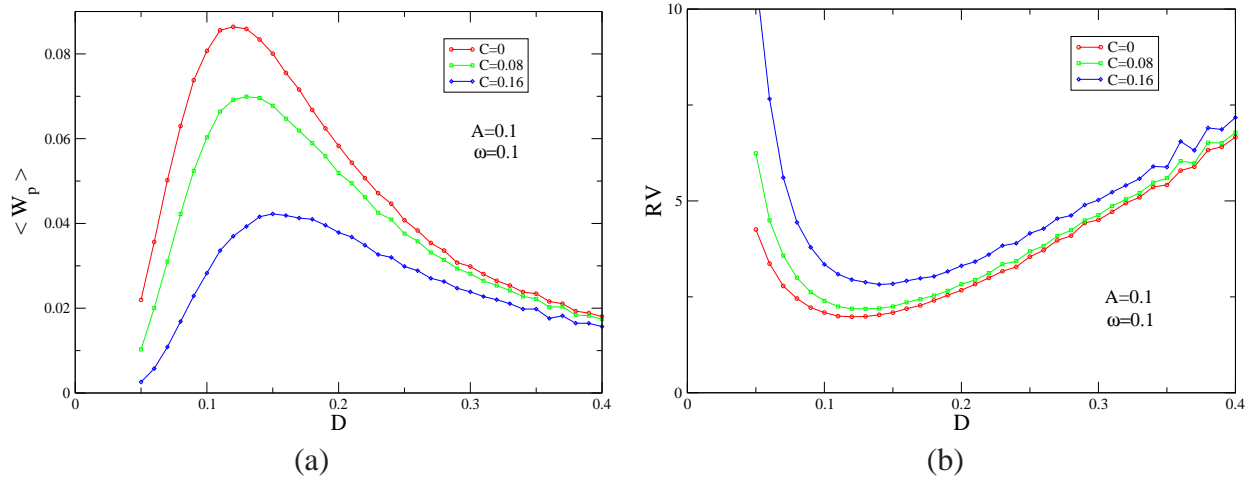


Figure 6.5: (a) Plots of $\langle W_p \rangle$ as a function of D for different values of the static tilt (c). (b) Corresponding plots of relative variance of W_p as a function of D . Fixed parameters are mentioned on the graphs.

Figure 6.5(a) shows the average input energy as a function of D for various values of c . From this, we notice that the input energy curves for higher value of c are below those with lower value of c (other parameters being fixed). As c increases SR peak becomes broadened and shifts towards higher values of D . We thus observe that in the presence of pumping induced by static tilt, SR weakens as mentioned in the introduction to this chapter. This is also corroborated

by the nature of relative work fluctuations as a function of D (figure 6.5(b)). From this figure we note that as we increase c , RV increases for a given value of D . The magnitude of the RV at the minimum becomes larger as we increase c . This implies degradation of SR signal in the presence of particle pumping induced by a static tilt.

The pumping due to static tilt makes the hysteresis loops asymmetric (figure 6.6). By increasing c , more pumping is achieved and this is reflected in the vertical shift of hysteresis loops. Thus from the above figures and discussions, we conclude that in the presence of biharmonic drive, SR increases while in the presence of static tilt, SR weakens.

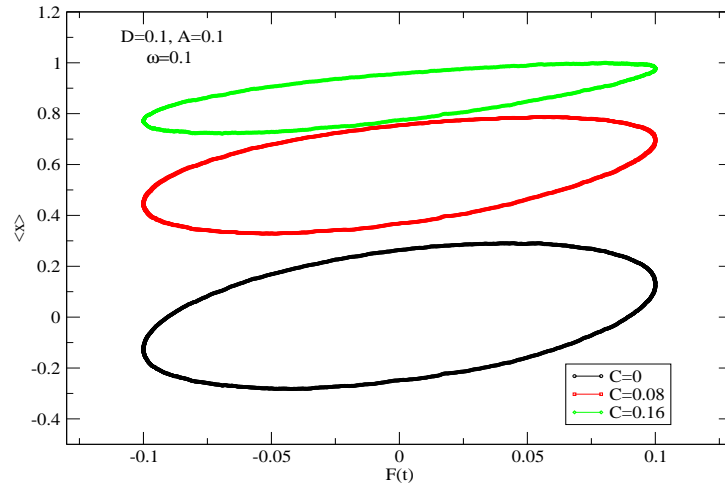


Figure 6.6: Plots showing hysteresis loops, $\langle x \rangle$ vs F , for different values of static tilt (c). Fixed parameters are: $D = 0.1, A = 0.1$ and $\omega = 0.1$.

6.3.3 SR as a function of driving frequency

In figure 6.7(a), we have plotted average input energy as a function of ω for various values of B . Once again we notice that SR signal even for this case is increased as we increase the biharmonic component B . Each curve exhibits a peak as a function of ω , thus establishing SR as a bona fide resonance. The peak shifts to the lower values of ω as we increase B . This is consistent with the fact that peaks in figure 6.1 shift towards larger values of D as we increase B . This is a requirement for the time scale matching between D and ω . Since increase in B

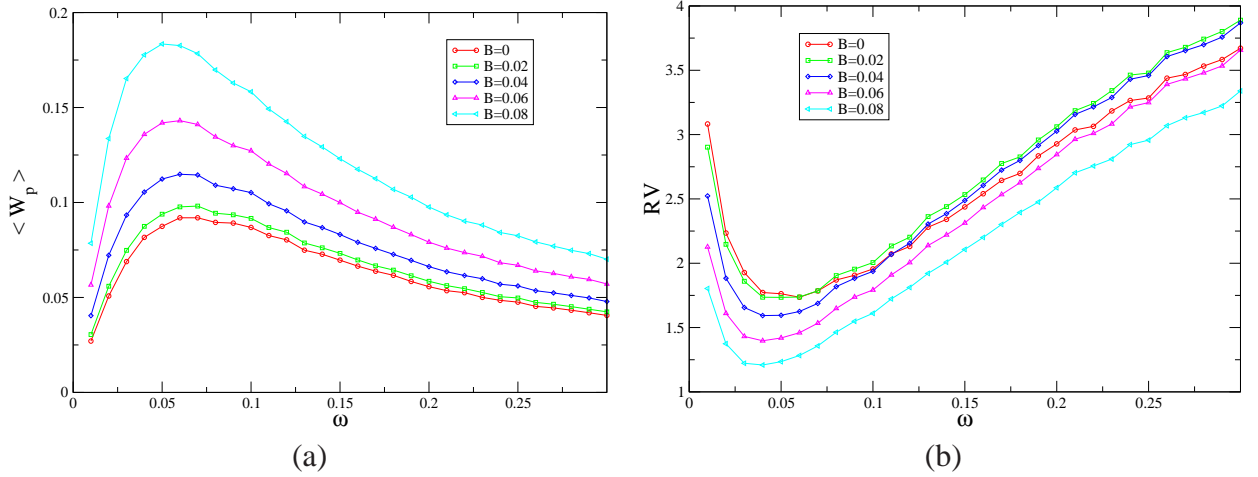


Figure 6.7: (a) The average input energy per period $\langle W_p \rangle$ as a function of frequency ω . (b) Relative variance (RV) of input energy vs frequency ω for different values of the strength of the second harmonic, B . The parameters used are: $\omega = 0.1$, $A = 0.1$, $\phi = 0$.

slows down the effective time averaged hopping rates between the wells, higher D is required to achieve resonance. This lowering of effective escape rate at given D in turn implies decrease in the resonant frequency. The enhancement of SR signal in the presence of B can be inferred from figure 6.7(b) where we have plotted relative variance across the SR as a function of ω for various values of B . Lower values of relative variance across the SR for larger values of B are suggestive of the fact that SR is enhanced in the presence of biharmonic drive, consistent with the conclusions of figure 6.1.

6.3.4 Energy fluctuations over a single period

Next, we analyze the nature of distribution functions of input energy $P(W_p)$, dissipated heat $P(Q_p)$ and internal energy $P(\Delta U_p)$ for different values of D . These distributions are plotted in figure 6.8 (a), (b), and (c) below resonance ($D = 0.05$), at resonance ($D = 0.12$), and above resonance ($D = 0.3$) respectively. The averaged internal energy $\langle U \rangle$ being a state function assumes the same value at the beginning and at the end of a period or periods in the time asymptotic regime. Hence average change in the internal energy $\langle \Delta U_p \rangle$ over a period is equal to zero and it is also expected that the distribution $P(\Delta U_p)$ is symmetric as is evident from figure 6.8 (a), (b) and (c). The nature of $P(\Delta U_p)$ is explained in [7] for a single harmonic

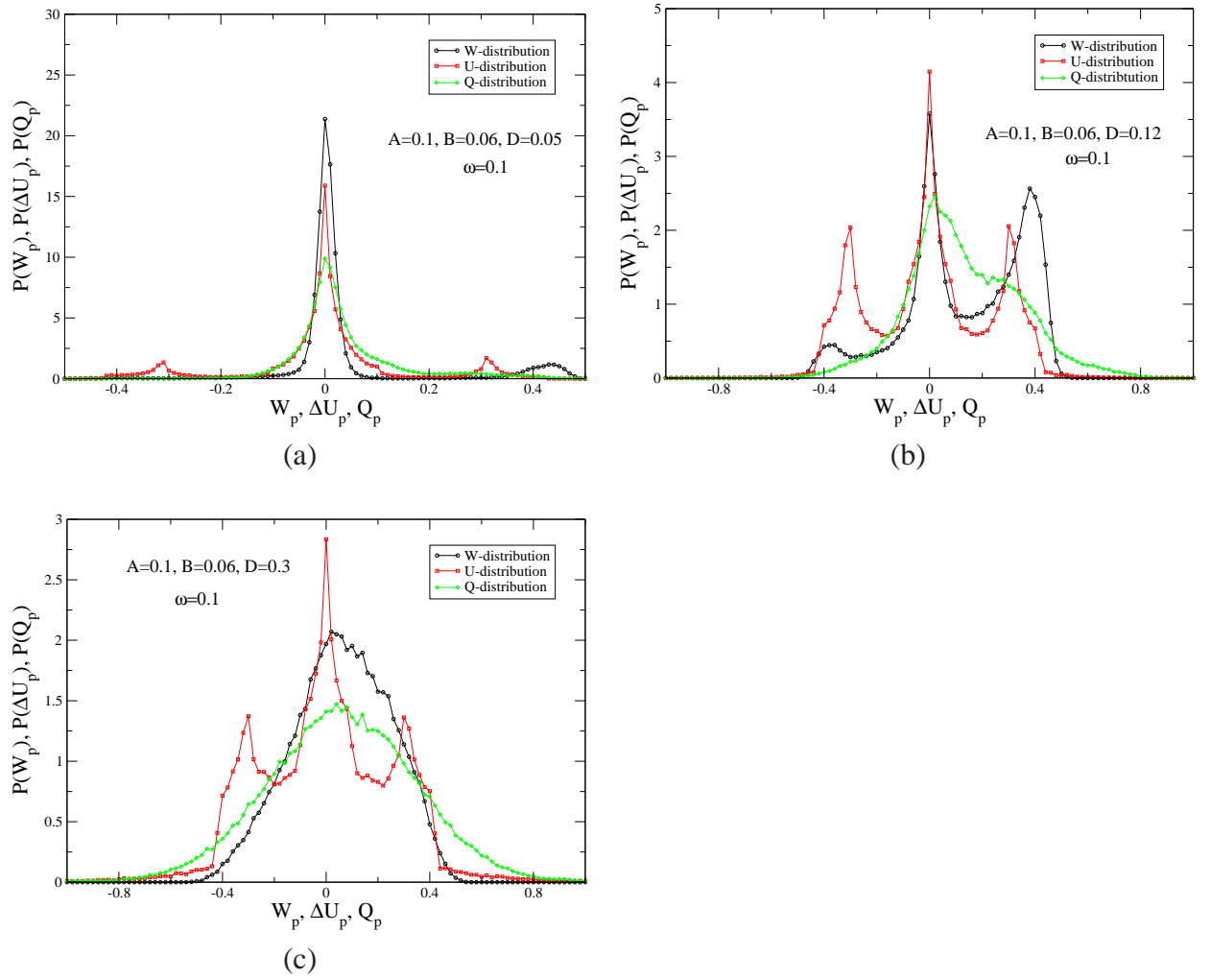


Figure 6.8: Plots (a), (b), and (c) show the distributions $P(W_p)$, $P(Q_p)$, and $P(\Delta U_p)$ for different values of D , below resonance ($D = 0.05$), at resonance ($D = 0.12$), and above resonance ($D = 0.3$), respectively. Other fixed parameters are also shown on the graphs.

drive. As opposed to ΔU_p , distributions for W_p and Q_p are asymmetric. These distributions keep on changing in shape depending on the number of cycles over which they have been obtained which will be discussed later in connection with steady state fluctuation theorem (SSFT). Probability distributions for work and heat have finite weights for the negative values of their arguments. These negative values correspond to the trajectories where the particle moves against the perturbing AC field over a short time. For small values of D ($D = 0.05$), peak for W_p or Q_p near the origin corresponds mainly to intrawell dynamics of the particle and is mostly confined to a single well. The occasional excursion of the particle into the other well as a function of time is clearly reflected as a small hump at higher values of W_p or Q_p in the plot of $P(W_p)$ and

$P(Q_p)$. As we increase D further ($D = 0.12$), interwell dynamics starts playing a dominant role, and hence the distributions become broader. Work distribution exhibits three prominent peaks including one at the negative side. For larger values of D beyond SR point, shapes of $P(W_p)$ and $P(Q_p)$ tend closer to Gaussian distribution with increased variance/fluctuations. For such high temperatures, particle makes several random excursions between the two wells during a single time period of the external drive. It may be noted that the relative variances in W_p and Q_p are larger than 1. Also, fluctuations in heat are larger than those of work when averaged over a single period.

6.3.5 Effect of phase difference on SR

We now analyze the role of phase difference (ϕ) between driving fields on pumping and energetics of the system. In figure 6.9 (a), we have plotted $\langle W_p \rangle$ as a function of noise strength D for various values of ϕ . Other physical parameters are held fixed as mentioned in the figure captions. In figure 6.9 (b), we have plotted relative variance of W_p as a function of D . It is interesting to note that $\langle W_p \rangle$ is insensitive to ϕ , even though the relative variance depends on ϕ . This is a rather surprising result, given the fact that different values of phase ϕ lead to different degrees of localization of the particle in one of the wells.

We have characterized this dynamic localization of particles by average position $\langle x \rangle$ of the particle in the double well potential which in fact can be large depending on D and ϕ . This is shown in figure 6.10 where we have plotted $\langle x \rangle$ as a function of ϕ for two different values of noise strength D . One can readily see that $\langle x \rangle$ is periodic in ϕ as expected.

The insensitivity of $\langle W_p \rangle$ on phase gets reflected in the hysteresis loop areas as shown in figures 6.11 (a) ($D = 0.1$) and (b) ($D = 0.05$) for different values of ϕ and fixed value of B ($B = 0.06$). We notice that the areas of the hysteresis loops remain same for different ϕ . However, their shapes are asymmetric and qualitatively different for different ϕ (i.e., sensitive dependence on phase ϕ). Due to the different degree of localization or pumping, loops are shifted in $\langle x \rangle - F$ plane.

The sensitivity of full probability distribution on the phase difference can be seen from

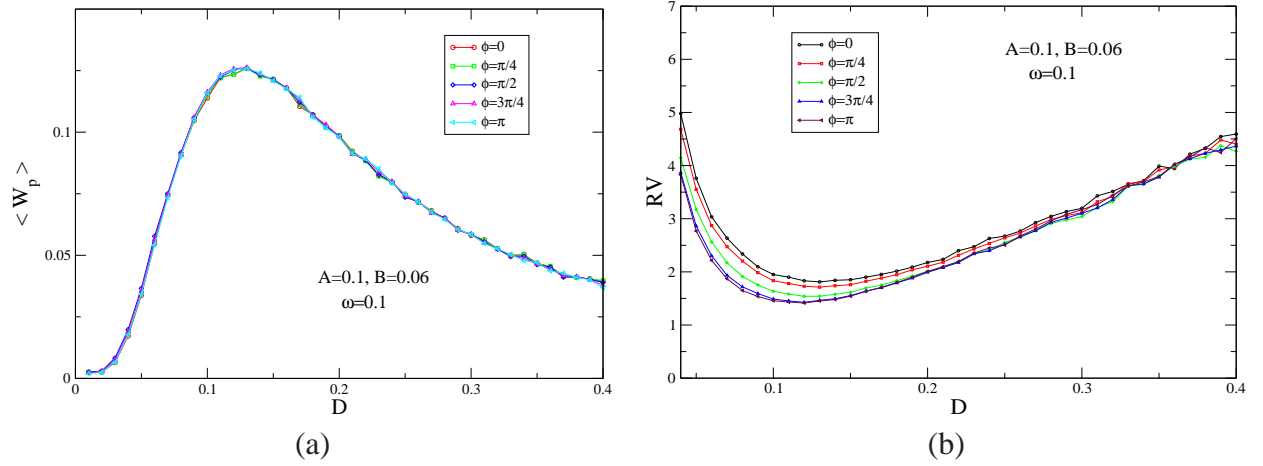


Figure 6.9: (a) The average input energy per period $\langle W_p \rangle$ as a function of D and frequency ω for various values of the phase difference ϕ . (b) relative variances (RV) of W_p versus D . Fixed parameters are shown on the graphs.

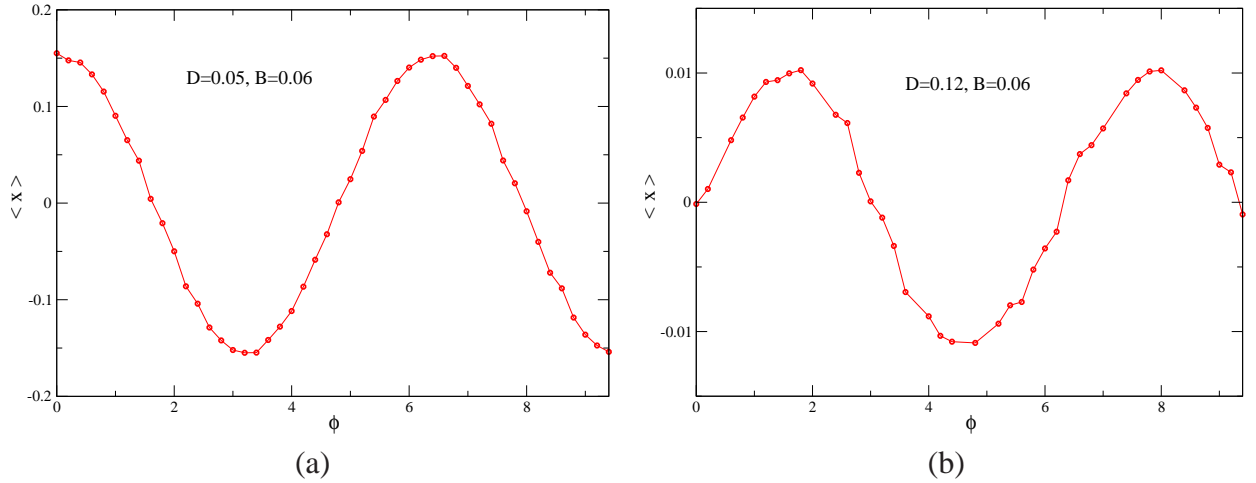


Figure 6.10: Average position $\langle x \rangle$ as a function of phase ϕ for two different values of D . In (a), $D = 0.05$, and in (b), $D = 0.12$. Other fixed parameters are: $B = 0.06$, $A = 0.1$, and $\omega = 0.1$

figures 6.12. In these figures we have plotted $P(W_p)$ and $P(Q_p)$ for different values of ϕ as indicated. Note that the distributions exhibit qualitative differences for different ϕ . We have also verified separately that for different values of rocking amplitudes, as long as we are in subthreshold regime, average input energy is not very sensitive to ϕ as opposed to full probability distribution. By tuning ϕ , one can achieve different degrees of particle confinement and can control the fluctuations in heat and work.

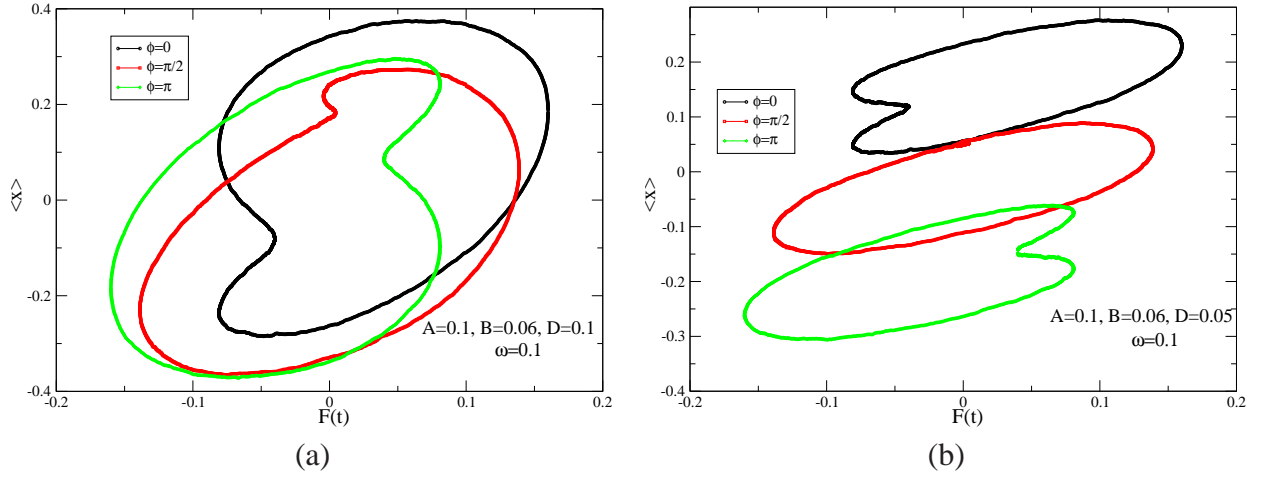


Figure 6.11: (a) Hysteresis loops for different values of ϕ at $D = 0.1$, (b) Hysteresis loops for different ϕ at $D = 0.05$, with other parameters $A = 0.1$, $B = 0.06$, and $\omega = 0.1$

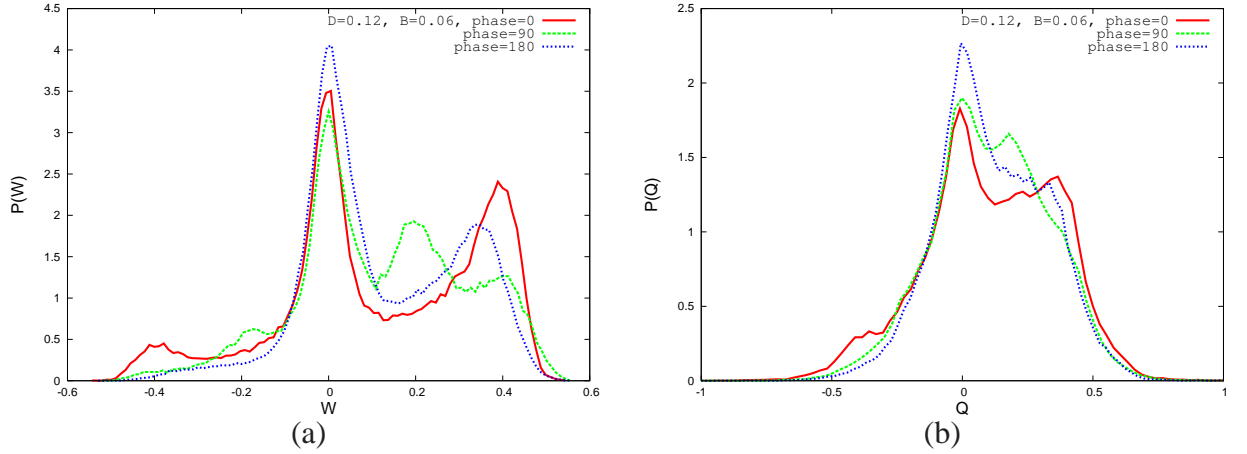
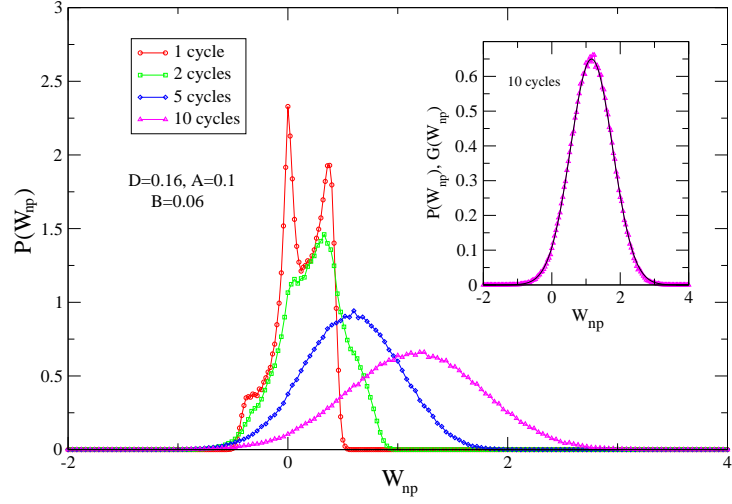


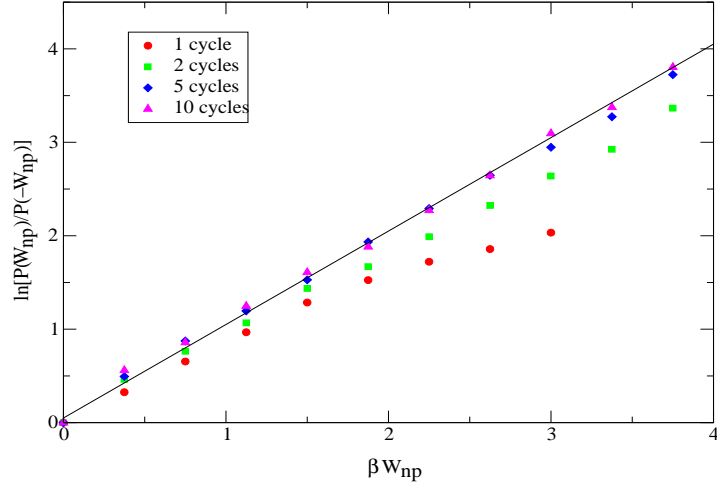
Figure 6.12: Figures (a) and (b) show the distributions $P(W_p)$ and $P(Q_p)$ respectively for three different values of phase: $\phi = 0, \pi/2$ and π . Here $D = 0.12$ and $B = 0.06$.

6.3.6 Energy fluctuations and SSFT

Finally we discuss the validity of SSFT in the present case of nonequilibrium time periodic steady state. Here, by SSFT we would mean the probability distribution of physical quantity A to satisfy relation $p(A)/p(-A) = e^{\beta A}$, where β is the inverse temperature of the bath and A is the work done on the system or the heat released to the bath over a long time of observation. For nonlinear systems it has been observed experimentally and theoretically that SSFT is satisfied if one considers work done over a large number of cycles [68, 69, 113]. In regard to heat, SSFT is known to be valid for $Q < \langle Q \rangle$ [114]. Since $\langle Q \rangle$ increases with the number of periods or



(a)



(b)

Figure 6.13: (a) The evolution of $P(W_p)$ over different periods. In the inset $P(W_{10p})$ is plotted together with its Gaussian fit $G(W)$. (b) The plot of symmetry function $(\ln \frac{P(W_{np})}{P(-W_{np})})$ versus βW_{np} for various values of periods. The parameters used are: $D = 0.16, \omega = 0.1, B = 0.06, A = 0.1, \phi = 0$. The solid line is the best fit for symmetry function calculated for 10 cycles.

measured time interval in the limit of large n ($n \rightarrow \infty$), $\langle Q \rangle \rightarrow \infty$ and hence the conventional SSFT is valid over an entire range of Q [115]. It may be noted that there exists an alternative relation for heat fluctuation, namely extended heat fluctuation theorem [40, 114].

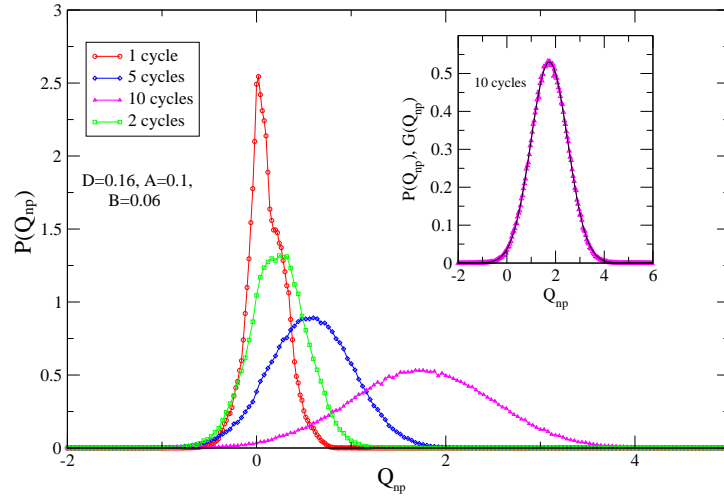
In figure 6.13(a) we have plotted probability distribution $P(W_{np})$ of work W_{np} integrated over different number (n) of periods. $P(W_{np})$ for a single period exhibits double peak struc-

ture. As we increase the number of periods the probability distribution shifts towards right as the mean value of work scales linearly with n . Fine structure in probability distributions get smeared out progressively and distribution tends towards a Gaussian. In the inset of figure 6.13 (a) we have shown the Gaussian fit for the obtained distribution for 10 cycles. From this fit we obtain $\langle W_{10p} \rangle = 1.16$ and variance $\sigma^2 \equiv \langle W^2 \rangle - \langle W \rangle^2 = 0.37$. From this we can obtain dissipation ratio $R_{diss} = \frac{\langle W^2 \rangle - \langle W \rangle^2}{2\langle W \rangle / \beta} \simeq 1$, i.e., the variance equals $\frac{2}{\beta} \langle W \rangle$ which is the required condition to satisfy SSFT when observed distribution is Gaussian [68, 116, 117].

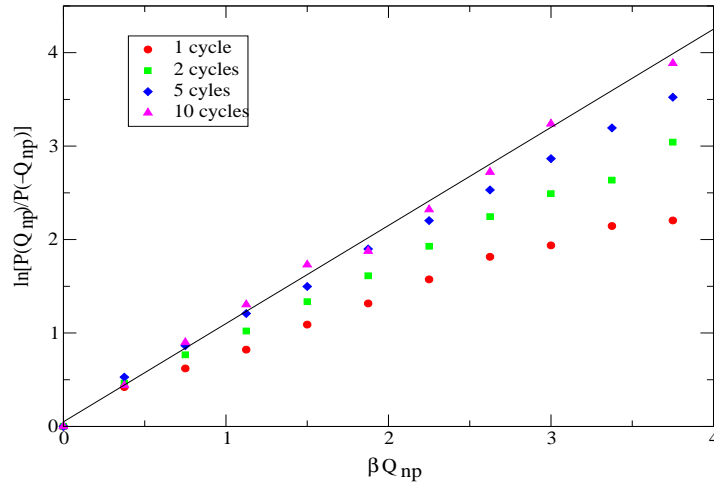
The validity of SSFT for work is also observed from figure 6.13(b) where we have plotted the symmetry function $(\ln \frac{P(W_{np})}{P(-W_{np})})$ versus βW_{np} for work evaluated over different cycles as indicated in the figure. As we increase the number of periods from 1 to 10 the slope of symmetry function approaches 1. The number of periods above which SSFT is valid depends sensitively on the parameters in the problem.

As already noted heat fluctuations over a cycle are large compared to work fluctuations. The heat fluctuations get an additional contribution from the internal energy (eq. (6.3)). The contribution from internal energy is supposed to dominate at very large values of Q , making the distribution $P(Q)$ exponential in the large Q limit [40, 114]. However, it may be noted that the distribution of the change in internal energy does not change with number of periods. Heat being an extensive quantity in time, distribution changes as we change the number of periods as shown in figure 6.14(a) where we have plotted $P(Q_{np})$ for various values of n . As anticipated, by increasing n , the distribution tends towards the a Gaussian (see for $n=10$ cycles). The Gaussian fit for the $P(Q_{np})$ (inset of figure 6.14(a)) gives the value for the variance as 0.56, and mean as 1.74. Thus dissipation ratio is 0.99, which is closer to unity, satisfying SSFT. In principle, one should be able to observe exponential tails for the distribution $P(Q)$ in the large Q limit [40]. However, our simulations will not be able to detect it due to lack of required precision. As mentioned earlier, in the limit $n \rightarrow \infty$, conventional SSFT holds for heat distributions [113].

In figure 6.14(b), we have plotted the symmetry functions $(\ln \frac{P(Q_{np})}{P(-Q_{np})})$ as a function of βQ_{np} . The slope of the symmetry function approaches unity as we increase n , thereby suggest-



(a)



(b)

Figure 6.14: (a) The evolution of $P(Q_p)$ over different periods. In the inset $P(Q_{10p})$ is plotted together with its Gaussian fit $G(Q)$. (b) The plot of symmetry function $(\ln \frac{P(Q_{np})}{P(-Q_{np})})$ versus βQ_{np} for various values of periods. The solid line is the best fit for symmetry function calculated for 10 cycles. The parameters used are same as in figure 13.

ing the validity of SSFT.

6.4 Conclusion

In conclusion, we have studied the nature of energy fluctuations in a biharmonically driven bistable system. This system is driven simultaneously with two periodic input signals of fre-

quencies ω and 2ω , having phase difference ϕ between them. The presence of additional periodic drive induces particle confinement or localization in a preferred potential well. The degree of confinement analyzed in terms of the averaged value of the particle position $\langle x \rangle$ depends on the system parameters. We have shown that in spite of confinement, SR signal when quantified via the averaged work per period exhibits enhanced response. This is in sharp contrast to the case when confinement is induced by static tilt, which degrades SR. Surprisingly, the average input energy over a period is not very sensitive to ϕ even though variation of ϕ leads to significant particle pumping. However, changes in ϕ does affect qualitatively the nature of hysteresis loop and distributions/fluctuations of work and heat. We have analyzed the fluctuations in work done, heat dissipated, and internal energy over a large but finite number of periods. Our data suggests that the SSFT for work and heat hold in this system for large number of periods.

Chapter 7

Summary and Conclusions

In this thesis, we have studied some exact relations, called fluctuation relations, that are valid for systems that are perturbed arbitrarily out of equilibrium. Such relations hold good for systems following several different dynamics, for example the Hamiltonian dynamics or stochastic dynamics. We have concerned ourselves mainly with the latter category of systems. There are several relations that are collectively referred to as the fluctuation theorems – the Jarzynski equality and Crooks fluctuation theorems for nonequilibrium work done on the system, the total entropy production fluctuation theorems (both integral and detailed forms) by Seifert, the Hatano-Sasa relation for transitions between steady states, etc.

In this thesis, we have studied the verification of some fluctuation theorems in different situations and model systems, and have put forward a few new ones.

We have observed that Seifert's detailed fluctuation theorem for the total entropy change is valid even in the transient case for a system trapped in a harmonic potential, provided it begins from a state of thermal equilibrium. We have further observed that the two frequently used statements of the second law in terms of total entropy production and dissipated work, are not equivalent. In fact one of them provides a better bound for the average work done. A new quantifier of irreversibility of a process has been proposed.

We have extended several fluctuation theorems, both in classical and the quantum regime, when the system is driven by a feedback controlled external drive. Here, we measure some

observable of the system, and change our drive accordingly. We find that all the relations now involve a corrections term that depend on the mutual information between the measurement outcomes and actual values of observables, when no feedback is applied along the reverse process. We also find that the correction term changes, if the algorithm for the feedback applied along the reverse process is changed. In contrast, the second form extended fluctuation theorems, that is expressed in terms of efficacy parameter (a parameter that decides the efficiency of a feedback), always retains the same form.

We have verified the fluctuation theorems for total entropy change, work done and dissipated heat, when the system is in a time-periodic steady state. In this case, a system present in a bistable potential has been considered, where the phenomenon of stochastic resonance has also been analyzed. In such systems, we have shown that although the fluctuation theorems for total entropy holds exactly over any number of cycles of the external drive, work and heat will follow the steady state fluctuation theorem only if a large enough number of cycles are observed in each experimental realization. In presence of biharmonic drive applied to the same system, we obtain particle confinement into one of the wells, along with a sharper stochastic resonance peak, in clear contrast to the behaviour in presence of a static drive.

Appendix A

Derivation of Crooks work theorem and Seifert's detailed fluctuation theorem for total entropy

A.1 Crooks Theorem for forward and reverse trajectories

The relation is given by [27]

$$\frac{P[X|x_0]}{\tilde{P}[\tilde{X}|\tilde{x}_\tau]} = e^{\beta Q}. \quad (\text{A.1})$$

The left hand side is the ratio of the probability density of a trajectory $X(t)$ in the forward process for initial point x_0 , to the probability density of a trajectory $\tilde{X}(t)$ along the reverse process for the initial point \tilde{x}_τ . Q is the heat dissipated by the system into the bath. The above relation has been proved systems obeying various dynamics, but here we would briefly discuss the case of stochastic dynamics of a Markovian overdamped system.

We first discretize time as $\{t_0 = 0, t_1, \dots, t_N = \tau\}$, and the forward trajectory as $\{x_0 \rightarrow x_1 \rightarrow \dots \rightarrow x_\tau\}$. The reverse trajectory will contain the same sequence of phase points as the forward trajectory but traversed in the opposite direction: $\{x_0 \leftarrow x_1 \leftarrow \dots \leftarrow x_\tau\}$. The external protocol as a function of time is given by $\{\lambda_0 \rightarrow \lambda_1 \rightarrow \dots \rightarrow \lambda_\tau\}$. Along the reverse process, this same sequence gets reversed as $\{\lambda_0 \leftarrow \lambda_1 \leftarrow \dots \leftarrow \lambda_\tau\}$. The forward trajectory

in presence of this protocol can thus be represented by [42]

$$x_0 \xrightarrow{\lambda_1} x_1 \xrightarrow{\lambda_2} x_2 \xrightarrow{\lambda_3} \dots \xrightarrow{\lambda_\tau} x_\tau. \quad (\text{A.2})$$

Each of these steps can once again be broken up as follows [42]:

$$(x_j, \lambda_j) \xrightarrow{\text{work step}} (x_j, \lambda_{j+1}) \xrightarrow{\text{heat step}} (x_{j+1}, \lambda_{j+1}), \quad (\text{A.3})$$

where in the first step, the position remains constant at x_j while the protocol changes from λ_j to λ_{j+1} . This step is called the *work step*. The work done by the protocol in this step is given by the change in the system's energy during this step: $W_j = E(x_j, \lambda_{j+1}) - E(x_j, \lambda_j)$. Here, $E(x, \lambda)$ is the energy of the state x when the value of the protocol is λ . In the second step, the protocol remains fixed at λ_{j+1} , while the position changes from x_j to x_{j+1} . This is called the *heat step*, in which the heat dissipated is $Q_j = -[E(x_{j+1}, \lambda_{j+1}) - E(x_j, \lambda_{j+1})]$.

We next assume that the transition probabilities between two states x_j and x_{j+1} , follow the condition of local detailed balance for a given value of protocol λ_{j+1} [42]:

$$\frac{p_{\lambda_{j+1}}(x_{j+1}|x_j)}{p_{\lambda_{j+1}}(x_j|x_{j+1})} = \exp\{\beta[E(x_j; \lambda_{j+1}) - E(x_{j+1}; \lambda_{j+1})]\} = e^{\beta Q_j}. \quad (\text{A.4})$$

This condition implies that if the parameter is held fixed for a long enough time interval, then the system would reach the equilibrium state that corresponds to this fixed value of the control parameter.

We then get the ratio between the forward and reverse trajectory as (using the Markovian property of the dynamics)

$$\frac{P[X|x_0]}{\tilde{P}[\tilde{X}|x_\tau]} = \frac{p_{\lambda_1}(x_1|x_0)p_{\lambda_2}(x_2|x_1) \cdots p_{\lambda_\tau}(x_\tau|x_{\tau-1})}{p_{\lambda_1}(x_0|x_1)p_{\lambda_2}(x_1|x_2) \cdots p_{\lambda_\tau}(x_{\tau-1}|x_\tau)} = e^{\beta \sum_j Q_j} = e^{\beta Q}, \quad (\text{A.5})$$

with the net dissipated heat in the forward path being given by $Q = \sum_{j=0}^{N-1} Q_j$. This is the well-known Crooks' theorem for the phase space trajectories [27].

For an underdamped system, the reverse trajectory will be given by [27] (as before, the tilde symbol represents switching of the signs of the velocities): $\{\tilde{x}_0 \leftarrow \tilde{x}_1 \leftarrow \dots \leftarrow \tilde{x}_\tau\}$. The Crooks theorem for underdamped systems can be derived using stochastic path-integral formulation¹ [41, 118], and is shown to remain the same as in the overdamped case (eq. (A.5)), except the fact the initial state of the reverse trajectory becomes \tilde{x}_τ instead of x_τ :

$$\frac{P[X|x_0]}{\tilde{P}[\tilde{X}|\tilde{x}_\tau]} = e^{\beta Q}. \quad (\text{A.6})$$

A.2 Crooks work theorem

If the system is initially at equilibrium with the reservoir, then the initial distribution for the forward process will be given by (with parameter value fixed at $\lambda(0) = A$)

$$p_{eq}(x_0) = \frac{e^{-\beta E(x_0)}}{Z(A)}, \quad (\text{A.7})$$

$Z(A)$ being the partition function corresponding to the initial value of the protocol. For the reverse process, the systems begins at thermal equilibrium with the same bath, but now with the value of the external protocol given by $\lambda(\tau) = B$, so that the initial distribution for the reverse process will be given by

$$\tilde{p}_{eq}(x_\tau) = \frac{e^{-\beta E(x_\tau)}}{Z(B)}. \quad (\text{A.8})$$

Here, $Z(B)$ is the partition function corresponding to the final value of the protocol. We have assumed that the equilibrium distribution is invariant under the time-reversal operation: $\tilde{p}_{eq}(\tilde{x}_\tau) = \tilde{p}_{eq}(x_\tau)$. Then from the Crooks heat theorem, we get

$$\begin{aligned} \frac{P[X]}{\tilde{P}[\tilde{X}]} &= \frac{P[X|x_0] p_{eq}(x_0)}{\tilde{P}[\tilde{X}|\tilde{x}_\tau] \tilde{p}_{eq}(x_\tau)} = e^{\beta Q} \frac{e^{-\beta E(x_0)}}{Z(A)} \cdot \frac{Z(B)}{e^{-\beta E(x_\tau)}} \\ &= e^{\beta(Q + \Delta U - \Delta F)}. \end{aligned} \quad (\text{A.9})$$

¹The same treatment can also be applied to the overdamped systems.

On application of the first law, we get

$$\frac{P[X]}{\tilde{P}[\tilde{X}]} = e^{\beta(W[X]-\Delta F)} \quad (\text{A.10})$$

Here, we have explicitly written the work done as a function of the forward trajectory X .

Now, the probability density for work \mathcal{W} done along the forward process is defined as

$$P(\mathcal{W}) \equiv \langle \delta(\mathcal{W} - W[X]) \rangle, \quad (\text{A.11})$$

where $W[X]$ is a path function. We then get

$$\begin{aligned} P(\mathcal{W}) &= \int \mathcal{D}[X] P[X] \delta(\mathcal{W} - W[X]) \\ &= \int \mathcal{D}[X] \tilde{P}[\tilde{X}] e^{\beta(W[X]-\Delta F)} \delta(\mathcal{W} - W[X]) \\ &= e^{\beta(\mathcal{W}-\Delta F)} \int \mathcal{D}[X] \tilde{P}[\tilde{X}] \delta(\mathcal{W} - W[X]) \\ &= e^{\beta(\mathcal{W}-\Delta F)} \int \mathcal{D}[\tilde{X}] \tilde{P}[\tilde{X}] \delta(\mathcal{W} + W[\tilde{X}]) \\ &= \tilde{P}(-\mathcal{W}) e^{\beta(\mathcal{W}-\Delta F)}. \end{aligned} \quad (\text{A.12})$$

Here we have used the relation $W[\tilde{X}] = -W[X]$, and $\mathcal{D}[\tilde{X}] = \mathcal{D}[X]$. The delta-function allows us to take the $e^{\beta\mathcal{W}}$ factor out of the integral, and $e^{-\beta\Delta F}$ is a constant. The above relation can be rewritten, by replacing the symbol \mathcal{W} by W , in the standard form:

$$\frac{P(W)}{\tilde{P}(-W)} = e^{\beta(W-\Delta F)}. \quad (\text{A.13})$$

A.3 Seifert's detailed fluctuation theorem for the total entropy

Using eq. (1.30), $P[X]/\tilde{P}[\tilde{X}] = e^{\Delta s_{tot}[X]}$, we have in steady state, the probability of obtaining a total entropy change of $\Delta \mathcal{S}_{tot}$ to be

$$\begin{aligned}
 P(\Delta \mathcal{S}_{tot}) &= \int \mathcal{D}[X] P[X] \delta(\Delta \mathcal{S}_{tot} - \Delta s_{tot}[X]) \\
 &= \int \mathcal{D}[X] \tilde{P}[\tilde{X}] e^{\Delta s_{tot}[X]} \delta(\Delta \mathcal{S}_{tot} - \Delta s_{tot}[X]) \\
 &= e^{\Delta \mathcal{S}_{tot}} \int \mathcal{D}[\tilde{X}] \tilde{P}[\tilde{X}] \delta(\Delta \mathcal{S}_{tot} + \Delta s_{tot}[\tilde{X}]) \\
 &= \tilde{P}(-\Delta \mathcal{S}_{tot}) e^{\Delta \mathcal{S}_{tot}}.
 \end{aligned} \tag{A.14}$$

The property of steady state has been used in the third step, where we have assumed that $\Delta s_{tot}[\tilde{X}] = -\Delta s_{tot}[X]$. In other words, we have assumed that, along with the medium entropy change, the change in system entropy also reverses sign along reverse path, which is possible only if the initial and final distributions interchange their forms along the reverse process. This condition holds for stochastic evolution only if the process starts and ends in equilibrium states, or in time-symmetric nonequilibrium steady states [27].

Once again, replacing the symbol $\Delta \mathcal{S}_{tot}$ by Δs_{tot} , and noting that the functional forms of P and \tilde{P} are same in a steady state, we can rearrange and write the final result in the standard form

$$\frac{P(\Delta s_{tot})}{P(-\Delta s_{tot})} = e^{\Delta s_{tot}}. \tag{A.15}$$

Appendix B

Dual dynamics and heat exchanges in steady state

B.1 The Hatano-Sasa identity

As shown by Hatano and Sasa [47], the following identity holds for systems making transitions between nonequilibrium steady states (we would deal with an overdamped system):

$$\left\langle \prod_{i=0}^{N-1} \frac{\rho_{ss}(x_{i+1}; \lambda_{i+1})}{\rho_{ss}(x_{i+1}; \lambda_i)} \right\rangle = 1. \quad (\text{B.1})$$

The steady state density $\rho_{ss}(x; \lambda)$ is assumed to be given by $e^{-\phi(x; \lambda)}$, where $\phi(x; \lambda)$ is an effective potential. To prove the identity, we would use the property of a steady state, that for a fixed value λ of the external non-autonomous drive, it remains in the same steady state:

$$\int dx' p(x|x'; \lambda) \rho_{ss}(x'; \lambda) = \rho_{ss}(x; \lambda). \quad (\text{B.2})$$

The left hand side can be explicitly written as

$$\left\langle \prod_{i=0}^{N-1} \frac{\rho_{ss}(x_{i+1}; \lambda_{i+1})}{\rho_{ss}(x_{i+1}; \lambda_i)} \right\rangle \equiv \int dx_0 \cdots dx_N \rho_{ss}(x_0; \lambda_0) \prod_{i=0}^{N-1} P(x_{i+1}|x_i; \lambda_i) \frac{\rho_{ss}(x_{i+1}; \lambda_{i+1})}{\rho_{ss}(x_{i+1}; \lambda_i)}. \quad (\text{B.3})$$

We therefore have,

$$\begin{aligned}
\left\langle \prod_{i=0}^{N-1} \frac{\rho_{ss}(x_{i+1}; \lambda_{i+1})}{\rho_{ss}(x_{i+1}; \lambda_i)} \right\rangle &= \int dx_1 \cdots dx_N \prod_{i=1}^{N-1} P(x_{i+1}|x_i; \lambda_i) \frac{\prod_{i=0}^{N-1} \rho_{ss}(x_{i+1}; \lambda_{i+1})}{\prod_{i=0}^{N-1} \rho_{ss}(x_{i+1}; \lambda_i)} \\
&\quad \times \int dx_0 \rho_{ss}(x_0; \lambda_0) P(x_1|x_0; \lambda_0) \\
&= \int dx_1 \cdots dx_N \prod_{i=1}^{N-1} P(x_{i+1}|x_i; \lambda_i) \frac{\prod_{i=0}^{N-1} \rho_{ss}(x_{i+1}; \lambda_{i+1}) \times \rho_{ss}(x_1; \lambda_0)}{\rho_{ss}(x_1; \lambda_0) \prod_{i=1}^{N-1} \rho_{ss}(x_{i+1}; \lambda_i)} \\
&= \int dx_1 \cdots dx_N \rho_{ss}(x_1; \lambda_1) \prod_{i=1}^{N-1} P(x_{i+1}|x_i; \lambda_i) \frac{\rho_{ss}(x_{i+1}; \lambda_{i+1})}{\rho_{ss}(x_{i+1}; \lambda_i)} \\
&= \cdots = \int dx_N \rho_{ss}(x_N; \lambda_N) = 1. \tag{B.4}
\end{aligned}$$

In the second step, we have used the property (B.2) to replace $\int dx_0 \rho_{ss}(x_0; \lambda_0) P(x_1|x_0; \lambda_0)$ by $\rho_{ss}(x_1; \lambda_0)$. In the third step, the factor $\rho_{ss}(x_1; \lambda_1)$ has been taken out of the product over $\rho_{ss}(x_{i+1}; \lambda_{i+1})$ in the numerator. The “ \cdots ” symbol in the last line implies repetition of the same sequence of steps $(N - 1)$ times.

B.2 Dual dynamics and its relation to steady state heat exchanges

The dual dynamics (denoted by the symbol \dagger) is defined through its transition probabilities as

$$\rho_{ss}(x_i; \lambda_i) p(x_{i+1}|x_i; \lambda_i) = \rho_{ss}(x_{i+1}; \lambda_i) p^\dagger(x_i|x_{i+1}; \lambda_i); \tag{B.5a}$$

$$\rho_{ss}(x_i; \lambda_i) p^\dagger(x_{i+1}|x_i; \lambda_i) = \rho_{ss}(x_{i+1}; \lambda_i) p(x_i|x_{i+1}; \lambda_i); \tag{B.5b}$$

Here, $p(x_{i+1}|x_i; \lambda_i)$ and $p^\dagger(x_{i+1}|x_i; \lambda_i)$ are the transition probabilities from state x_i to the state x_{i+1} at the parameter value λ_i , in the original and the dual dynamics, respectively. Eq. (B.5b) is obtained by taking dual transformation of both sides of eq. (B.5a). Under such a dynamics, if the system is allowed to relax to a steady state with a fixed value of λ , then one would find that the steady state density $\rho_{ss}(x; \lambda)$ retains its form while the probability current changes sign.

Now, proceeding along the lines of Hatano and Sasa, we rewrite the identity (B.1) as

$$\begin{aligned}
\left\langle \prod_{i=0}^{N-1} \frac{\rho_{ss}(x_{i+1}; \lambda_{i+1})}{\rho_{ss}(x_{i+1}; \lambda_i)} \right\rangle &= \left\langle \frac{\rho_{ss}(x_N; \lambda_N) \prod_{i=0}^{N-2} \rho_{ss}(x_{i+1}; \lambda_{i+1})}{\rho_{ss}(x_1; \lambda_0) \prod_{i=1}^{N-1} \rho_{ss}(x_{i+1}; \lambda_i)} \right\rangle \\
&= \left\langle \frac{\rho_{ss}(x_N; \lambda_N) \rho_{ss}(x_0; \lambda_0) \prod_{i=0}^{N-2} \rho_{ss}(x_{i+1}; \lambda_{i+1})}{\rho_{ss}(x_0; \lambda_0) \rho_{ss}(x_1; \lambda_0) \prod_{i=1}^{N-1} \rho_{ss}(x_{i+1}; \lambda_i)} \right\rangle \\
&= \left\langle e^{-\Delta\phi} \prod_{i=0}^{N-1} \frac{\rho_{ss}(x_i; \lambda_i)}{\rho_{ss}(x_{i+1}; \lambda_i)} \right\rangle \\
&= \left\langle e^{-\Delta\phi} \prod_{i=0}^{N-1} \frac{p^\dagger(x_i|x_{i+1}; \lambda_i)}{p(x_{i+1}|x_i; \lambda_i)} \right\rangle = 1. \tag{B.6}
\end{aligned}$$

In the first step, the last factor from the product in the numerator and the first factor from the product in the denominator, have been taken out of the respective product signs, consequently changing the limits of these products. In the second step, we have multiplied the numerator and denominator of $\frac{\rho_{ss}(x_N; \lambda_N)}{\rho_{ss}(x_1; \lambda_0)}$ by the factor $\rho_{ss}(x_0; \lambda_0)$. We have used the relation $\Delta\phi = -\ln[\rho_{ss}(x_N; \lambda_N)/\rho_{ss}(x_0; \lambda_0)]$ in the next step, and have made use of the relations (B.5a) and (B.5b) in the final step.

Comparing with the Hatano-Sasa equality, eq.(1.37), we find that the product within the angular brackets in eq. (B.6) must be equal to $e^{-\beta Q_{ex}}$. Therefore,

$$e^{\beta Q_{ex}} = \prod_{i=0}^{N-1} \frac{\rho_{ss}(x_{i+1}; \lambda_i)}{\rho_{ss}(x_i; \lambda_i)} = \prod_{i=0}^{N-1} \frac{p(x_{i+1}|x_i; \lambda_i)}{p^\dagger(x_i|x_{i+1}; \lambda_i)} = \prod_{i=0}^{N-1} \frac{p^\dagger(x_{i+1}|x_i; \lambda_i)}{p(x_i|x_{i+1}; \lambda_i)}. \tag{B.7}$$

The second equality follows from eq. (B.5b). To derive a similar expression for the housekeeping heat, we begin with the Crooks theorem:

$$\begin{aligned}
e^{\beta Q} &= \prod_{i=0}^{N-1} \frac{p(x_{i+1}|x_i; \lambda_i)}{p(x_i|x_{i+1}; \lambda_i)} = \prod_{i=0}^{N-1} \frac{p(x_{i+1}|x_i; \lambda_i)}{p(x_i|x_{i+1}; \lambda_i)} \times \frac{p^\dagger(x_{i+1}|x_i; \lambda_i)}{p^\dagger(x_{i+1}|x_i; \lambda_i)} \\
&= \prod_{i=0}^{N-1} \frac{p(x_{i+1}|x_i; \lambda_i)}{p^\dagger(x_{i+1}|x_i; \lambda_i)} \times \frac{p^\dagger(x_{i+1}|x_i; \lambda_i)}{p(x_i|x_{i+1}; \lambda_i)} = e^{\beta Q_{ex}} \prod_{i=0}^{N-1} \frac{p(x_{i+1}|x_i; \lambda_i)}{p^\dagger(x_{i+1}|x_i; \lambda_i)}. \tag{B.8}
\end{aligned}$$

In the final step, eq. (B.7) has been used. Thus, we get

$$e^{\beta Q_{hk}} = e^{\beta(Q - Q_{ex})} = \prod_{i=0}^{N-1} \frac{p(x_{i+1}|x_i; \lambda_i)}{p^\dagger(x_{i+1}|x_i; \lambda_i)}. \quad (\text{B.9})$$

Equations (B.7) and (B.9) thus provide the expressions for the excess heat and the housekeeping heat, respectively.

Appendix C

Calculation of variance of W , and the Fourier transform of $P(\Delta s_{tot})$ for a system in a harmonic potential

C.1 Calculation of variance of W :

Using equation (2.2a),

$$\begin{aligned} W - \langle W \rangle &= - \int_0^t (x(t') - \langle x(t') \rangle) \dot{f}(t') dt' \\ &= - \int_0^t dt' \dot{f}(t') \left[x_0 e^{-kt'/\gamma} + e^{-kt'/\gamma} \int_0^{t'} e^{kt''/\gamma} \xi(t'') dt'' \right], \end{aligned}$$

$$\begin{aligned} \therefore \langle (W - \langle W \rangle)^2 \rangle &= \langle x_0^2 \rangle \int_0^t dt' \dot{f}(t') e^{-kt'/\gamma} \int_0^t dt_1 \dot{f}(t_1) e^{-kt_1/\gamma} \\ &\quad + \frac{1}{\gamma^2} \int_0^t dt' \dot{f}(t') e^{-kt'/\gamma} \int_0^t dt_1 \dot{f}(t_1) e^{-kt_1/\gamma} \int_0^{t'} dt'' e^{kt''/\gamma} \int_0^{t_1} dt_2 e^{kt_2/\gamma} \langle \xi(t'') \xi(t_2) \rangle \\ &= \langle x_0^2 \rangle \int_0^t dt' \dot{f}(t') e^{-kt'/\gamma} \int_0^t dt_1 \dot{f}(t_1) e^{-kt_1/\gamma} \\ &\quad + \frac{2T}{\gamma} \int_0^t dt' \dot{f}(t') e^{-kt'/\gamma} \int_0^t dt_1 \dot{f}(t_1) e^{-kt_1/\gamma} \int_0^{t'} dt'' e^{kt''/\gamma} \int_0^{t_1} dt_2 e^{kt_2/\gamma} \delta(t'' - t_2). \end{aligned}$$

In the second line, we have got an integral of the form

$$\begin{aligned}
I &= \int_0^t dt' \dot{f}(t') e^{-kt'/\gamma} \int_0^t dt_1 \dot{f}(t_1) e^{-kt_1/\gamma} \int_0^{t'} dt'' e^{kt''/\gamma} \int_0^{t_1} dt_2 e^{kt_2/\gamma} \delta(t'' - t_2) \\
&= I_1 + I_2,
\end{aligned} \tag{C.1}$$

where I_1 and I_2 are contain the same integrands, but the contributions come from the region $t' \leq t_1$ and from $t' > t_1$, respectively. Then we have,

$$\begin{aligned}
I_1 &= \int_0^t dt' \dot{f}(t') e^{-kt'/\gamma} \int_0^t dt_1 \dot{f}(t_1) e^{-kt_1/\gamma} \int_0^{t'} dt'' e^{2kt''/\gamma} \\
&= \frac{\gamma}{2k} \int_0^t dt' \dot{f}(t') e^{-kt'/\gamma} (e^{2kt'/\gamma} - 1) \int_0^t dt_1 \dot{f}(t_1) e^{-kt_1/\gamma} \\
&= \frac{\gamma}{2k} \int_0^t dt' \dot{f}(t') (e^{kt'/\gamma} - e^{-kt'/\gamma}) \int_0^t dt_1 \dot{f}(t_1) e^{-kt_1/\gamma}
\end{aligned} \tag{C.2}$$

Therefore we have,

$$\begin{aligned}
\langle (W - \langle W \rangle)^2 \rangle_{t' \leq t_1} &= \frac{T}{k} \int_0^t dt' \dot{f}(t') e^{-kt'/\gamma} \int_0^t dt_1 \dot{f}(t_1) e^{-kt_1/\gamma} \\
&\quad + \frac{T}{k} \int_0^t dt' \dot{f}(t') (e^{kt'/\gamma} - e^{-kt'/\gamma}) \int_0^t dt_1 \dot{f}(t_1) e^{-kt_1/\gamma} \\
&= \frac{T}{k} \int_0^t dt' \dot{f}(t') e^{kt'/\gamma} \int_0^t dt_1 \dot{f}(t_1) e^{-kt_1/\gamma} \\
&= \frac{T}{k} \int_0^t dt' \int_0^t dt_1 \dot{f}(t') \dot{f}(t_1) e^{-k(t_1-t')/\gamma}.
\end{aligned} \tag{C.3}$$

Similarly, one gets

$$\langle (W - \langle W \rangle)^2 \rangle_{t' > t_1} = \frac{T}{k} \int_0^t dt' \int_0^t dt_1 \dot{f}(t') \dot{f}(t_1) e^{-k(t'-t_1)/\gamma}. \tag{C.4}$$

Therefore, we can write in compact notation,

$$\langle (W - \langle W \rangle)^2 \rangle = \frac{T}{k} \int_0^t dt' \int_0^t dt_1 \dot{f}(t') \dot{f}(t_1) e^{-k|t'-t_1|/\gamma}$$

$$\begin{aligned}
&= \frac{2T}{k} \int_0^t dt' \int_0^{t'} dt_1 \dot{f}(t') \dot{f}(t_1) e^{-k(t'-t_1)/\gamma} \\
&= \frac{2T}{k} \int_0^t dt' \dot{f}(t') e^{-kt'/\gamma} \int_0^{t'} dt_1 \dot{f}(t_1) e^{kt_1/\gamma}. \tag{C.5}
\end{aligned}$$

Note that eq. (C.5) is obtained only when the contributions from eq. (C.3) or (C.4) are summed up, which leads to an integrand that is symmetric with respect to t' and t_1 (see the first line of eq. (C.5)). Partial integration of the integral over t_1 gives

$$\langle W^2 \rangle - \langle W \rangle^2 = \frac{2T}{k} \int_0^t dt' \dot{f}(t') f(t') - \frac{2T}{\gamma} \int_0^t dt' \dot{f}(t') e^{-kt'/\gamma} \int_0^{t'} e^{kt_1/\gamma} f(t_1) dt_1.$$

Noting that $\langle x(t') \rangle = \frac{e^{-kt'/\gamma}}{\gamma} \int_0^{t'} e^{kt_1/\gamma} f(t_1) dt_1$ and $W = - \int_0^t \dot{f}(t') \langle x(t') \rangle dt'$, we finally get

$$\langle (W - \langle W \rangle)^2 \rangle = \frac{2T}{2k} f^2(t) + \frac{2T}{\gamma} \langle W \rangle = 2T \left[\langle W \rangle + \frac{f^2(t)}{2k} \right].$$

C.2 Calculation of cross correlation $\langle Wx \rangle - \langle W \rangle \langle x \rangle$:

We have, from (2.2a) and (2.13),

$$\begin{aligned}
\langle W(t) \rangle \langle x(t) \rangle &= \left[- \int_0^t \langle x(t') \rangle \dot{f}(t') dt' \right] \times \langle x(t) \rangle \\
&= \left[- \int_0^t \left(\frac{1}{\gamma} \int_0^{t'} e^{-k(t'-t'')/\gamma} f(t'') dt'' \right) \dot{f}(t') dt' \right] \times \left[\frac{1}{\gamma} \int_0^t e^{-k(t-t_1)/\gamma} f(t_1) dt_1 \right] \\
&= - \frac{1}{\gamma^2} \int_0^t dt' \dot{f}(t') \int_0^{t'} dt'' e^{-k(t'-t'')/\gamma} f(t'') \int_0^t dt_1 e^{-k(t-t_1)/\gamma} f(t_1). \tag{C.6}
\end{aligned}$$

On the other hand,

$$\begin{aligned}
W.x &= \left(- \int_0^t x(t') \dot{f}(t') dt' \right) x(t) \\
&= \left[- \int_0^t \left(x_0 e^{-kt'/\gamma} + \frac{1}{\gamma} \int_0^{t'} e^{-k(t'-t'')/\gamma} (f(t'') + \xi(t'')) dt'' \right) \dot{f}(t') dt' \right] \\
&\quad \times \left[x_0 e^{-kt/\gamma} + \frac{1}{\gamma} \int_0^t e^{-k(t-t_1)/\gamma} (f(t_1) + \xi(t_1)) dt_1 \right]
\end{aligned}$$

$$\begin{aligned}
\therefore \langle Wx \rangle &= - \int_0^t \langle x_0^2 \rangle e^{-k(t+t')/\gamma} \dot{f}(t') dt' \\
&\quad - \frac{1}{\gamma^2} \int_0^t dt' \dot{f}(t') \int_0^{t'} dt'' e^{-k(t'-t'')/\gamma} \int_0^t dt_1 [f(t'')f(t_1) + \langle \xi(t'')\xi(t_1) \rangle] e^{-k(t-t_1)/\gamma} \\
&= - \frac{T}{k} \int_0^t e^{-k(t+t')/\gamma} \dot{f}(t') dt' \\
&\quad - \frac{1}{\gamma^2} \int_0^t dt' \dot{f}(t') \int_0^{t'} dt'' e^{-k(t'-t'')/\gamma} \int_0^t dt_1 [f(t'')f(t_1) + 2T\gamma\delta(t_1 - t'')] e^{-k(t-t_1)/\gamma},
\end{aligned} \tag{C.7}$$

where we have used the fact that $\frac{1}{2}k\langle x_0 \rangle^2 = \frac{1}{2}T$, and $\langle \xi(t)\xi(t') \rangle = 2T\gamma\delta(t - t')$. Also, x_0 and $\xi(t)$ are uncorrelated, and the average of each is zero. From (C.6) and (C.7),

$$\begin{aligned}
\langle W(t)x(t) \rangle - \langle W(t) \rangle \langle x(t) \rangle &= - (T/k) \int_0^t e^{-k(t+t')/\gamma} \dot{f}(t') dt' \\
&\quad - (2T/\gamma) \int_0^t dt' \dot{f}(t') \int_0^{t'} e^{-k(t'-t'')/\gamma} e^{-k(t-t'')/\gamma} dt'' \\
&= - (T/k) e^{-kt/\gamma} \int_0^t e^{-kt'/\gamma} \dot{f}(t') dt' \\
&\quad - (2T/\gamma) e^{-kt/\gamma} \int_0^t dt' \dot{f}(t') e^{-kt'/\gamma} \int_0^{t'} e^{2kt''/\gamma} dt''.
\end{aligned} \tag{C.8}$$

Finally, one obtains

$$\langle W(t)x(t) \rangle - \langle W(t) \rangle \langle x(t) \rangle = -\frac{T}{k} e^{-kt/\gamma} \int_0^t dt' \dot{f}(t') e^{kt'/\gamma} dt'. \tag{C.9}$$

On integrating by parts, the integral on the RHS becomes

$$\left[e^{kt'/\gamma} f(t') \right]_0^t - \int_0^t \frac{k}{\gamma} e^{kt'/\gamma} f(t') dt' = e^{kt/\gamma} f(t) - \frac{k}{\gamma} \int_0^t e^{kt'/\gamma} f(t') dt'.$$

Using this, equation (C.9) reduces to

$$\langle W(t)x(t) \rangle - \langle W(t) \rangle \langle x(t) \rangle = \frac{T}{k} [k\langle x(t) \rangle - f(t)]. \tag{C.10}$$

Finally, from (C.10) and (2.17b), we get

$$\sigma^2 = \frac{T}{T} [2\langle W \rangle - k\langle x \rangle^2 + 2\langle x \rangle f] = 2\langle \Delta s_{tot} \rangle. \quad (\text{C.11})$$

C.3 Calculation of the Fourier transform of $P(\Delta s_{tot}, t)$

$$\begin{aligned} \hat{P}(R, t) &\equiv \int_{-\infty}^{\infty} d\Delta s_{tot} e^{iR\Delta s_{tot}} P(\Delta s_{tot}, t) \\ &= \int_{-\infty}^{\infty} dx dx_0 P(x_0, x, t) \exp \left[iR \left(\frac{\alpha}{2} x_0^2 + \frac{\beta}{2} x^2 + \kappa \right) \right] \\ &= e^{iR\kappa} \int_{-\infty}^{\infty} dx dx_0 P(x_0, x, t) \exp \left[iR \left(\frac{\alpha}{2} x_0^2 + \frac{\beta}{2} x^2 \right) \right]. \end{aligned} \quad (\text{C.12})$$

The factor $\exp \left[iR \left(\frac{\alpha}{2} x_0^2 + \frac{\beta}{2} x^2 \right) \right]$ in (C.12) can be written as

$$\exp \left[iR \left(\frac{\alpha}{2} x_0^2 + \frac{\beta}{2} x^2 \right) \right] = e^{\frac{1}{2} iR \mathbf{a}^\dagger \cdot \mathbf{B} \cdot \mathbf{a}}, \quad (\text{C.13})$$

with

$$\mathbf{a} = \begin{pmatrix} x_0 \\ x \end{pmatrix}; \quad \mathbf{B} = \begin{pmatrix} \alpha & 0 \\ 0 & \beta \end{pmatrix}. \quad (\text{C.14})$$

Therefore, from (C.12), we have,

$$\begin{aligned} \therefore \hat{P}(R, t) &= \frac{e^{iR\kappa}}{2\pi \sqrt{\det \mathbf{A}}} \int_{-\infty}^{\infty} d\mathbf{a} e^{-\frac{1}{2} \mathbf{a}^\dagger \cdot \mathbf{A}^{-1} \cdot \mathbf{a} + i\frac{R}{2} \mathbf{a}^\dagger \cdot \mathbf{B} \cdot \mathbf{a}} \\ &= \frac{e^{iR\kappa}}{2\pi \sqrt{\det \mathbf{A}}} \int_{-\infty}^{\infty} d\mathbf{a} e^{-\frac{1}{2} \mathbf{a}^\dagger \cdot (\mathbf{A}^{-1} - iR\mathbf{B}) \cdot \mathbf{a}} \\ &= \frac{e^{iR\kappa}}{2\pi \sqrt{\det \mathbf{A}}} \int_{-\infty}^{\infty} d\mathbf{a} e^{-\frac{1}{2} \mathbf{a}^\dagger \cdot \mathbf{A}^{-1} \cdot (\mathbf{I} - iR\mathbf{A} \cdot \mathbf{B}) \cdot \mathbf{a}} \\ &= \frac{e^{iR\kappa}}{2\pi \sqrt{\det \mathbf{A}}} \frac{2\pi}{\sqrt{\det(\mathbf{A}^{-1}) \det(\mathbf{I} - iR\mathbf{A} \cdot \mathbf{B})}} \\ &= \frac{e^{iR\kappa}}{\sqrt{\det(\mathbf{I} - iR\mathbf{A} \cdot \mathbf{B})}}. \end{aligned} \quad (\text{C.15})$$

which is equation (2.37).

The determinant $\det(\mathbf{I} - iR\mathbf{A}\cdot\mathbf{B})$ is given by

$$\begin{aligned} \det(I - iR\mathbf{A}\cdot\mathbf{B}) &= \frac{T - iR(\sigma_x^2 - T)}{k\langle x^2 \rangle} + \left(\frac{\sigma_x^2 - T}{k\langle x^2 \rangle} \right) e^{-2kt/\gamma} [(1 + iR)^2 \\ &\quad + R(i - R) \left\{ \left(\frac{\sigma_x^2 - T}{T} \right) e^{-2kt/\gamma} - \frac{\sigma_x^2}{T} \right\}]. \end{aligned} \quad (\text{C.16})$$

C.4 Proof of $\langle \Delta F(\tau) \rangle \geq \Delta F$ for harmonic potential

In this appendix, our motivation is to evaluate $\langle \Delta F(\tau) \rangle$ and show that $\langle \Delta F(\tau) \rangle \geq \Delta F$.

Let us consider the potential

$$U(x, t) = \frac{1}{2}kx^2 - xf(t), \quad (\text{C.17})$$

where $f(t)$ is an arbitrary protocol. The protocol $\lambda(t) = f(t)$ is assumed to be equal to zero at time $t = 0$. Thus, $\lambda(0) = 0$. After time τ , $\lambda(\tau) = f(\tau)$. The equilibrium free energy, calculated from the partition function, at parameter value $\lambda(0)$, is $F_A = T \ln \left(\sqrt{\frac{k}{2\pi T}} \right)$. The equilibrium free energy corresponding to the final value of the protocol is

$$F_B = T \ln \left(\sqrt{\frac{k}{2\pi T}} \right) - \frac{f^2}{2k}. \quad (\text{C.18})$$

Here,

$$\Delta F = F_B - F_A = -\frac{f^2}{2k}. \quad (\text{C.19})$$

The initial probability density of the particle position is

$$p(x_0) = \sqrt{\frac{k}{2\pi T}} \exp \left(\frac{-kx_0^2}{2T} \right). \quad (\text{C.20})$$

The final time-evolved solution for $p(x, \tau)$ is

$$p(x, \tau) = \sqrt{\frac{k}{2\pi T}} \exp \left(\frac{-k(x - \langle x \rangle)^2}{2T} \right). \quad (\text{C.21})$$

where $\langle x(\tau) \rangle$ is obtained from equation (2.5) on replacing t by τ . Using the definition (2.42) for nonequilibrium free energy, and the variance $\langle (x - \langle x \rangle)^2 \rangle = T/k$, we then have

$$\langle \Delta F(\tau) \rangle = \langle \Delta U(\tau) \rangle - T \langle \Delta s(\tau) \rangle = \frac{1}{2} k \langle x^2 \rangle - \langle x \rangle f - \frac{T}{2}.$$

Thus,

$$\begin{aligned} \langle \Delta F(\tau) \rangle - \Delta F &= \frac{1}{2} k \langle x^2 \rangle - \langle x \rangle f - \frac{T}{2} + \frac{f^2}{2k} \\ &= \frac{1}{2} k \left(\frac{T}{k} + \langle x \rangle^2 \right) - \langle x \rangle f - \frac{T}{2} + \frac{f^2}{2k} \\ &= \frac{1}{2} k \left(\langle x \rangle^2 - 2 \langle x \rangle \frac{f}{k} + \frac{f^2}{k^2} \right) \\ &= \frac{1}{2} k \left(\langle x \rangle - \frac{f}{k} \right)^2 \geq 0. \end{aligned} \tag{C.22}$$

In the second step, we have used the fact that $\langle x^2 \rangle - \langle x \rangle^2 = T/k$, so that $\langle x^2 \rangle = T/k + \langle x \rangle^2$.

C.5 Explicit expressions for free energy changes in a sinusoidally driven system in harmonic potential

When $f(t) = A \sin \omega t$, the instantaneous change in free energy is given by

$$\begin{aligned} \langle \Delta F(t) \rangle &= \frac{1}{2} k \langle x(t) \rangle^2 - \langle x(t) \rangle f(t) \\ &= \frac{k A^2 e^{-2kt/\gamma}}{2(k^2 + \gamma^2 \omega^2)^2} [\gamma \omega + e^{kt/\gamma} (-\gamma \omega \cos \omega t + k \sin \omega t)]^2 \\ &\quad - \frac{A^2 e^{-kt/\gamma} \sin \omega t}{k^2 + \gamma^2 \omega^2} [\gamma \omega + e^{kt/\gamma} (-\gamma \omega \cos \omega t + k \sin \omega t)]. \end{aligned} \tag{C.23}$$

and change in equilibrium free energy is given by

$$\Delta F = -\frac{A^2 \sin^2 \omega t}{2k}. \tag{C.24}$$

For a protocol of time interval between $t = 0$ to $t = \tau = \pi/2\omega$, we therefore get

$$\langle \Delta F(\tau) \rangle = -\frac{A^2 [k^3 + (2 - e^{-k\pi/\gamma\omega}) k\gamma^2\omega^2 + 2e^{-k\pi/2\gamma\omega}\gamma^3\omega^3]}{2(k^2 + \gamma^2\omega^2)^2}; \quad (\text{C.25})$$

$$\langle \Delta F \rangle = -\frac{A^2}{2k}. \quad (\text{C.26})$$

Appendix D

Heun's method of numerical integration

Here we describe briefly the Heun's method of integration [67]. Let the slope of a curve $g(t)$ at some point be t given by the function

$$\frac{dg(t)}{dt} \equiv f(t, g(t)). \quad (\text{D.1})$$

Consider the solution curve to be the blue curve in the figure below. The actual value of $g(t+h)$

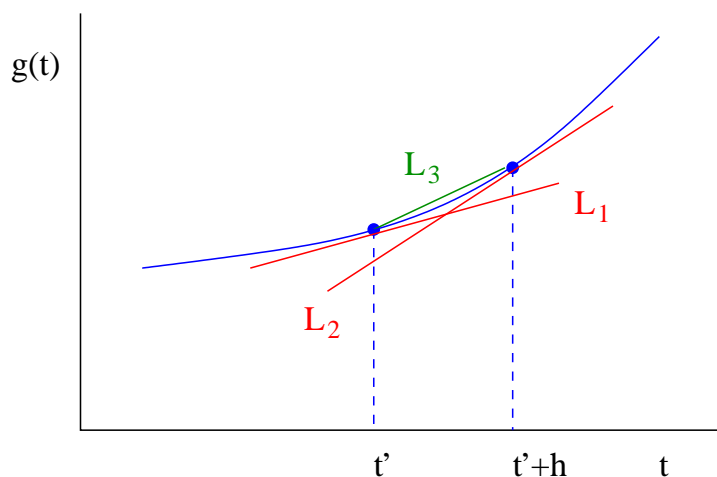


Figure D.1

must be given by, from eq. (D.1),

$$g(t+h) = g(t) + \int_t^{t+h} ds f(s, g(s)). \quad (\text{D.2})$$

Now, we exaggerate one of the time steps, denoted by h , to show the essential principle which the method relies on. Suppose that the region of the curve considered be convex, as depicted in the figure. As is obvious from the figure, the slope corresponding to $t = t'$ (line L_1) is smaller and that at $t = t' + h$ (line L_2) is higher than the desired slope given by the line L_3 . One can decrease the inaccuracy of computation by substituting either of these slopes with the average of the slopes¹ at the two points $t = t'$ and $t = t' + h$:

$$\text{slope} = \frac{1}{2}[f(t', g(t')) + f(t' + h, g(t' + h))]. \quad (\text{D.3})$$

To do this, we first calculate the slope at the point t' . To get the slope at the right end, Heun's method approximates $g(t' + h)$ by the value obtained through the Euler method, $g(t' + h) \simeq g(t') + hf(t', g(t'))$, and then computes the slope $f(t' + h, g(t' + h))$. We then write

$$g(t' + h) = g(t') + h \cdot f_{Heun}(t', g(t')), \quad (\text{D.4})$$

where

$$f_{Heun}(t', g(t')) = \frac{1}{2}[f(t', g(t')) + f(t' + h, g(t') + hf(t', g(t')))]. \quad (\text{D.5})$$

The Heun's method is accurate up to $O(h^2)$ (per step) for deterministic integrals [67]. In [67], it has been shown that this method reproduces the equilibrium distribution faithfully for stochastic systems.

The entire analysis remains similar if the considered region of the curve is concave instead of being convex.

¹This is the basic principle of the trapezoidal method of integration.

Bibliography

- [1] L. D Landau and E. M. Lifshitz, *Statistical Physics*, 3rd ed., part 1 (Butterworth-Heinemann, 1980).
- [2] L. P. Pitaevskii, *Phys.-Usp.* **54**, 625 (2011).
- [3] G. M. Wang, E. M. Sevick, E. Mittag, D. J. Searles, and D. J. Evans, *Phys. Rev. Lett.* **89**, 050601 (2002).
- [4] F. Ritort, *J. Phys. Condens. Matter* **18**, R531 (2006).
- [5] U. Seifert, *Rep. Prog. Phys.* **75**, 126001 (2012).
- [6] M. Campisi, P. Hänggi, and P. Talkner, *Rev. Mod. Phys.* **83**, 771 (2011).
- [7] S. Ciliberto and C. Laroche, *Journal de Physique IV* **8**, 215 (1998).
- [8] J. Liphardt, S. Dumont, S. B. Smith, I. Tinoco Jr., and C. Bustamante, *Science* **296**, 1832 (2002).
- [9] A. Petrosyan, F. Douarche, I. Rabbiosi and S. Ciliberto, *Europhys. Lett.* **70**, 593 (2005).
- [10] E. H. Trepagnier, C. Jarzynski, F. Ritort, G. E. Crooks, C. J. Bustamante and J. Liphardt, *Proc. Natl. Acad. Sci.* **101**, 15038 (2004).
- [11] F. Douarche, S. Joubaud, N. B. Garnier, A. Petrosyan and S. Ciliberto, *Phys. Rev. Lett.* **97**, 140603 (2006).
- [12] R. von Zon, S. Ciliberto and E. G. D. Cohen, *Phys. Rev. Lett.* **92**, 130601 (2004).

- [13] T. Speck, V. Blickle, C. Bechinger and U. Seifert, *Europhys. Lett.* **79**, 30002 (2007).
- [14] V. Blickle, T. Speck, L. Helden, U. Seifert and C. Bechinger, *Phys. Rev. Lett.* **96**, 070603 (2006).
- [15] S. Joubaud, N. B. Garnier and S. Ciliberto, *Europhys. Lett.* **82**, 30007 (2008).
- [16] P. Jop, A. Petrosyan and S. Ciliberto, *Europhys. Lett.* **81** 50005 (2008).
- [17] A. Imparato, P. Jop, A. Petrosyan and S. Ciliberto, *J. Stat. Mech.* P10017 (2008).
- [18] P. Talkner and P. Hänggi, *J. Phys. A: Math. Theor.* **40**, F569 (2007).
- [19] M. Campisi, P. Talkner, and P. Hänggi, *Phys. Rev. Lett.* **102**, 210401 (2009).
- [20] M. Campisi, P. Talkner and P. Hänggi, *Phys. Rev. Lett.* **105**, 140601 (2010).
- [21] T. Sagawa and M. Ueda, *Phys. Rev. Lett.* **100**, 080403 (2008).
- [22] C. Jarzynski, *Annu. Rev. Condens. Matter Phys.* **2**, 329 (2011).
- [23] K. Sekimoto, *J. Phys. Soc. Jpn.* **66**, 1234 (1997).
- [24] K. Sekimoto, *Prog. Theor. Phys. Supp.* **130**, 17 (1998).
- [25] H. B. Callen, *Thermodynamics and an introduction to thermostatistics*, 2nd ed. (John Wiley & Sons, 2006).
- [26] M. W. Zemansky, *Heat and thermodynamics*, 5th ed. (McGraw-Hill, 1968).
- [27] G. E. Crooks, *Phys. Rev. E* **60**, 2721 (1999).
- [28] Udo Seifert, *Phys. Rev. Lett.* **95**, 040602 (2005).
- [29] Udo Seifert, *Eur. Phys. J. B* **64**, 423 (2008).
- [30] D. J. Evans, E. G. D. Cohen and G. P. Morriss, *Phys. Rev. Lett.* **71** , 2401 (1993); **71**, 3616 (1993) [errata].

- [31] D. J. Evans and D. J. Searles, Phys. Rev. E **50**, 1645 (1994).
- [32] G. Gallavotti and E. G. D. Cohen, Phys. Rev. Lett. **74**, 2694 (1995); J. Stat. Phys. **80**, 31 (1995).
- [33] C. Jarzynski, Phys. Rev. Lett. **78**, 2690 (1997).
- [34] C. Jarzynski, Phys. Rev. E **56**, 5018 (1997).
- [35] D. J. Evans and D. J. Searles, Adv. Phys. **51**, 1529 (2002).
- [36] R. J. Harris and G. M. Schütz, J. Stat. Mech. p07020 (2007).
- [37] F. Ritort, Sem. Poincare **2**, 63 (2003).
- [38] J. Kurchan, J. Stat. Mech. p07005 (2007).
- [39] R. van Zon and E. G. D. Cohen, Phys. Rev. E **67**, 046102 (2003).
- [40] R. van Zon and E. G. D. Cohen, Phys. Rev. E **69**, 056121 (2004).
- [41] O. Narayan and A. Dhar, J. Phys. A: Math. Gen. **37**, 63 (2004).
- [42] G. E. Crooks, J. Stat. Phys. **90**, 1481 (1998).
- [43] J. Kurchan, J. Phys. A: Math. Gen. **31**, 3719 (1998).
- [44] C. Jarzynski, Phys. Rev. E **73**, 046105 (2006).
- [45] David Chandler, *Introduction to Modern Statistical Mechanics* (Oxford University Press, USA, 1987).
- [46] Y. Oono and M. Paniconi, Prog. Theor. Phys. Supp. **130**, 29 (1998).
- [47] T. Hatano and S. Sasa, Phys. Rev. Lett. **86**, 3463 (2001).
- [48] H. Risken, *The Fokker-Planck Equation: Methods of Solutions and Applications*, 2nd ed. (Springer, 1996).

- [49] M. Esposito and C. Van den Broeck, Phys. Rev. Lett. **104**, 090601 (2010).
- [50] R. E. Spinney and I. J. Ford, Phys. Rev. Lett. **108**, 170603 (2012).
- [51] R. Garcia-Garcia, V. Lecomte, A. B. Kolton and D. Dominguez, J. Stat. Mech. P02009 (2012).
- [52] V. Y. Chernayk, M. Chertkov and C. Jarzynski, J. Stat. Mech. P08001 (2006).
- [53] L. Gammaitoni, P. Hänggi, P. Jung and F. Marchesoni, Rev. Mod. Phys. **70**, 223 (1998).
- [54] R. Benzi, G. Parisi, A. Sutera and A. Vulpiani, Tellus **34**, 10 (1982).
- [55] T. Iwai, Physica A **300**, 350 (2001).
- [56] D. Andrieux and P. Gaspard, J. Stat. Mech. P02006 (2007).
- [57] J. L. Lebowitz and H. Spohn, J. Stat. Phys. **95**, 333 (1999).
- [58] C. Jarzynski, J. Stat. Phys. **98**, 77 (2000).
- [59] A. Saha, S. Lahiri and A. M. Jayannavar, Phys. Rev. E **80**, 011117 (2009).
- [60] R. Kawai, J. M. R. Parrondo and C. Van den Broeck, Phys. Rev. Lett. **98**, 080602 (2007).
- [61] A. Gomez-Marin, J.M.R. Parrondo and C. Van den Broeck, Europhys. Lett. **82**, 50002 (2008).
- [62] A. Gomez-Marin, J. M. R. Parrondo and C. Van den Broeck, Phys. Rev. E **78**, 011107 (2008).
- [63] A. Gomez-Marin, J. M. R. Parrondo and C. Van den Broeck, arxiv/cond-mat: 0710.4290.
- [64] Jordan Horowitz and Christopher Jarzynski, Phys. Rev. E **79**, 021106 (2009).
- [65] M. Evstigneev, P. Riemann and C. Bechinger, J. Phys.: Condens. Matter **17**, S3795 (2005).
- [66] Debasis Dan and A. M. Jayannavar, Physica A **345**, 404 (2005).

- [67] R. Mannella, in: J.A. Freund and T. Poschel (Eds), *Stochastic Process in Physics, Chemistry and Biology, Lecture Notes in Physics*, vol. 557 (Springer-Verlag, Berlin, 2000) .
- [68] Shantu Saikia, Ratnadeep Roy and A.M. Jayannavar, *Phys. Lett. A* **369**, 367 (2007).
- [69] Mamata Sahoo, Shantu Saikia, Mangal C. Mahato, A.M. Jayannavar, *Physica A* **387**, 6284 (2008).
- [70] Navinder Singh, Sourabh Lahiri and A. M. Jayannavar, *Pramana J. Phys.* **74**, 331 (2010).
- [71] Sylvain Joubaud , Nicolas B. Garnier and Sergio Ciliberto arxiv:cond-mat/0610031.
- [72] E. Trepagnier, C. Jarzynski, F. Ritort, G. Crooks, C. Bustamante and J. Liphardt, *PNAS* **101**, 15038 (2004).
- [73] O. Mazonka and C. Jarzynski, cond-mat/arxiv: 9912121.
- [74] T. Speck and U. Seifert, *Eur. Phys. J. B* **43**, 521 (2005).
- [75] A. M. Jayannavar and Mamata Sahoo, *Phys. Rev. E* **75**, 032102 (2007).
- [76] Hong Qian, *Phys. Rev. E* **65**, 016102 (2001).
- [77] C. Jarzynski, *Eur. Phys. J. B* **64**, 331 (2008).
- [78] L. Szilard, *Maxwells Demon: Entropy, Information, Computing*, edited by H. S. Leff and A. F. Rex (Princeton University Press, Princeton, NJ, 1990).
- [79] J. M. Horowitz and S. Vaikuntanthan, *Phys. Rev. E* **82**, 061120 (2010).
- [80] T. M. Cover and J. A. Thomas, *Elements of information theory*, 2nd ed. (Hoboken, NJ: Wiley-Interscience, 2006).
- [81] S. Liang, D. Medich, D.M. Czajkowsky, S. Sheng, J. Yuan, and Z. Shao, *Ultramicroscopy* **84**, 119 (2000).
- [82] T. Sagawa and M. Ueda, *Phys. Rev. Lett.* **104**, 090602 (2010).

- [83] T. Sagawa and M. Ueda, Phys. Rev. E **85**, 021104 (2012).
- [84] S. Lahiri, S. Rana and A. M. Jayannavar, J. Phys. A: Math. Theor. **45**, 065002 (2012).
- [85] S. Rana, S. Lahiri and A. M. Jayannavar, arxiv/cond-mat: 1202.1097.
- [86] M. Ponmurugan, Phys. Rev. E **83**, 031129 (2010).
- [87] D. Abrieu and U. Seifert, Phys. Rev. Lett. **108**, 030601 (2012).
- [88] S. Rana, S. Lahiri and A. M. Jayannavar, arxiv:1111.6229; accepted for publication in Pramana J. Phys.
- [89] F. J. Cao and M. Feito, Phys. Rev. E **79**, 041118 (2009).
- [90] U. Weiss, *Quantum dissipative systems* (World Scientific, 1993).
- [91] S. Lahiri and A. M. Jayannavar, arxiv/cond-mat: 1206.338.
- [92] S. Toyabe, T. Sagawa, M. Ueda, E. Muneyuki and M. Sano, Nature Physics **6**, 988 (2010).
- [93] A. Kundu, Phys. Rev. E **86**, 021107 (2012).
- [94] M. Esposito and C. van den Broeck, Phys. Rev. E **82**, 011143 (2010).
- [95] M. Esposito and C. van den Broeck, Phys. Rev. E **82**, 011144 (2010).
- [96] S. Lahiri and A. M. Jayannavar, Eur. Phys. J. B **69**, 87 (2009).
- [97] P. Hanggi, P. Talkner, M. Borkovec, Rev. Mod. Phys. **62**, 251 (1990).
- [98] L. Gammaitoni, F. Marchesoni and S. Santucci, Phys. Rev. Lett. **74**, 1052 (1995).
- [99] M. C. Mahato and A. M. Jayannavar, Phys. Rev. E **55**, 6266 (1997).
- [100] M. C. Mahato and A. M. Jayannavar, Mod. Phys. Lett. B **11**, 815 (1997).
- [101] M. C. Mahato and A. M. Jayannavar, Physica A **248**, 138 (1998).

- [102] D. Dan and A. M. Jayannavar, *Physica A* **345**, 404 (2005).
- [103] R. Krishnan and A. M. Jayannavar, *Physica A* **345**, 61 (2005).
- [104] N. Singh, S. Lahiri and A. M. Jayannavar, *Pramana J. Phys.* **74**, 331 (2010).
- [105] M. Borromeo and F. Marchesoni, *Europhys. Lett.* **68**, 783 (2004).
- [106] S. Savelev et al., *Europhys. Lett.* **67**, 179 (2004).
- [107] M. Borromeo and F. Marchesoni, *Phys. Rev. E* **71**, 031105 (2005).
- [108] M. Borromeo and F. Marchesoni, *Acta Physica Polonica B* **36**, 1421 (2005).
- [109] M. C. Mahato, A. M. Jayannavar, *Phys. Lett. A* **209**, 21 (1995).
- [110] D. R. Chialvo and M. M. Millonas, *Phys. Lett. A* **209**, 26 (1995).
- [111] A. Ajdari, D. Mukamel, L. Peliti, and J. Prost, *J. Phys. (Paris)-I*, **4**, 1551 (1994).
- [112] J. M. R. Parrondo and B. J. De Cisneros, *Appl. Phys. A: Mater. Sci. Process.* **75**, 179 (2002).
- [113] P. Jop, S. Ciliberto, A. Petrosyan, *Europhys. Lett.* **81**, 50005 (2008).
- [114] R. van Zon and E. G. D. Cohen, *Phys. Rev. E* **67** (2002) 046102
- [115] S. Joubaud, N. B. Garnier and S. Ciliberto, *J. Stat. Mech.*, P09018 (2007).
- [116] A. M. Jayannavar and M. Sahoo, *Phys. Rev. E* **75**, 032102 (2007).
- [117] M. Sahoo and A. M. Jayannavar, *Pramana J. Phys.* **70** 201(2008).
- [118] A. Imperato, L. Peliti, *Phys. Rev. E* **74**, 026106 (2006).